

Sheffield Hallam University

Deposition of cobalt on iron powder.

SAYLAM, Haydar.

Available from the Sheffield Hallam University Research Archive (SHURA) at:

<http://shura.shu.ac.uk/20331/>

A Sheffield Hallam University thesis

This thesis is protected by copyright which belongs to the author.

The content must not be changed in any way or sold commercially in any format or medium without the formal permission of the author.

When referring to this work, full bibliographic details including the author, title, awarding institution and date of the thesis must be given.

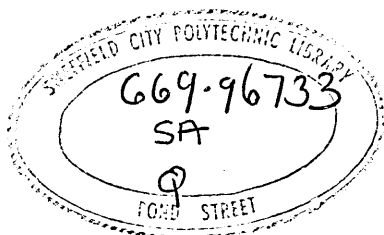
Please visit <http://shura.shu.ac.uk/20331/> and <http://shura.shu.ac.uk/information.html> for further details about copyright and re-use permissions.

DEPOSITION OF COBALT ON IRON POWDER

by

Haydar Saylam

This thesis is submitted in fulfilment of the requirements of Master of Philosophy of the Council of National Academic Awards. The work was carried out at Sheffield City Polytechnic Department of Metallurgy in collaboration with London and Scandinavian Metallurgical Ltd. March 1982.



7910749-01

PREFACE

All the work written in this thesis was carried out between 1st July, 1979 - 1st December, 1981 at Sheffield City Polytechnic. No part of this thesis has been submitted for a degree of any other institution.

During the course of the research programme the following advanced courses were attended

Corrosion and heat resistant alloys.

Continuous Casting.

Powder Metallurgy.

Each being a part of module 3 of the M.Sc. in Metallurgical Process Management.

ACKNOWLEDGMENTS

Many thanks are due specially to Dr. A.J. Fletcher for his regular support and constructive advice throughout the duration of this work.

Thanks must also be expressed to the technical staff of the Department of Metallurgy of Sheffield City Polytechnic and particularly to Mr. D. Latimer, Mr. G. Gregory, Mr. R. Rhodes and Mr. K. Woodhouse.

I also would like to express my sincere thanks and gratitude to Dr. A.W. Hills, Head of the Department of Metallurgy of Sheffield City Polytechnic for providing the opportunity for my research work.

DEPOSITION OF COBALT ON
IRON POWDER

By: H Saylam

SYNOPSIS

The cementation reaction



although theoretically possible, is not normally considered to be of significance since the negative electrode potential of the reaction is very small and the rate of deposition is usually extremely low. However, a previous investigation of the corresponding reaction between nickel and iron suggests that such reactions may occur at a relatively rapid rate, provided the specific surface area of the iron is very high, as in the case of a fine powder,

In the present work the cementation reaction has been followed in a three phase fluidized bed, which maintained the powder in suspension in the solution and ensured that all particles had an equal chance of contact with cobalt ions. An investigation was made of the effect on the reaction of certain process variables including temperature, PH, type of anion in the solution and concentration of iron powder in the cell and cobalt ions in the solution. This has allowed, under optimum conditions, cobalt deposition at a relatively high rate. In view of the relative cost of iron and cobalt this reaction may be a suitable way of extracting cobalt from waste solutions.

An examination of the morphology of the deposit

suggested that deposition always took place irregularly, so that some parts of the iron powder remained in contact with the solution. Thus the cementation reaction did not come to a rapid conclusion, on account of the formation of a continuous layer of cobalt on the iron surface. This irregular deposit was maintained even when electrodeposition occurred simultaneously with the cementation reaction.

GLOSSARY

A	: Constant
A'	: Atomic mass of elements (Atm/g)
A''	: Surface area per unit volume of electrode (cm^{-1})
A _s	: Surface area of the powder in 1 l solution.
a _m	: Activity of reduced metal
a _{mⁿ⁺}	: Activity of a metal ion in solution.
b	: Constant
C _o	: Concentration of the reducible cations at X = 0 (g/l)
C ₁	: Bulk solution concentration of reactant ions.
C ₂	: Bulk solution ion concentration of reductant metal.
C _m	: Metal ion concentration.
C _{m.s}	: Catholyte concentration at the metal surface.
C _{H₂O}	: Water concentration in the diffusion layer.
D	: Diffusion coefficient (cm^2s^{-1}).
E	: Electrode potential in volts.
E ^o	: Standard electrode potential referring to that of hydrogen (V).
E _{rev}	: Reversible potential (V).
E _c ^o	: Standard electrode potential of more noble metal.
E _a ^o	: Standard electrode potential of less noble metal.
E _a	: Potential of an anode operating irreversibly (V).
E _c	: Potential of a cathode operating irreversibly (V).
E _K	: Compromise potential in the case of short circuit.
E _{dic}	: Discharge potential.
F	: Faraday constant (96.493 C/equivalent).

g	:	gram
ΔG^*	:	Activation energy.
h	:	Time (hour)
I	:	Current (Ampere)
I_e	:	Electron current resulting from the transfer of metal cation of charge z.
I_c	:	Cathodic current.
I_a	:	Anodic current.
I_o	:	Exchange current density.
I_c^o	:	Actual cathodic current.
I_a^o	:	Actual anodic current.
I_p	:	Limiting passivation current.
k_o	:	Cementation reaction rate constant.
k_p	:	Reaction equilibrium constant of constant pressure $(k_p = \frac{a_m}{a_{m^{n+}}})$
k_s	:	Rate constant for the surface reaction.
\mathcal{K}	:	Transmission coefficient.
l or lt:	:	litre
L	:	Electrode length under working conditions (cm)
η	:	Overpotential
n	:	Number of electrons reacting, in per gram atom.
η_a	:	activation overpotential.
η_c	:	Concentration overvoltage.
η_r	:	Resistance overvoltage.
n'	:	Number of molecules reacting
n_1	:	Number of electrons involved in cementation reaction.

n_2	:	Valency electron number of reductant ^{five} metal, in cementation reaction.	x
R	:	Gas constant (1.987 cal/deg. mol. 8.314 joule/deg mol.)	
r	:	Corrosion rate (mg/cm ² .h.)	
r.d.s.	:	Rate determining step.	
S	:	Electrode surface area.	
S_a	:	Actual anodic area.	
S_c	:	Actual cathodic area.	
T	:	Temperature in kelvin.	
t	:	Time (second).	
$\frac{U}{V}$:	Electrolyte flow velocity (cm/min). Mean solution volume.	
V_F	:	Flade potential	
V_p	:	Passivation potential.	
V_{pp}	:	Complete passivation potential.	
V_o	:	Voidage fraction.	
X	:	Diffuse double layer thickness.	
W	:	Mass of an element.	
Z	:	Electrochemical equivalent.	
z_1	:	Number of electrons required for the total reduction process.	
μ_a	:	Anodic chemical potential.	
μ_c	:	Cathodic chemical potential.	
γ	:	Activity coefficient.	
ϕ	:	Effective potential at electrode surface.	
ψ_o	:	Potential at outer Helmholtz plane.	
ψ_x	:	Potential at diffusion double layer.	

CONTENTS

	<u>PAGE</u>
1. INTRODUCTION	12
2. REVIEW OF LITERATURE	14
2.1 Electrolytic Reactions	14
2.1.1 Electrode Potential	14
2.1.2 Activity Coefficient	16
2.1.3 Faraday's Law	16
2.1.4 The Electrode Layer	17
2.1.5 The Diffuse Double Layer	19
2.1.6 Polarization	20
2.1.7 Activation Overvoltage	23
2.1.8 Resistance Overvoltage	24
2.1.9 Concentration Overpotential	24
2.1.10 Passivation Phenomena	27
2.1.11 Characteristics of Active and Passive States	29
2.2 Non-Electrolytic Reactions	33
2.2.1 The Cementation Reaction	33
2.2.2 Hydrogen Reduction	37
2.2.3 Electroless Deposition	40
2.3 Cobalt Extraction in Aqueous Media	43
2.3.1 Cobalt Plating Solutions	45
2.3.2 Cobalt Sulphate Plating Solutions	46
2.3.3 Cobalt Chloride Plating Solutions	49
2.3.4 Other Cobalt Plating Solutions	50
2.4 The Properties of Cobalt Coatings	51
2.4.1 Corrosion Resistant Properties	51
2.4.2 Mechanical Properties	53
2.4.3 Effect of Certain Additions in the Solution on the Properties of Cobalt Coatings.	54

2.5	Metallic Powder Coating in a Fluidized Bed.	55
2.5.1	Mechanism of the Fluidized Bed Cell Operation.	56
2.5.2	Current Efficiency and Limiting Current Density.	59
2.5.3	Gas Fluidization	60
2.5.4	Application of fluidized Bed Cell to the Production of Metal and Composite Coatings.	61
3.	EXPERIMENTAL PROCEDURE	66
3.1	The Cementation Cells.	66
3.1.1 a)	Mechanically Stirred Cell	66
3.1.1 b)	Experimental Procedure in the Mechanically Stirred Cell	67
3.1.2 a)	Fluidized Bed Cell	68
3.1.2 b)	Experimental Procedure in the Fluidized Bed Cell	70
3.1.2 c)	Coating of Cobalt onto Iron Powder by Cementation in the Fluidized Bed Cell.	71
3.2	Raw Materials.	71
3.2.1	Metallic Powder	71
3.2.2	Cobalt Plating Solutions	72
3.2.3	Anode Materials.	72
3.2.4	Cathodes	73
3.3	Metallographic Study.	73
4.	RESULTS	75
4.1	Deposition of Cobalt in the Mechanically Stirred Cell.	75
4.1.1	Influence of Temperature on the Deposition of Cobalt in the Mechanically Stirred Cell.	77
4.1.2	Prolonged Deposition of Cobalt in the Mechanically Stirred Cell.	78
4.2	Deposition of Cobalt in the Fluidized Bed Cell.	79
4.2.1	Presence of Froth in the Fluidized Bed Cell.	79

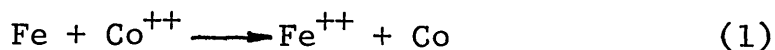
4.2.2	The Results in the Fluidized Bed Cell.	80
4.2.3	Effect of Iron Powder Concentration on the Deposition of Cobalt.	81
4.2.4	Influence of PH on the Rate of Cobalt Deposition.	83
4.2.5	Effect of Boric Acid Addition on The Rate of Cobalt Deposition From CoCl_2 and CoSO_4 solutions.	85
4.2.6	Effect of Temperature on the Cobalt Cementation Rate.	87
4.2.7	Effect of Cobalt Ion Concentration on the Cobalt Deposition Rate.	90
4.2.8	Effect of Sodium Sulphate on Cobalt Deposition Rate.	91
4.2.9	Electrodeposition of Cobalt onto Iron Powder in the Fluidized Bed Cell.	92
4.3	Metallographic Results	94
4.3.1	Distribution of Cobalt Deposit on the Iron Powder.	94
4.3.2	Sections Through Cobalt Coated Iron Particles.	96
4.3.3	Type of Morphology of Cobalt Deposits.	99
4.3.4	Effect of Time on the Type of Deposit.	101
4.3.5	Effect of Current Applications on the Deposit Morphology.	102
5.	DISCUSSION	103
5.1.1	Cobalt Cementation in the Mechanically Agitated Cell.	103
5.1.2	Influence of Boric Acid on Cobalt Deposition in the Mechanically Stirred Cell.	107
5.2.1	Cobalt Cementation in the Fluidized Bed Cell.	107
5.2.2	Influence of Iron Powder Concentration on the Rate of Cobalt Deposition.	108
5.2.3	The Influence of PH on the Cobalt Cementation Rate.	110
5.2.4	Effect of Boric Acid on the Cobalt Cementation	112

5.2.5	Effect of Temperature on the Cobalt Cementation.	115
5.2.6	Effect of Cobalt Salt Concentration on the Rate of Cobalt Deposition.	119
5.2.7	Effect of Additions of Sodium Sulphate on Cobalt Cementation.	120
5.3	Electrodeposition in the Fluidized Bed Cell.	121
5.4	Morphology of the Layer of Cobalt Deposited on the Iron Powder.	122
6.	CONCLUSIONS	127
7.	RECOMMENDATIONS	128
	REFERENCES	130
	TABLES	136
	FIGURES	175

1. INTRODUCTION

This investigation is part of a continuing study of the deposition of metallic materials on iron powder in a three phase fluidized bed. Previous work has included an investigation of the deposition of nickel onto iron powder^(1,2).

In this study an attempt has been made to deposit cobalt from chloride and sulphate solutions onto iron powder under various conditions. In the absence of an applied electric potential this process would involve the cementation reaction,



A similar reaction has been observed in the case of nickel deposition on iron powder⁽³⁾, but the electrode potential that is the driving force of such reactions is considerably smaller in the case of iron-cobalt than with the iron-nickel. However, the commercial interest would be greater in the former case on account of the greater difference in the values of equal quantities of cobalt and iron. The large specific surface area associated with powders is of the greatest importance in these reactions, since neither nickel nor cobalt can normally be deposited on iron by this means when the specific surface areas are similar to those found in large pieces of material.

The present investigation was carried out in three stages:

- 1) Cementation of cobalt on iron powder in a simple mechanically stirred cell.
- 2) Cementation of cobalt onto iron powder in a fluidized bed cell, using nitrogen as the fluidizing agent.
- 3) Electrolytic deposition of cobalt onto iron powder in the fluidized bed cell.

During the course of the investigation the effect of the following variables on the cementation reaction were studied.

- 1) PH of the solution.
- 2) Temperature of the solution.
- 3) Minor additions (boric acid and sodium sulphate).
- 4) Concentration of cobalt ions in the solution.
- 5) Concentration of iron powder in the cell.

2. REVIEW OF LITERATURE

2.1 Electrolytic Reactions

There are relatively few publications available concerned with cobalt cementation but the mechanism of it is not markedly different from the cementation of other metals: therefore principal electrochemical electrode reactions can be considered.

2.1.1 Electrode Potential

The change in free energy which accompanies a chemical reaction measures the driving force of that reaction and the extent to which it can proceed to completion. The Van't Hoff isochore equation relates the change in free energy for the reaction to the equilibrium constant at constant pressure⁽⁴⁾.

$$\Delta G^\circ = - RT \ln K_p \quad \dots\dots (2)$$

The equilibrium constant in equation (2) is defined as the ratio of the thermodynamic activities of the products to those of the reactants. For instance the reaction,



will proceed in a forward direction when K_p is positive, which makes ΔG° negative⁽⁴⁾.

The electrical potential which is necessary to drive such a reaction forward is related to the free energy by

$$\Delta G = -nEF \quad \dots\dots (4)$$

When a metal is immersed in a solution containing its

own ions a potential difference is established between the metal and the solution, and this is expressed by the Nernst equation

$$E = E_0 - \frac{RT}{nF} \ln (a_m/a_m^{n+}) \quad \dots\dots (5)$$

The potential depends on the ion activity, and the unit ion activity $E = E_0$. Thus the standard electrode potential of a metal is the electro motive force (e.m.f.) produced when a half-cell of the element, in a 1 molar solution of its ions is coupled to a molar hydrogen electrode.

At 25°C, and assuming that the metal electrode is in a standard thermodynamic state ($a_m = 1$),

$$E = E_0 + \frac{0.0591}{n} \log a_m^{n+} \quad \dots\dots (6)$$

Change of concentration will have a major effect on the electrode potential. Assuming that activity and concentration are equivalent, dilution of the solution shifts the electrode potential to more negative values⁽⁴⁾ (see table 1).

The standard electrode potential of a metal is an indication of its basicity or nobility. A metal with a high negative E_0 value must have a large positive ΔG° value for the ion reduction reaction; metals of this type (e.g. Na, K, Al) form very stable ions which in an aqueous solution can not be electrodeposited. In contrast metals with a positive E_0 value and therefore negative ΔG° values, (e.g. Cu, Ag) for unit ion reduced electrodeposit quite

readily. Table 2 lists some of the more important values relative to hydrogen, which has zero standard electrode potential.

This change in electrode potential depends upon the number of exchanged electrons and is illustrated in fig. 1 which shows that univalent ions have a larger effect than ions of higher valency.

2.1.2. Activity Coefficient

It is important to discriminate between concentration and activity when complexing agents are present in solution. The activity of a metal ion in solution is related to the concentration of the ion, by the activity coefficient.

$$a_{m^{n+}} = \gamma \cdot C_{m^{n+}} \quad \dots (7)$$

The value of the γ depends on the nature of the anions present. Most of the metals of importance in hydrometallurgy are bivalent, and the anions are usually also bivalent, sulphate being the most common one. However in this study monovalent anion (chloride) was used as well. The potential values of the reactions, given by equation 6, change relative to γ .

2.1.3 Faraday's Law

The two laws governing quantitatively the electrode reactions during electrolysis are:-

- a) The mass of an element liberated in electrolysis is proportional to the current and the time:

$$W = Zit \quad \dots (8)$$

b) For a given quantity of charge the mass of an element discharged is proportional to its electrochemical equivalent

$$W = \frac{i \cdot t \cdot A'}{n \cdot F} \quad \dots\dots (9)$$

During the electrolysis process all the ions in solution carry current and the contribution from an individual ion depends upon its concentration and mobility⁽⁴⁾. Under ideal conditions the mass of electrodeposited cobalt referring to the equation 9 is $W = 1.099 \text{ g/Ah}$.

2.1.4 The Electrode Double Layer

At any metal/electrolyte solution interface, a potential difference exists whose magnitude is a function of both the composition and the nature of the phases. The potential differences are produced by the electrical double layer. The structure of the double layer is responsible for many of the properties of a given system: the double layer itself arising from an excess of charges at the interface which may be ions, electrons or oriented dipoles.

In the case of an electrode dipping into an electrolyte, it is seen that the excess charge residing on the electrode surface must be exactly balanced by an equal charge of an opposite sign on the solution side. When only electrostatic interaction operates, ions from the solution phase may approach the electrode only so far as their inner solvation shells will allow. The ions are cushioned from the electrode surface by a layer of solvent

molecules (fig. 2). The line drawn through the centre of such ions at this distance of closest approach, marks a boundary known as the outer Helmholtz plane. The region within this plane constitutes the whole of the double layer or the Helmholtz layer. The size of the ions forming up at the outer Helmholtz plane are such, that there are insufficient of them in contact to neutralize the charge on the electrode. The remaining charges are held with increasing disorder as the distance from the electrode surface increases: this is due to a progressive reduction in electrostatic forces and a simultaneous increase in thermal motion. This less ordered arrangement of charges of a sign opposite to that on the electrode constitutes the diffuse part of the double layer. Thus all the charges which neutralize that on the electrode are held in a region between the outer Helmholtz plane and the bulk of the electrolyte solution. The variation of potential with distance from the electrode surface is shown in fig. 3. This is only the case for purely electrostatic interaction between the electrode and ions in a solution. Most anions are specifically adsorbed, thereby losing most, if not all of their inner hydration shell. This behaviour contrasts with that of most cations which retain their hydration molecules. Specifically adsorbed species can evidently approach much closer to the electrode surface (fig. 4). A line drawn through the centres of such species aligned at the electrode surface

defines a further boundary within the Helmholtz layer called the inner Helmholtz layer. The extent to which specific adsorption occurs is controlled by the nature of ions in solution, as well as the nature of the electrode material and the potential applied to it⁽⁵⁾.

Uncharged species, if they are less polar than the solvent or are attracted to the electrode by chemical forces, will accumulate at the interface. These species are called surfactants. If the adsorption occurs the charge distribution in the diffuse layer changes to maintain electroneutrality⁽⁵⁾.

2.1.5 The Diffuse Double Layer

The diffuse double layer is the space between the centre of the solvated ions (outer Helmholtz layer), and the plane where the electrical potential is zero. Fig. 5 illustrates the diffusion double layer in the absence of an applied potential. The diffusion double layer potential (Ψ_x) for $0 < x < x'$ becomes zero for $x = x'$,⁽⁶⁾. The electrode potential (E) and the diffusion double layer potential are independent and the diffusion double layer potential may be considered constant if the ionic strength is held constant and there is an excess of electrolyte. For the ions in the Helmholtz double layer the effective potential is $\phi = E - \Psi_0$. The diffuse double layer potential varies from $\Psi = \Psi_0$ at $x = 0$ to zero at $x \gg x'$. The relation between Ψ_x and the diffuse double

layer thickness is given by the equations, ⁽⁶⁾

$$\Psi_x = \frac{2RT}{nF} \ln \text{Coth}^{1/2} (X+a) \quad \dots (10a)$$

and
$$a = -\ln \tanh \left| \frac{\Psi_{nF}}{4RT} \right| \quad \dots (10b)$$

For metal deposition by cation transport to the metal surface the diffuse layer will exert a retarding influence if $Z \cdot \Psi_x$ is positive. Under steady state conditions the ion flow is the same for any value of X and will also be equal to the rate of surface reaction. For metal deposition the dissolution reaction may be neglected and the net rate of the surface reaction approximated by ⁽⁶⁾

$$I_e = -Z_s k_s C_0 \quad \dots (11)$$

The effect of the potential in the diffuse layer is to diminish the cation concentration at values of $X < X'$ below that expected for diffusion alone, as shown in fig. 5. As can be seen from the above equation decreasing the C_0 will decrease the net rate of reaction.

2.1.6 Polarization

When a metal electrode is partially immersed into a solution of metal ions an equilibrium between two opposite reactions is established,



and the electrode gives a potential depending on the conditions of the equilibrium. An increase in the forward reaction rate will give a more negative electrode

potential on the metal and more electrons will accumulate there.

The potential, when the system is in equilibrium, is called reversible potential. If the electrode is included in a circuit and connected to a source of potential which is slightly more positive than the reversible potential of the electrode, electrons will pass from the electrode into the circuit. Simultaneously the metal electrode dissolves to form the ions in the solution. In this situation the electrode is referred to as an anode. If the externally applied potential at the electrode is only very slightly more positive than the reversible electrode potential, the rate of electron flow from the electrode will be small and the electrode reaction easily replenishes the lost electrons. Under these conditions the electrode will maintain its reversible potential and operates reversibly as an anode⁽⁵⁾.

If the applied potential is much more positive than the reversible potential of the electrode, electrons will leave the electrode at a greater rate than in the reversible reaction. If the metal dissolution is hindered for any reason (e.g. surface oxide layers) the anode reaction will slow down and the anode overpotential will increase. In that case the electrode is said to be polarized and operates irreversibly.

The relationship between the potentials of reversible and irreversible reactions can be stated as:

$$E_A > E_{rev} \quad \dots\dots (13)$$

If the above situation is reversed, then cathodic polarization occurs, which can be written as,

$$E_C < E_{rev} \quad \dots\dots (14)$$

For an electrode to behave as a cathode it must have an applied potential which is more negative than its reversible potential, while anodic behaviour requires a potential which is more positive than its reversible potential.

The deviation of an electrode's potential from its reversible potential is called overvoltage and can be calculated from

$$\eta = E - E_{rev} \quad \dots\dots (15)$$

Some electrodes never show reversible potentials under normal conditions because the attainment rate of the electrode equilibrium is low. Under these circumstances even a small cathodic or anodic current requires a potential much greater than the equilibrium value to be applied⁽⁵⁾. For such cases a current-voltage curve will be the form shown in fig. 6. η_c and η_a gives the minimum value needed to obtain a net current for a cathodic or anodic reaction.

The next section considers three major types of over-

voltage, including their origin, control and the way they influence the progress of an electrochemical reaction.

2.1.7 Activation Overvoltage

In order for the electron transfer reaction to proceed the activation energy barrier must be overcome. This requires that the applied potential must exceed the equilibrium potential. This excess potential is called the activation overpotential. The slow rate-determining step in the process is the electron transfer due to the high activation energy barrier which the electrons must cross.

Activation overpotential usually obeys the Tafel law,

$$\eta_a = a + b \log i \quad \dots\dots (16a)$$

$$a = \frac{2.303 R}{n F} \log I_o \quad \dots\dots (16b)$$

$$b = \frac{2.303 RT}{n F} \quad \dots\dots (16c)$$

$$I_o = I_a = I_c \quad \dots\dots (16d)$$

The values of I_o , a and b are different for each electrode reaction. Exchange current density values of metals varies between 10^{-3} to 10^{-2} A/cm² for different metals.

Cathodic deposition in simple ion solutions proceeds with very little activation overpotential and the E/I curves are therefore relatively shallow. An important consequence of a high degree of polarization, is that the deposits produced from complexed ions are smoother, more amenable to brightening and gives better metal distribution or throwing power(5).

2.1.8 Resistance Overpotential

Resistance overpotential arises from the electrical current and resistance of the solution which surrounds the electrodes. The electrolyte resistance to the current flow produces an ohmic drop in potential between the anode and cathode. Another cause of the ohmic overpotential is the formation of an adherent layer of poor electrical conductivity on the electrode surface, e.g. surface oxide films.

2.1.9 Concentration Overpotential

When a metal dissolves very rapidly the water molecules in the double layer may not be sufficient to solvate all the dissolving ions. Therefore a limiting current density is reached for which $C_{H_2O} \rightarrow 0$; this limits the rate of anodic dissolution.

The reverse situation applies with the cathodic reaction; when cathodic deposition proceeds very quickly, dissolved metal ions may not diffuse sufficiently quickly from the bulk of the solution to the cathode surface. Therefore a limiting current density is reached but this time $C_{m^{n+}} \rightarrow 0$. In both cases a diffusion layer is built up in which either water or metal ions vary in concentration from zero on the electrode surface to bulk concentration on the solution side of the layer. For the above reasons a departure from the linear Tafel relationship occurs which is called concentration overpotential (fig.7).

The concentration overpotential can be expressed as, (5)

$$\eta_c = \frac{RT}{nF} \ln \frac{I_{lim}}{I_{lim} - I} = \frac{RT}{nF} \ln \frac{C_o}{C_{ms}} \dots\dots (17)$$

Finally the overvoltage of an electrode can be expressed as the sum of the three overvoltages,

$$\eta = \eta_a + \eta_c + \eta_r \dots\dots (18)$$

The total polarization for a cell includes the anode and cathode over-potentials.

$$\eta = (\eta_c + \eta_a)_{anode} + (\eta_c + \eta_a)_{cathode} + \eta_r \dots\dots (19)$$

There are some major differences between the above three overvoltages, viz:-

- a) Resistance overvoltage appears and disappears instantaneously when the polarizing circuit is made or broken.
- b) Activation overpotential increases rapidly and exponentially after a polarization current has started to flow and similarly decreases when the current flow is stopped. The exponential growth and decay of activation overpotential is a function of the activation energy of the electrode process. The magnitude of activation-overpotential is affected by the physical and chemical nature of the electrode material.
- c) Concentration overpotential grows and decays slowly after interruption to the current flow at a rate dependent

upon the diffusion coefficient of the ions involved. Concentration overvoltage is the only form of overvoltage which is affected by stirring and is unaffected by the nature of the electrode. Stirring decreases the diffusion layer thickness and concentration overvoltage.

Increasing the diffusion coefficient by raising the temperature also decreases the concentration overvoltage. The result of the reduced concentration overvoltage is a higher limiting current density during deposition. Therefore to obtain rapid electrodeposition it is necessary to select a highly soluble metal salt or compound, a high degree of solution agitation and as high a temperature as is practicable. Increase in temperature and agitation may reduce polarization at both electrodes but specific depolarization can also be important. For instance, a cathode may be polarized by slow diffusion of hydrogen ions or atoms following discharge, which lead to the formation of bubbles on the electrode surface. However if an oxidizing agent is available in solution an alternative cathode reaction will be available at the electrode surface, and depolarization takes place.

From an examination of a polarization curve (see fig. 7), it is possible to distinguish three separate zones⁽⁴⁾,

a) The first zone, associated with the lowest current density, where over potential is proportional to $\log i$.

This is the Tafel region of activation overpotential, where the rate-controlling process is an electron transfer between ion and metal electrode with the possibility of a catalytic effect.

b) The second zone, where overpotential is proportional to current. The rate controlling stage is probably the diffusion of ions through a surface layer of electrolyte.

c) This affects the solution of gas in the electrode since at this stage gas bubbles fail to reach the critical size for evolution and the gas generated diffuses into the electrode.

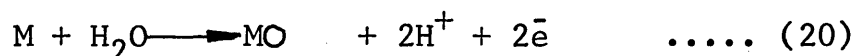
2.1.10 Passivation Phenomena

A metal may be called passive when the amount of metal consumed by a chemical reaction in a given time is significantly lower under conditions corresponding to a greater decrease in the free energy, than that obtained under conditions corresponding to a lower reduction in this parameter⁽⁷⁾. Passivation of a metal electrode also reduces the current passed from the electrode, (see fig.8).

A metal in solution exhibits chemical passivity when the partial anodic and cathodic currents become equal at a potential sufficiently greater than the reversible potential (see passive region of I-V curve in Fig. 8). The comparison of such a steady state potential with its dissolution potential in a specific medium is defined by Tomashov and Chernova as a degree of passivity⁽⁸⁾. The

same authors have given another approximate calculation of the degree of passivity, using as the relevant factor the ratio of anodic and cathodic polarization at a certain potential. This has produced the following series in decreasing order of passivity: Zr, Ti, Ta, Nb, Al, Cr, Be, Mo, Ni, Co, Fe, Mn, Zn, Cd, Sn, Pb, Cu.

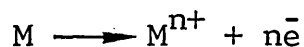
In the active point of the I-V curve (fig. 8) metal ions go into the solution as shown by equation 12. At still higher potentials the polarization curve deviates from a simple logarithmic relationship because the dissolution is hindered by another anodic process: that is the formation of a protective film through a reaction of the type⁽⁸⁾,



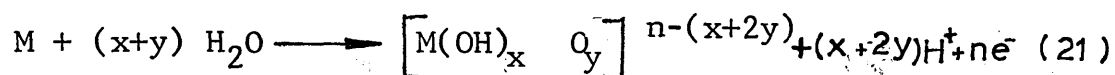
This deviation point from the logarithmic relationship is defined by some authors as Flade potential⁽⁹⁾. At the passivation potential, V_p , a limiting passivation current i_p , is reached and the rate of acceleration of metal dissolution becomes equal to the rate of retardation of the process. With a further increase in potential the rate of metal dissolution is increasingly hindered by the passivation process, which terminates at the fully passive potential. Thereafter the dissolution rate is independent of potential. The increase in current at some higher potential is determined by the overpotential of oxygen discharge. The region is called "transpassive".

2.1.11 Characteristics of Active and Passive States

An anodic dissolution process progresses as in equation 12.

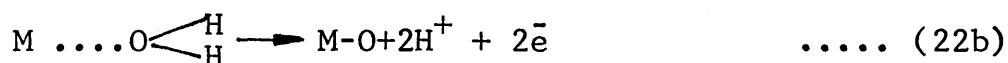
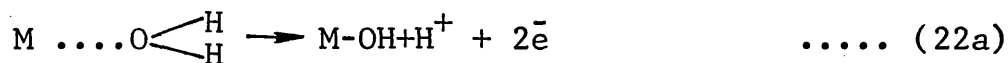


and a passivation process involves



In all cases dissolution of a metal ion requires more energy than the oxide formation; this is due to a large negative free energy of hydration.

Similarly water molecules in the Helmholtz double layer at a metal surface under anodic conditions tend to orientate with oxygen atoms towards the metal, presenting the possibility of the following reactions⁽¹⁰⁾,

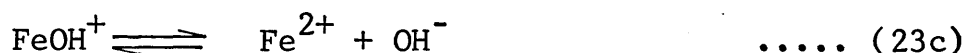


Again the formation of a surface monolayer of solid hydroxide or oxide needs a smaller energy due to the large negative free energy for cation association with the surrounding oxide ions.

The reactions 21 and 22 may prevent the anodic dissolution or the cathodic deposition; this depends on the potential, the composition of the solvent, the specimen geometry and microstructure and the properties of the

solid film. The surface oxide film separates the reacting substances, and further reaction is possible only if there is diffusion of the reacting species through the oxide layer. The diffusion of the ions depends on the properties of the oxide film such as; crystal structure, thermodynamic stability, adhesion to anode surface, thickness, conductivity, and transport processes to and from the boundary⁽⁷⁾.

Bockris et al⁽¹¹⁾ have suggested the following mechanism for iron dissolution



It has been reported that the critical OH^- concentration for passivation of mild steel with a given chloride level and PH in the range 5-11 reached higher values in solutions not containing sulphate⁽¹⁰⁾. Rice et al⁽¹²⁾ reported cobalt passivation at $\text{PH} > 6$ by the formation of a stable complex oxide. Ohatsku and Sato⁽¹³⁾ pointed out that cobalt passivates in alkaline solutions but this effect is minimal in acid solutions. Fig. 9 shows a polarization curve as well as cobalt dissolution versus potential and film charge potential relationships in borate buffer solution at PH of 8.4. In addition to the active dissolution region, the passive potential range may be divided into three regions. Passive 1,

passive 2, and passive 3. The transpassive region appears beyond the passive regions. These passive regions tie up with the stability regions for a divalent cobalt oxide CoO , for a spinal type oxide Co_3O_4 , and for a trivalent oxide Co_2O_3 respectively. Ohatsku and Sato⁽¹³⁾ also applied a cathodic reduction technique to measurements of the passive film formed in different potential regions. The film formed in the passive 1 potential region was cathodically reduced. Further, no cobaltous ions entered the solution from the film during cathodic reduction: possibly direct reduction of cobaltous oxide to metallic cobalt took place instead.

The film formed in the potential region, passive 2 and passive 3, dissolves during cathodic reduction, producing cobaltous (Co^{2+}) ions in the solution as shown in fig. 10, which gives the amount of dissolved cobaltous ions against the cathodic charge passed. The broken line indicates the theoretical reduction curve of Co_3O_4 to cobaltous ions. The film formed in the passive 2 region follows the broken line in its initial stage of reduction, which may be evidence that the outer layer of the film has a composition close to Co_3O_4 ⁽¹³⁾. The film in the passive 3 region shows an initial induction^{Period} where small quantities of cobaltous ions appear in the solution before it follows the same slope as that of the broken line. Ohatsku and Sato also concluded that the outer layer in the passive 3 region is composed of Co_2O_3 . The film previously formed

in the passive 2 region is not a single layer but two layers with different optical constants.

Reduction of the passive film which is formed in the passive 3 region, progresses in three stages, as shown in fig. 11. In the first stage the outer Co_2O_3 layer changes to Co_3O_4 with little reduction in the film thickness: subsequently the Co_3O_4 film is reduced to CoO and finally to Co^{++} (13). Fig. 12 shows the thickness of the film which is estimated by the ellipsometric technique as a function of potential. The thickness of the outer layer increased almost linearly with the potential⁽¹³⁾. The almost linear relationship between the thickness of this layer and the potential suggests that the outer layer acts as a barrier which gives rise to the greater part of the overpotential.

In aqueous solutions film formation may be effected by electrochemical reduction or oxidation, chemical dissolution, mechanical disruption, and specially by the presence of active anions (chlorides). These may either encourage the activation of the 'weak' sites in the film (mechanical flaws, inclusions) or introduce new ones. Depassivation was usually observed by a fairly rapid fall in potential to a value slightly more noble than that required for passivation (the Flade potential).

Finally the observed relationship between current and potential is a function of several processes including

film formation, film dissolution and metal dissolution. The latter was suggested by Ohatsku and Sato⁽¹³⁾ to be mostly responsible for the magnitude of the current at all potentials. In the active potential region dissolution was hindered by a decrease in the free electrode area, and in the passive region dissolution depended on the properties of the passive film.

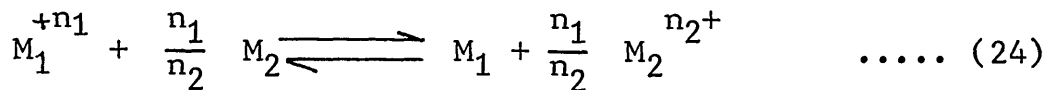
2.2 Non Electrolytic Reactions

2.2.1 The Cementation Reaction

Cementation is defined as electrochemical precipitation of a more noble metal from its ionic solutions onto the surface of a less noble metal.

The reduction of metals in solution by precipitation using metals which are more electropositive may be viewed in terms of electrode processes. Unfortunately the application of electrochemical parameters is limited, since the cells are essentially short circuited and anodic and cathodic processes can not be separated unambiguously by adjustment of the electrode potentials. The theory of slow discharge may be used in explaining cementation kinetics⁽⁶⁾. Generally, contact reduction systems are electrochemical processes and their kinetics are usually diffusion controlled. In some systems, particularly at low temperatures and high concentrations, mixed control as well as surface control have been observed.

In general contact reduction may be written as



As indicated in fig. 13 electrons will flow from the anode to the cathode. The electrode potential (E) will be less than the equilibrium potential of the cathode (E_c), and greater than the equilibrium potential of the anode. If we rewrite the Nernst equation for cathodic and anodic reactions in the reduction process it becomes;

$$E_c = E_c^o + \frac{RT}{n_1 F} \ln C_1 \quad \dots\dots (25a)$$

$$E_a = E_a^o + \frac{RT}{n_2 F} \ln C_2 \quad \dots\dots (25b)$$

assuming an activity coefficient of unity. The potential (E_k) for a short circuited system will usually be the same for both the cathode and the anode. This potential is referred to by Drozdov⁽¹⁴⁾ as the compromise potential and he pointed out that the potential need not always be the same at the cathode or the anode since there may be an internal or ohmic resistance between the growing cathodic deposit and the anode. Also by the use of slow discharge theory and the assumption of zero ohmic resistance all processes, before or after the slow step, may be considered to be in equilibrium. Hence the total free energy change for the process (ΔG) may be considered equal to the difference in chemical potential for the slow steps according to⁽⁶⁾

$$\Delta G = \mu_c - \mu_a \quad \dots\dots (26)$$

If the slow discharge is controlled by diffusion or reaction at the cathode surface the anode will be at equilibrium and the compromise potential will be equal to the equilibrium potential of the cathode: that is the overpotential at the anode will be near to zero.

Wadsworth⁽⁶⁾ described the cementation reaction rate as;

$$\frac{I}{n_1 F} = -C_1 k_o \left(1 - \frac{C_2^{n_1/n_2}}{C_1} \exp \left[- \frac{z_1(E_c - E_a)F}{R.T.} \right] \right) \quad \dots\dots (27)$$

and he proposed that the $C_2^{n_1/n_2}/C_1$ ratio in a cementation reaction would not exceed 10^3 . The maximum observed value of this ratio, in fluidized bed cells is in the case of Co^{2+}/Fe cementation, 39.57. Wadsworth⁽⁶⁾ also suggested that the reverse reaction kinetics, would not be important when

$$C_2^{n_1/n_2}/C_1 * \exp (-n_1(E_c - E_a)F/RT) < 10^{-2}.$$

The maximum value of this term in Co^{2+}/Fe cementation is 5.4143×10^{-15} . Therefore the reverse reaction kinetics of cobalt cementation onto iron are not important.

Wadsworth⁽⁶⁾ also stated that reversible reaction kinetics would not be detectable if $n_1(E_c - E_a) > 0.3$ volt. The $n_1(E_c - E_a)$ value at $25^\circ C$ for the $Co-Fe$ cementation system is 0.326V. Therefore reverse reaction rates should be un-

detectable in the case of cobalt deposition onto iron powder. If a cathode surface reaction is rate controlling the cementation kinetics would be a function of effective potential which is dependent upon anodic potential. If the anodic overvoltage is near zero, the effective potential is approximately equal to $E_a - \Psi_o$. Under the above conditions, slow discharge at the cathode would be influenced by anolyte concentration since it affects anode potential, the potential of the outer Helmholtz plane, and the reaction rate constant⁽⁶⁾. When the kinetics are diffusion controlled, they would be independent of anolyte concentration. Under non-equilibrium conditions the kinetics of the electrode reaction may be influenced by certain processes that occur in the solution in the immediate vicinity of the electrode. These include the formation of a boundary diffusion layer, the precipitation of cathodic material or the precipitation of certain salts when the PH is high.

The current density developed in the electrode reactions are normalized values related to the measured projected geometric area (S). Under steady state conditions

$$I_c \cdot S = -I_a \cdot S \quad \dots (28)$$

The actual cathodic and anodic current densities differ from I_c and I_a because the actual anodic and cathodic areas change, due to the cementation. Therefore

equation 28 may change as⁽⁶⁾,

$$I_c^0 \cdot S_c = -I_a^0 S_A \quad \dots\dots (29)$$

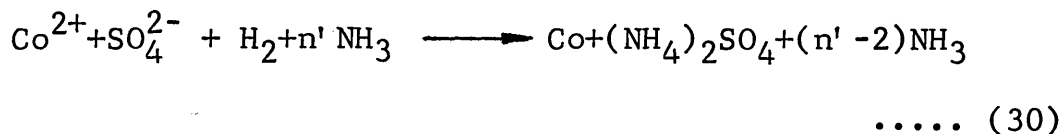
The character of the deposit varies with the rate of deposition. Drazdov⁽¹⁴⁾ has noted that rapid deposition of copper on nickel and copper, and silver on zinc produced dense but porous layers made up of very fine needles that offered little resistance to additional reaction. Slowly deposited films or deposits in the presence of certain additions produced dense films which retarded the reaction rate. During the course of the cementation reaction the rate per unit area may increase due to an increased proportion of cathodic area. The true area of the anodic surface is not important if the process is controlled by reactions at the cathode, and the anodic sites are freely exposed to the electrolyte. These anodic areas may be highly localized because of lattice defects and impurities.

2.2.2 Hydrogen Reduction

Recovery of metals from their solution can be achieved either by electrolysis or by chemical reduction. Some workers have used hydrogen as a cheap reducing agent for the production of nickel, cobalt, copper⁽¹⁵⁾, and silver⁽¹⁶⁾. The product is usually metal powder, and the physical characteristics of the powder may be controlled by control of the process variables.

Metal reduction by hydrogen can also be used to

produce coatings of some metals on solids suspended in the solution. The commercial method for the precipitation of cobalt metal powder is similar to that used to obtain nickel from ammoniacal ammonium sulphate solutions. The relevant reaction is⁽¹⁵⁾;



The suggested values of n' in equation 30 lay between 2 and 2.3 and the reaction was carried out at 174-204°C with a hydrogen pressure of 14-25 atmospheres. In the production of cobalt powder the essential deposition surface was provided by cobalt seed powder.

For the production of composite powders, the usual cobalt seed powder was replaced by the desired core powder and the cobalt bearing solution was then subjected to a hydrogen reduction process, with the cobalt precipitated onto the surface of the core powder⁽¹⁵⁾.

When the core powder offered a surface that was weakly catalytic, the first few particles of cobalt acted as preferred sites for the subsequent deposit instead of the bare, almost inert, core powder surface. Although all of the reduced cobalt was deposited onto the core surface, not all of the core surface was covered with cobalt⁽¹⁵⁾. To activate the seed metal powder surface antraquinone was used by "Sherrit Gordon Mines Limited".

Kaneki and Wadsworth⁽¹⁷⁾ discussed the hydrogen reduction of cobaltous sulphate solutions using colloidal graphite as a nucleation catalyst. Kaneki and Wadsworth found that the maximum reduction rate occurred when the molar ratio of NH_3 to cobalt was 2 and therefore deduced that the cobaltous diamine sulphate complex was the most readily reducible.

In the Sherritt Gordon process the nuclei for the first batch reductions were produced by adding 2.8 g/l sodium cyanide and 0.2 g/l sodium sulphite to a cobalt solution containing 35 g/l cobalt⁽¹⁸⁾. Growth of cobalt particles came from a few active sites on the surface but the final shape of the particles was strongly affected by the tendency of these particles to agglomerate and become welded together during the deposition of more metal⁽¹⁵⁾. Shaufleberger has precipitated Cu, Ni, Co, elemental powders by reducing with hydrogen of 200°C and 35kg/cm² pressure in ammoniacal solutions⁽¹⁹⁾. In the case of aqueous amine ammonium solutions at a pressure of 15kg/cm² hydrogen and a temperature of 150°C were found to be the minimum required for satisfactory cobalt reduction rates⁽²⁰⁾. A variety of reagents containing sulphur in their molecular structure and which are capable of forming CoSO_4 with cobalt in the solution can be used as the catalyst for the reduction process⁽²⁰⁾.

2.2.3 Electroless Deposition

The formation of silver or copper films on glass by the reaction between metal salts and organic reducing agents has been used for many years. Such reduction of one metal onto a substrate by a reducing agent is referred to as electroless deposition. More recently nickel, copper and some other metals have been deposited onto ceramics and plastics. The deposits were used as protective coatings, and in various applications in the electronics industry, including printed circuits.

Usually a strong bond does not exist between the electrolessly deposited layer and the substrate. Thus adhesion of the metal is usually poor unless there is a mechanical interlocking of the deposited particles. This is achieved by roughening the surface of the substrate by use of sand blasting or etching⁽²¹⁾. It is essential to remove surface barriers, such as grease and air envelopes. Methods of pretreatment, sensitizing metal deposition, and testing for adhesive strength in the case of plastic substrate have been discussed by Narcus⁽²¹⁾.

All non conductors (ceramics, plastics) can be electrolessly plated but only a few give good adhesion and appearance. A highly active unstabilized electroless bath can coat any object it contacts including its container. This process is called encapsulating because there is little or no adhesion between the metal deposit and the substrate. Highly active baths are used rarely

in nonconductor plating.

The stable baths do not plate spontaneously on any nonconductor, so the surface must first be coated with an active catalyst to initiate the electroless deposition. The most common method available involves the deposition of palladium; here the solid to be treated, is immersed for one minute in a solution of stannous chloride containing sufficient hydrochloric acid to prevent precipitation. A wetting agent is also usually added. The solid is then immersed in a solution of PdCl_2 at 50°C . The solid is then transferred to the bath in which electroless deposition of the metal coating is to be carried out⁽²²⁾.

An electroless plating bath is basically a solution of a salt of the metal to be plated, and a reducing agent. The reducing agent may be present initially at a relatively high concentration or it may be added continuously while plating proceeds and so maintains the concentration at a lower value. To obtain optimum electroless deposition the PH and the temperature of the solution must be carefully controlled. If a simple electroless deposition bath is used either a metal salt of the reducing acid, or a metal hydroxide formed by oxidation of the reducing acid would precipitate. The use of suitable complexing agents prevent the formation of hydroxides, insoluble salts and stabilize the metal

reduction. Often the complexing agent is used as a buffering agent, which stabilizes the PH of the solution as metal deposition proceeds⁽¹⁸⁾. The stabilizers are sometimes used to prevent sudden decomposition of plating baths. These stabilizers are usually organic compounds, and they adhere onto solid surfaces and precipitate metal ions present in solutions. Other substances that behave as stabilisers are heavy metal cations, which form insoluble sulphides under the conditions of the bath.

Hypophosphite is a very strongly reducing ion, and has been used to plate Co, Cu, Fe, Ag, and Au. Other commonly used reducing agents include hydrazine⁽²³⁾ (for cobalt, nickel, gold and palladium), and alkylamine⁽²⁴⁾, or metal borohydrides⁽²⁵⁾ (for cobalt and nickel).

In the first cobalt electroless deposition process sodium hypophosphite was used as a reducing agent. About twenty years ago it was thought that the electroless deposition of cobalt from acid solutions was impractical so that a mixture of cobalt-chloride, sodium hypophosphite, sodium citrate and ammonium chloride was the only solution available. The presence of Cd^{2+} , Zn^{2+} , Mg^{2+} , Fe^{2+} and PO_3^{3-} decreased the deposition rate, while in the presence of CN^- and SCN^- there was no deposition. Divalent copper and aluminium did not affect the reaction⁽²⁶⁾. More recently Zeilmaker⁽²⁷⁾ has reported the use of hydrazine for cobalt electroless deposition. One patent suggests a solution that contains a sulphur-containing compound such as thiourea, thio-acetamide, carbon disulphate, phenyl thiourea, thiobarbituric acid, thiosulphates, in addition

to sodium pyrophosphate⁽²³⁾. Pearlstain and Werghtman⁽²⁸⁾ have reported the use of a cobalt-boron alloy electrolessly deposited in a cobalt sulphate (25g/l $\text{CoSO}_4 \cdot 7\text{H}_2\text{O}$) solution at a temperature of 70°C and a pH of 5.

Sadakov and Suvalova⁽²⁹⁾ have studied the electroless cobalt deposition by hypophosphite in ammoniacal solutions. With increased hypophosphite concentration, and PH the rate of cobalt deposition increased and the potential became more negative. The rate of hypophosphite oxidation was equal to the rate of cobalt reduction. With increasing cobalt chloride concentration the electroless deposition rate of cobalt rose sharply and after an optimum concentration had been reached, the deposition rate decreased⁽²⁹⁾. Rao et al⁽³⁰⁾ studied electroless cobalt plating onto tungsten carbide and iron powders using sodium hypophosphite and observed that the cobalt content of the powder was increased during the first 90 minutes, after which little more cobalt reduction occurred. Furthermore Sullivan⁽²⁴⁾ and Mc.Leod⁽²⁵⁾ have patented two cobalt electroless plating solutions in basic and acidic conditions. Finally Pew⁽³¹⁾ studied the electroless deposition of Co-P alloys onto activated surfaces of nonconductors.

2.3 Cobalt Extraction in Aqueous Media

In addition to the previously described reduction processes, cobalt can be extracted from its aqueous scrap or ore solutions by using various selective extractants.

Carboxylic acid isomers are the most commonly used cobalt selective extractors although both sulphur dioxide and hydrogen sulphide have also been used as a cobalt reducer.

Ivanov et al⁽³²⁾ proposed the use of trialkylebenzyl-ammonium chloride in polyalkile benzene diluter for the solvent extraction removal of Co, Fe, Cu, Zn, Cd, As in the case of nickel electrolytes. Use of trioctylephosphine oxide has also led to selective solvent extraction of cobalt from sulphuric nickel leach solutions⁽³³⁾.

Ashbrook⁽³⁴⁾ extracted cobalt from its ammonium sulphate solutions (PH = 6-7.5) by using Versatic 911* as the extraction reagent. Another worker used Versatic 10* to extract cobalt from its dilute solutions⁽³⁵⁾.

The presence of SO_4^{2-} and Cl^- ions reduces the extent to which cobalt may be extracted by Versatic 911 and di-2-ethyl hexyl phosphoric acid (D2EHPA) because SO_4^{2-} and Cl^- form complex ions with divalent cobalt. The effect of the Cl^- ion is smaller than that of the sulphate ion, and the distribution coefficient of cobalt slightly decreases with increasing Cl^- ion concentration⁽³⁶⁾.

Zhelibo et al⁽³⁷⁾ studied the effect of electrolysis conditions on the properties of fine cobalt particles, and have showed that when the electrolyte concentration was reduced, and the rate of flow of the organic additive

* :Versatic 911 and 10 : Code names for Shell company
produced carboxylic acid isomer.

and the pressure of the nitrogen atmosphere, were increased the cobalt particle size was reduced. It has been shown that during the production of cobalt powder from cobalt chloride solutions with certain organic additions, an increase in PH from 1.75 to 6 reduced the particle size of the powder from 1.5-2 μm to 0.5-1 μm ⁽³⁸⁾.

Recently S. Harada⁽³⁹⁾ studied the extraction of ultrafine cobalt and cobalt alloy particles (60-700 \AA) by using protein in the presence of a magnetic field. Edwards and Lowering⁽⁴⁰⁾ also reported successful application of organic amines on electroless cobalt extractions.

Victorovich et al⁽⁴¹⁾ have used H_2S as a competitor to the hydrogen reduction process, in order to precipitate cobalt and nickel from various sulphate solutions: they found that the precipitation of cobalt started only after an incubation period. Filmer et al⁽⁴²⁾ have selectively extracted cobalt from cobalt containing copper sulphate solutions by injecting sulphur dioxide at 80-90 $^\circ\text{C}$ in a solution with a PH of 3.

2.3.1 Cobalt Plating Solutions

The electroless deposition process involves the production of metals from solutions of their salts by means of ionic exchange, and the electrodeposition process involves the production of metals from solutions of their salts by means of an electric current. The salts may be fused or aqueous but commercial processes generally employ

aqueous solutions, since these offer the advantage of easy handling, good durability and stability, together with economic competitiveness. A major requirement is that the deposited metal is available in a sufficient concentration in the solution to give the required thickness under favourable economic conditions. The deposit is desired to be as uniform as possible, with satisfactory adhesion to the substrate: it must also be as ductile as possible.

Cobalt and its alloys can be deposited from a large number of aqueous solutions, both acidic and alkaline⁽⁴³⁾. Most cobalt and cobalt alloy electrodeposition is carried out using aqueous acid solutions, such as sulphate, chloride, sulphamate, fluoborate and sulphate-chlorate. Typical compositions and operating ^{conditions} for a number of baths are given in table 3 and 4.

Cobalt sulphate and cobalt chloride baths are major concerns of this study, although other cobalt solutions are industrially applied, usually for cobalt-alloy electrodeposition. These plating solutions will be studied with detail in the following paragraphs.

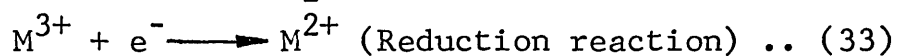
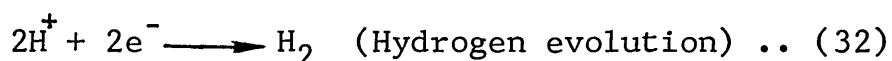
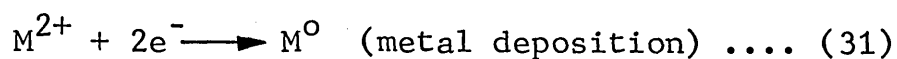
2.3.2 Cobalt Sulphate Plating Solutions

This bath is popular for cobalt deposition because it is cheap and easy to operate and control, and also can be used at relatively low temperatures. The simplest commercial bath consists of cobalt sulphate, with a boric acid buffer which prevents an excessively high value of

PH: it also hinders the formation of basic hydroxides. Current densities used in the baths are generally below $5A/dm^2$, in order to avoid the production of rough dark deposits.

In most cases a soluble pure cobalt anode is used, such anodes are usually bagged to collect any insoluble sludge forming and to prevent this from interfering with the plating process that occurs at the cathode. Bath contamination may still be a problem, and continuous filtration of the electrolyte is often used in commercial processes. Lakshiminarayanan et al⁽⁴⁴⁾ reported a process which incorporated an insoluble platinum anode into a cobalt sulphate plating solution. The addition of a sufficient amount of electrochemically active substance, such as vanadium pentoxide, to the bath suppressed the formation of Co^{3+} ions and cobalt trioxide (Co_2O_3) at the anode, thereby improved the efficiency of the operation.

The anodic current efficiency of these baths, depends on the other plating variables (PH, metal ion concentration, current density etc)^(45,46). Often a reduction in the PH of the solution, results in an increase in efficiency but unfortunately this leads to other problems by increasing the hydrogen uptake in the deposits. The cathodic reactions are:



Encapsulation of hydrogen into the deposit has detrimental effects because it causes pitting and raises the level of internal stress: it has shown that the amount of hydrogen present in deposit increases as the PH decreases⁽⁴⁷⁾. This problem may be lessened by the incorporation of a wetting agent into the bath which facilitates the formation and release of hydrogen gas bubbles from the cathode surface, so reducing the amount which can be included in the coating.

Cobalt is usually plated with an alloying element deposited from a complex bath containing sulphate ions, although Armyanow⁽⁵⁰⁾ electrodeposited cobalt from a sulphate solution.

The early work on the deposition of various cobalt alloys from sulphate baths has been reviewed by Morral^(48, 49). More recent publications have reported the deposition of Co-Cr⁽⁵¹⁾, Co-Ni-Fe^(52,53), Co-V^(54,53), Co-Mo^(45,55), Co-W^(55,56), Co-B-C-N⁽²⁸⁾, Co-Ni^(57,46), Fe-Co-Cd⁽⁵⁸⁾, Co-Re⁽⁵⁹⁾, Co-P^(60,31), Fe-Co^(3,61), and several other ternary alloys from sulphate baths⁽⁶²⁾.

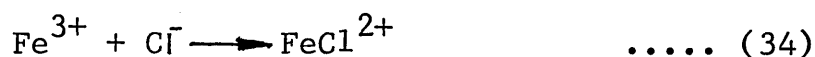
There is always a relationship between the amount of cobalt present in the alloy deposit and the cobalt sulphate concentration in the solution, although certain other factors also affect the alloy composition on cobalt alloy electroplating operations. Thus Yamamoto⁽⁴⁶⁾ et al concluded that cobalt content of Co-Ni electrodeposits was

reduced as the current density was increased. However, in the Fe-Co-Cd electroplating process greater amounts of iron deposition were observed at higher current densities, iron sulphate concentration, and PH⁽⁵⁸⁾.

2.3.3 Cobalt Chloride Plating Solutions

Pure chloride solutions are not usually employed for cobalt deposition, although most of the cobalt alloy plating solutions include $\text{CoCl}_2 \cdot 6\text{H}_2\text{O}$ as a major cobalt constituent. The use of chloride ions in the electro-deposition of cobalt is less common than is the case with nickel deposition.

The chloride ion has a particular influence on the kinetics of iron powder surface: Heusler and Fischer⁽⁶³⁾ studied the kinetics of pit initiation and the effect of chloride on the electrochemical process of passive iron in buffered neutral solutions, and showed that chloride "islands" occur on the passive iron oxide surface. Then;



if the oxide was completely removed locally during the lifetime of an island pitting occurs. Otherwise a steady state condition was established which was characterised by a large corrosion rate. Surface concentration of the pits formed simultaneously during the onset of pitting were between $1 \cdot 10^4 \text{ cm}^{-2}$ and the diameters were 10^{-3} to 10^{-6} cm.

Anode efficiency in the cobalt chloride solutions is

important as it is in the other electroplating solutions. Sard et al⁽⁴⁷⁾ proposed that low anode efficiency in cobalt electroplating is associated with low chloride ion concentration because chloride ions prevent the formation of other inhibitive reaction products which at high temperature (around 60°C) diffuse rapidly to the cathode and inhibit the cobalt deposition. Furthermore Sard et al claimed that chloride ions in cobalt electroplating solutions prevent hydrogen from acting as an inhibitor.

Sadakov⁽²⁹⁾ studied the connection between steady state potential and the rate of deposition and concentration of compounds, in the solution in the electroless deposition of cobalt from an ammoniacal chloride solution. His conclusion was that with increase in $\text{CoCl}_2 \cdot 6\text{H}_2\text{O}$ concentration the deposition rate increased sharply and then decreased. The higher the PH, the higher the cobalt deposition and the potential became more negative.

2.3.4 Other Cobalt Plating Solutions

In addition to the solutions discussed above some other solutions have been employed for commercial cobalt alloy plating. A cobalt citrate solution was used to electrodeposit Co-Au alloys for the electronics industry⁽⁶⁴⁾ and Sadama and Yajimo⁽⁶⁵⁾ have used cobalt citrate solutions for Co-Bi alloy deposition. A cobalt acetate solution was used to electrodeposit Co-Ni-Mo alloys at $2\text{A}/\text{dm}^2$ current density and PH of 5⁽⁶⁶⁾. In this

solution the cobalt content of the electroformed alloy was reduced as the current density, PH, and temperature increased. Wearmouth and Belt⁽⁶⁷⁾ used cobalt sulphamate baths to electrodeposit Co-Ni alloy for zinc die casting applications.

2.4 The Properties of Cobalt Coatings

The electroless or electroplating of cobalt is used industrially because of the superiority of certain of the properties of these deposits. These are closely related to the plating conditions. Therefore the maintenance of these conditions during the plating operation is necessary in order to obtain the required specifications. The effect of these variables on the properties of the coating are discussed below.

2.4.1 Corrosion Resistant Properties

Cobalt is sometimes plated onto metallic substrates because of its corrosion resistance which is often superior to that of nickel. Jackson and Wilkinson⁽⁶⁸⁾ have investigated the corrosion rate of cobalt in 8.4 mol/l hydrochloric acid with and without the presence of thiourea, phenyl thiourea, and tolyl thiourea, over the temperature range 20-80°C. It was observed that a distinct diminution in the corrosion rates occurred at higher concentrations of the active reagent, and they proposed that the difference in behaviour was one of degree rather than one involving a completely different mechanism.

Rice et al⁽¹²⁾ examined the corrosion of cobalt and indicated that cobalt passivation occurred by the formation of stable complex corrosion product scales. The rapid, initial surface reaction on cobalt involved the formation of hydroxides, although subsequently an oxide was formed by either hydroxide dissociation or interaction with oxygen. They also suggested that cobalt surfaces exposed to humid air, initially formed complex oxyhydroxides. These surfaces adsorbed significant quantities of water at selected points. Relative humidity had a profound influence on cobalt corrosion and followed an exponential dependence on the relative humidity,

$$r = A.e^{bRh}. \quad \dots (35)$$

The partial pressure of SO₂, Cl₂, and NH₃ significantly influenced cobalt corrosion while H₂S, NO₂, O₃ showed little effect⁽¹²⁾.

Cobalt has sometimes been electrodeposited as an alloy to obtain good corrosion resistance in acidic media, and has sometimes replaced nickel. Schuler et al⁽⁶⁹⁾ stated that Co-Cr alloys (2.5-6.8%Co) electrodeposited in CoCl₂ + Cr₂O₃ solutions at room temperature possessed good resistance to corrosion in dilute mineral acids. Carter⁽⁷⁰⁾ has observed that severe microcracking occurred in normal chromium topcoats when cobalt, which had been electrodeposited from chloride solution, replaced nickel in the under-coat, but the use of microdiscontinuous chromium on top of cobalt bearing deposits led to an increase in the

period of protection of the substrate to a level similar to that obtained with a nickel under-coat.

McLeod⁽²⁵⁾ claimed good corrosion resistance from an electrolessly deposited Co-Bi alloy which had been deposited at a PH of 5 and a temperature of 70-75°C.

2.4.2 Mechanical Properties

For protective reasons high hardness in the cobalt plating is desired but for powder metallurgy applications soft deposit is usually more suitable. Since hard cobalt a platings are usually required most of the recent work covers the hardness of the cobalt alloys. Greco⁽⁵⁹⁾ obtained 1200KHN from Co-Re alloys which is the maximum reported value for these materials, while Yamamoto et al⁽⁴⁶⁾ have observed that as the cobalt content, in Co-Ni alloy electrodeposits, increased up to 30% cobalt the hardness of the alloy likewise increased. Also a low plating temperature usually gives a higher hardness in the coating. Takei⁽⁷¹⁾ reported that a reduction in the rate of the electrodeposition of metals in the vertical direction corresponded to a decrease in the grain size and an increase in the hardness of the deposit. High hardnesses in electrodeposited cobalt usually depended on a small grain size, high internal stress, and the presence of exluded hydrogen, codeposited metallic oxides, hydroxides, addition agents and impurities⁽⁷²⁾. Read and Lindsay⁽⁷³⁾ have observed that the strength and ductility of the electroplated cobalt decreased as the PH of the

solution increased.

The coefficient of friction of cobalt deposits has an influence on the compressibility of cobalt plated powders. Buckley⁽⁷⁴⁾ has observed the lowest coefficients of friction and adhesion (0.36 and 0.05) in the case of sliding on cobalt surfaces with both movements on the (0001) plane.

Browning and Turns⁽⁵⁶⁾ have studied the mechanical properties of Co-30%W electrodeposits and have obtained 116500 p.s.i. ultimate tensile strength. Wearmouth and Belt⁽⁶⁷⁾ have observed freedom from high temperature embrittlement in the case of Co-Ni electroplated alloys for zinc die casting.

2.4.3 Effect of Certain Additions in the Solution on the Properties of Cobalt Coatings

Complexing agents are usually used in electroplating and electroless plating operations to improve certain characteristics of the processes. Boric acid is commonly used as a buffer for commercial plating solutions. Sirivastava and Nigam⁽⁷⁵⁾ have studied the effects of dextrine, gum-arabic and gelatine on the electrodeposition of Co-Ni alloys in acidic sulphate solutions. The additions of dextrine slightly increased the percentage of nickel in the alloy and shifted the cathode potential to more negative values. The addition of arabic gum produced more finely grained deposits than those obtained

under the same conditions but without this addition. The addition of gelatine to the bath hindered deposition while dextrine increased the throwing number. Subrahmanyam and Rama Cahar⁽⁷⁶⁾ have obtained good results from potassium pyrophosphite and ammonium citrate in the case of Co-Fe-Ni alloy plating at a PH of 8-9. Other additions were also used in order to improve certain properties: e.g. glycerine as a buffer, saccharin to improve the uniformity of the deposits, and ascorbic acid to minimize oxidation. Kukos and Terentieva⁽⁵³⁾ studied the effects of several bath additions on the quality of Kovar type (Fe-Co-Ni) coatings and concluded that the best results were obtained with amino-acetic acids as the addition agents. In another study Still and Dennis⁽⁵⁵⁾ used sodium-heptonate as a complexing agent to electrodeposit Co-Mo and Co-W alloys. It was concluded that optimum deposits were obtained from the bath composition given in table 4. Pearlstarn and Weightman⁽²⁸⁾ have used sodium sulphate, sodium succinate and dimethyl amine boron as complexing agents to codeposit electrolessly Co-B-C-N.

Sometimes impurity metal ions are eliminated by the addition of another metal, e.g. the use of a tellurium addition in a cadmium solution at PH of 5 in order to precipitate cobalt⁽⁷⁷⁾.

2.5 Metallic Powder Coating in a Fluidized Bed

The coating of metal and composite powders such as iron and tungsten carbide with nickel, cobalt and copper by

the hydrogen reduction method is rather expensive, because of the cost of the equipment and the difficulty of sealing at high temperature (175°C) and pressure (15 Atm). Therefore the application of the fluidized bed for powder coating may be a cheaper alternative to conventional hydrogen pressure vessels, such as those described by Meddings⁽¹⁵⁾.

2.5.1 Mechanism of the Fluidized Bed Cell Operation

To produce an even coating in a fluidized bed solution the powder particles have to be kept in suspension (65,78). The diffusion layer thickness of the particles in suspension in a fluidized bed solution will be lower than those in a plating solution which is agitated by an external agitator.

However in a solution circulated fluidized bed, solution flow has great advantages over conventional plating cells in metal extraction and powder coating operations (see Sabacky and Evans⁽⁷⁹⁾). These workers suggested a correlation between these advantages and the electronic properties of the bed; they also suggested three possible mechanisms for charge transport within the bed cell. These are:

1. Electrolyte phase conduction; simple ionic conduction within the electrolyte caused by movement of the ions under the influence of the electric field. Ionic conduction is also coupled with short circuiting of the

conduction paths through the particles, as shown in fig. 14-A.

2. Particulate phase conduction;

a) Simple electronic conduction, through particles which are in contact, this conduction path proceeding as far as the current feeder. This mechanism is illustrated in fig. 14-b and called by Sabacky the charge conductive mechanism.

b) The convective mechanism as presented by Fleischman and Oldfield⁽⁸⁰⁾. Here it is visualized that the electrical double layer of a particle becomes charged by contact with the current feeder or a particle of different charge, moves to a different part of the bed cell and then discharged, either by charge sharing with another particle or by electrochemical reaction; this possibility is illustrated in fig. 14-c.

In conventional electrowinning processes the electrode is a good conductor of electricity. Therefore voltage drops and power losses in the electrodes are low, in an electrowinning cell. It was observed by Evans and Sabacky⁽⁷⁸⁾ that the fluidized bed electrode itself presented a significant electrical resistance, power loss and voltage drop. They also pointed out that the electrode resistivity in the fluidized bed depended on the bed expansion (voidage) and was relatively independent of particle size, electrolyte conductivity, and frequency of the applied current. Furthermore they have reported higher

reaction rates at the current feeder and cell divider than the middle of the bed cell, caused by extreme values of the ratio of electrode conductivity to electrolyte conductivity.

Goodridge and Vance⁽⁸¹⁾ have observed a similar mechanism and have shown that the most active regions of the rectangular-shaped solution-circulated, fluidized beds were near the current feeder and the diaphragm while the middle of the fluidized bed possessed the minimum potential. Increased bed expansion resulted in an intensification of the active zone near the current feeder. Current efficiencies obtained during the deposition of copper on the fluidized cathode were increased when the current density increased because there was no cathodic protection of the bed below a critical current density⁽⁸²⁾.

Even if the anodic and cathodic regions in a fluidized bed are not separated, cathodic and anodic regions usually exist in the bed. Furthermore Hutin and Couret⁽⁸⁴⁾ showed the presence of a dissolution zone within the electrodes of a fluidized bed in which current and electrolyte flowed in the same direction. Backhurst⁽⁸³⁾ et al concluded that their fluidized bed was much more active in the proximity of the current feeder than at points removed from it. Hutin and Coeuret⁽⁸⁴⁾ observed that with fluid flow parallel to the current flow in a fluidized bed there was an anodic region which was approximately 80% of the bed depth and this anodic region was increased with

increased bed porosity.

2.5.2 Current Efficiency and Limiting Current Density

Fluidized bed electrodes usually give higher current efficiencies and higher limiting current densities than in conventional electroplating electrodes.⁽⁸⁵⁾ The reason for these higher values is probably associated with a smaller diffuse double layer thickness in the fluidized beds. Tangappan et al⁽⁸⁵⁾ in a review have also reported higher current efficiencies in the fluidized beds than the other electroplating cells.

Various factors affect the diffusion layer thickness in a fluidized bed cell such as the nature of the agitation, the fluidized powder size, and the porosity in the bed. Fleischmann et al⁽⁸⁶⁾ reported diffusion controlled deposition throughout fluidized bed electrodes. Garbin and Gabe⁽⁸⁷⁾ studied the effects of fluidized bed porosity and particle size on the electrodeposition of copper onto glass blatoni beads from copper sulphate solutions in an electrolyte circulated fluidized bed electrode. These workers concluded that the limiting current density increased with increased particle size. The larger particles were always more effective at reducing the diffusion layer thickness. Tangappan et al⁽⁸⁸⁾ used a higher limiting current density (65-80 A/dm²) in a fluidized bed electrode with a more uniform current distribution than was used with conventional baths. Backhurst

et al⁽⁸³⁾ have investigated the fluidized bed electrodes by using electrically conducting particles. They pointed out that the maximum operation performance of their fluidized bed electrodes was achieved with a voidage in the vicinity of 0.50-0.58 (5-25% expansion) and the total current supported by the bed scaled up linearly with the height except over an initial region, corresponding to a very low bed height where the relationship was non-linear. Furthermore Hutin and Coeuret⁽⁸⁴⁾ observed a higher current efficiency in a fluidized bed with a soluble anode than with an insoluble anode besides which the higher current densities gave the higher current efficiencies. Wilkinson and Haines⁽⁸⁹⁾ obtained high current efficiencies on copper extraction from copper sulphate solutions in a fluidized bed.

Ultrasonic vibration has also been applied by Alkateev⁽⁹⁰⁾. Interruption of the ultrasound could, under certain conditions, produce increased rates of cementation and reduced energy consumption relative to the values of these parameters obtained with constant vibration⁽⁹¹⁾.

2.5.3 Gas Fluidization

Fluidization of the electrode powder in the fluidized bed cells by an inert gas is not often reported although a few previous studies have been published.

Hutin and Coeuret⁽⁸⁴⁾ have obtained a 7% higher current efficiency by using nitrogen gas for fluidization,

instead of fluidizing by solution circulation. Doig and Alferdson⁽⁹²⁾ have studied bed expansion behaviour of pulsed fluidized bed and have observed that some small bubbles often appeared about two thirds of the way up the bed and rose ahead of the initial large bubbles formed at the bottom of the bed. They suggested that this was due to the pressure drop from the bottom of the bed to its surface. The mass velocity of gas required for interstitial flow fell towards the top of the bed and excess gas formed new bubbles while the gas was flowing. Many bubbles and slugs appeared to rise from parts about half way between the surface of the solution and the membrane, mainly by the displacement of the particles falling through the roof of the bubble.

2.5.4 Application of the Fluidized Bed Cell to the Production of Metal and Composite Coatings.

Industrial application of the fluidized bed has been mainly applied to copper production. The amount of metal in solution has been reduced to a few parts per million by using various types of fluidized beds.

The design of a fluidized bed has a great influence on its efficiency. In a rectangular-shaped solution circulated, fluidized bed, ionic metal concentration can be reduced by a factor of 100 if the dimensional ratio (L/λ) is kept at 5, where⁽⁸⁰⁾

$$\lambda = \frac{X \cdot U}{D \cdot V_0 \cdot A''} \quad \dots \dots (36)$$

Benson and Wenger⁽⁹³⁾ have used graphite powder bed electrodes with stream fluidization to reduce the divalent copper ions from 0.8 g/l. to 0.001g/l. Germain and Goodridge⁽⁸²⁾ used a fluidized bed cell with rectangular shaped geometry to electrodeposit copper from acidified aqueous solutions, enabling them to reduce the copper ion from 2g/l to 0.001 g/l with a 95% current efficiency.

The impurities in the solutions used in the production of plated metal have great influence on the efficiency of the fluidized beds, and the quality of the deposit metal. Simson⁽⁹⁴⁾ claimed to produce recovered copper of good quality from dilute solutions by using a rectangular shaped fluidized bed which included copper particles near the cathode together with an insoluble anode. Tangappan et al⁽⁸⁸⁾ obtained hydrogen free electroformed copper from a fluidized bed electrode. If any ferrous iron is present in a fluidized bed with a low concentration of copper solution (2g/l Cu), anolyte and catholyte have to be separated, otherwise ferrous iron will be oxidized and the oxidation will reduce the current efficiency⁽⁹⁵⁾.

The electrodeposition of cobalt onto nickel plated copper or titanium powder, in acid killed laterite leach liquor, was hindered by hexavalent chromium ions in a fluidized bed electrowinning process. The same impurity (Cr^{6+}) may also cause problems when it is present in solutions prepared from cobalt scrap. An increase in the PH to 5 precipitated the chromium from the laterite solution⁽⁹⁶⁾.

The addition of tellurium at PH of 5 facilitated cobalt precipitation in cadmium containing solutions⁽⁷⁷⁾.

Cobalt deposited onto other types of powder in a fluidized bed, improves the magnetic properties of the sintered material produced from that powder. Asti and Cavalotti⁽⁹⁷⁾ have observed that cobalt coated barium ferrite powder had a greater saturation magnetization and remanence than Co-Ni or Co-Ni-P coated powders, with improved mechanical properties, an increased orienting power of the dispersed powder in a magnetic field and optimum magnetic properties. Sintered material prepared from nickel coated iron powder that had been prepared in a fluidized bed, sometimes possessed mechanical properties superior to similar material prepared by commercial means⁽¹⁾. Thus a 3% nickel plated iron powder, mixed with 0.3% carbon had a higher tensile strength than prealloyed or blended sintered material, at the same pressure level.

Further improvements in the mechanical properties of the electroformed deposits in the fluidized bed, is possible by codepositing the metal with another ceramic powder or metal. The composition of the electroformed alloy is always different from the ratio of the metal ions in the solution. The more noble metal ion in an electroplating solution will be present in a higher proportion in the electroformed alloy than in the solution, owing to the replenishment of the cathodic diffusion layer with the more noble metal ions⁽⁹⁸⁾. Mc Farlon⁽⁹⁹⁾ claimed that

an increased current density reduced the amount of cobalt in Co-Ni alloys codeposited in a fluidized bed.

Dispersoid powders have also been codeposited with cobalt, nickel and other metals in order to obtain better high temperature properties. Co-Al₂O₃ and Co-Ni-Al₂O₃ (3 μm) codeposition in a fluidized bed which has included a device that applies a flush current with superimposed alternating current on the direct current, gave better high temperature properties than cobalt and Co-Ni electroforms produced by conventional means⁽⁵⁷⁾. Foster et al⁽¹⁰⁰⁾ have worked on the codeposition of various conducting and nonconducting composite powders onto a steel substrate. It has been shown that the particle volume contents in the electrodeposited composite coatings vary with current density: the highest contents were found to occur at the lowest current densities. Cobalt deposition at a particle cathode interface will depend on the conductivity of the particle. Thus non-conducting particles are gradually engulfed by the metal while conducting particles are rapidly engulfed⁽¹⁰⁰⁾.

Various factors influence the metal composite codeposition, such as temperature, additions etc. Kariapper and Foster⁽¹⁰¹⁾ stated that additions of thallium and rubidium sulphate promoted codeposition of aluminium oxide and nickel in a fluidized bed. Groves and Smith⁽¹⁰³⁾ studied the effects of the electrolyte on the charge carried by suspended ceramic particles in a fluidized bed

and concluded that positive ions were absorbed by contact on suspended ceramic particles (SiO_2 , SiO_2 and chromium diborate). The degree of adsorption increased as the metal ion concentration was raised, and decreased as the temperature rose.

3. EXPERIMENTAL PROCEDURE

3.1 The Cementation Cells

The coating of cobalt onto iron powder, by the cementation process, was carried out in two different types of cell. Preliminary experiments were carried out in a mechanically stirred beaker but this was discontinued after the completion of the fluidized bed cell. Henceforth all work was carried out in the latter.

3.1.1 (a) Mechanically Stirred Cell

The cell consisted of a 3l glass beaker, a mains driven electric motor, and a 20cm stirrer.

One end of the stirrer column was fixed to the electric motor while the other end was attached to a sheet steel paddle measuring 10x20x1.5mm; both of these were coated with a chemically neutral lacquer. The rotational speed of the motor was controlled by the dial on the top of the electric motor.

When in use the stirrer was suspended in the solution by means of a clamp and a retort stand. Initial heating of the solution in the beaker was maintained by a hot plate but this was later superseded by a hot water tank, which was heated by an immersion heater.

The dimensions of the glass beaker are shown in fig. 15.

To determine the possibility of cobalt cementation

onto iron powder (as in equation 1), some initial experiments were carried out in the mechanically agitated cell. The operation of this cell was as described in the following section.

3.1.1 (b) Experimental Procedure in the Mechanically Stirred Cell

To carry out the experiments in the mechanically agitated cell the steps as indicated below were followed:

1. The hot plate was heated or the hot water tank was heated to 5°C above the required solution temperature.
2. The beaker was filled with 1.5 l. of distilled water and placed on the hot plate, after that the desired amount of cobalt salt was introduced into the cell; then the cell was heated to a temperature of 5°C above the experimental temperature.
3. The stirrer was placed along the central axis of the cell keeping the stirring paddle 1 cm above the bottom.
4. The PH meter electrode was inserted and the thermocouple fixed about 1 cm away from the inside surface of the cell.
5. The required amount of iron powder was added to the stirred solution.
6. Samples of powder were taken at 15 minute intervals; simultaneously the PH and temperature of the solution were measured.
7. PH adjustment of the solution was maintained by hydrochloric acid in cobalt chloride solutions, and by

sulphuric acid in cobalt sulphate solutions.

8. The samples of powder were washed thoroughly in a filter paper with distilled water and then dried on the hot plate in a metal box under a nitrogen gas atmosphere.

3.1.2 (a) Fluidized Bed Cell

After the initial experiments showed that upto 68.5% cobalt could be produced by cementation onto iron powder, further experiments were carried out in the fluidized bed cell which had a more uniform stirring motion.

The fluidized bed cell consisted of two cylindrical sections made of OUF glass with a sintered polythene membrane made from Vyon D and C, which was bolted between the two glass sections. The top section of the bed (fig.16-1) included the cobalt solution and the powder, and the bottom part was used as a reservoir for the hot nitrogen gas, see fig. 16 and 17.

Blowing of nitrogen gas from the bottom section (no; 3 fig. 16), to the upper section (no: 1 fig. 16), through the membrane (no. 2 fig. 16) maintained the fluidization of the iron powder in the solution in the upper section.

The incoming nitrogen gas was heated by an electrical heater placed in a glass tube which made up part of the gas supply line. The fluidized bed cell was also contained within a water tank of dimensions 45x60x60cm, which was used to heat the bed and to keep it at a constant temperature within the range 50-80°C. The tank was made from

aluminium sheet with a perspex window for observation of the interior of the fluidized bed.

The hot nitrogen gas, emerging from the glass heating tube (9), passed through a section of hard plastic pipe (8) (approximately 30cm long 1cm ϕ), followed by a section of copper pipe (7) (50cm long and 1cm ϕ). These pipes carried the hot gas from the heating tube (9) through the hot water bath (10), into the bottom section of the chamber underneath the bed (3). The cold nitrogen gas supplied to the heating tube came from a cylinder through a gas flowmeter.

The hot water tank was heated by an electrical resistance heater, the output of which was controlled by a thermostat. Another thermocouple was attached to the outgoing side of the heating tube.

Electrical current was also used to plate cobalt onto iron powder in the fluidized bed cell. Twenty four cathode rods were screwed to a copper plate of 17 cm ϕ and 3mm thickness, and then the cathode plate was placed on the upper section of the cell, to keep the cathode rods vertically in the cell with the lower end of the rods 1cm above the membrane.

The copper cathode plate had a hole of 5cm diameter in the centre through which the stainless steel anode bar was immersed into the cell. The upper end of the anode bar was connected to the potential source while the lower

end, which was kept within the cell, was in contact with a cluster of cobalt pellets contained within a fabric anode bag. The purpose of the anode bag was to prevent the iron powder making contact with the anode and to contain the sludge generated from the impurities in the cobalt pellet, which had 99.9% cobalt.

3.1.2 (b) Experimental Procedure in the Fluidized Bed Cell

The use of the fluidized bed cell involved the following procedure for electrodeposition of cobalt onto iron powder.

1. A known volume of cobalt solution of known composition was heated to 15°C above the operation temperature in a beaker, and then poured into the plating cell.
2. Hot nitrogen gas, at a low flow rate (5.5 l/min), was passed through the fluidizing membrane.
3. A known mass of iron powder was poured into the plating cell.
4. The flow rate of nitrogen gas was adjusted to achieve complete suspension of the powder with random movement of the iron powder particles in the plating solution.
5. The assembly of cathodes, the electrodes of the PH meter, and the anode bag were placed in position, and then connected to the power sources.
6. Potential and current readings were recorded when the powder samples were taken from the bed.
7. Samples of the powder and the plating solutions were

removed after 15, 30, 60 and 90 minutes; the PH and temperature of the solution were also read at the same time.

8. When necessary, adjustments were made to the PH by addition of dilute HCl or H₂SO₄.
9. The plated powder samples were washed thoroughly in a filter paper with distilled water and then dried on a hot plate in a mild steel box under a nitrogen gas atmosphere. The cobalt content of the samples were then determined.

3.1.2 (c) Coating of Cobalt onto Iron Powder by Cementation in the Fluidized Bed Cell

During the process the anode bag and cathode assembly were taken out of the fluidized bed cell which was kept in a hot water bath at a temperature between 65-90°C. A cobalt solution of similar composition to that used in the cobalt cementation coating experiment, was heated to 5°C above the required temperature and then poured into the cell. The measured amount of Atomet 25 iron powder was then added to the cell and the gas flow was adjusted to obtain an optimum suspension of the iron powder in the fluidized bed cell. Subsequently samples of the iron powder were taken by a glass pipette, as described above.

3.2 Raw Materials

3.2.1 Metallic Powder

Atomized iron powder was used, the commercial name of

which is ATOMET 25. The chemical and sieve analysis of the Atomet 25 are shown in table 6 and 7.

3.2.2 Cobalt Plating Solutions

Three different solutions have been used for the cobalt coating experiments, at various concentrations, these are:

A) Cobalt chloride solutions including

$\text{CoCl}_2 \cdot 6\text{H}_2\text{O}$	100-300 g/l
H_3BO_3	20-60 g/l
KCl	10-20 g/l

B) Cobalt sulphate solutions, including

$\text{CoSO}_4 \cdot 7\text{H}_2\text{O}$	100-300 g/l
H_3BO_3	20-60 g/l

C) Mixed cobalt chloride and sulphate solutions, including

$\text{CoSO}_4 \cdot 7\text{H}_2\text{O}$	90.5 g/l
$\text{CoCl}_2 \cdot 6\text{H}_2\text{O}$	8 g/l

Mixed cobalt chloride and sulphate solutions were only used in cementation experiments involving the mechanical stirrer.

3.2.3 Anode Materials

The anode was a 30cm long stainless steel rod with a diameter of 5mm which contained Ni 9.05%, Cr 17.50%. Small clusters of 99.9% cobalt were placed in a fabric anode bag into which the anode rod was inserted. The bag

was stretched over the pellets to hold them firmly against the anode .

3.2.4 Cathodes

Cathodes were formed from niobium stabilized 18-8 stainless steel rods of diameter 3.5mm and 30cm length; these were placed in two concentric rings. To give electrical contact to the power supply each was screwed into a 3mm thick sheet of electrolytic copper.

3.3 Metallographic Study

In order to determine the morphology of the cobalt deposits on the iron powder a number of powder samples were studied using scanning electron microscopy (S.E.M.). A Phillips P.S.E.M.-500 scanning electron microscope was used for this purpose and an Edax non-dispersive x-ray analyser, which was connected to the S.E.M., was also used for the x-ray analysis of both the scanned surfaces and points within these surfaces.

Samples for the S.E.M. were prepared in two ways, firstly, powder samples for coating surface morphology study, secondly, for cross-sectional study of the powder samples.

The cobalt coated iron powder samples for surface morphology study were prepared in the following steps:

1. Apply some colloidal silver (liquid) onto the standard scanning electron microscopy (S.E.M.) stub.

2. Press the wet surface of the stub onto the iron powder sample.
3. Leave the stub to dry for a few minutes.
4. Coat the powder surface on the stub with a 300 angstrom layer of gold in a ion sputter coating machine.
5. Place the stub into the S.E.M.

The preparation of the powder samples for cross-sectional study was as indicated in the following procedure :

1. The powder sample was mounted in electrically conductive bakelite using a Metaserv automatic mounting press using a mounting time of 8 minutes at a temperature of 160°C.
2. The surface of the mounted powder was ground until a section approximately halfway through the powder was obtained: this section was then given a 600 ground finish and 1 μm of diamond compound polishing the sample until it gave a smooth surface.
3. The sample was etched in 2% nital solution for 30 seconds.
4. The sample was placed in the S.E.M.

4. RESULTS

4.1 Deposition of Cobalt in the Mechanically Stirred Cell.

Prior to the setting-up of the fluidized bed some preliminary experiments were carried out in a mechanically agitated suspension of powder in the appropriate solution.

Some of the words in the tables of the results are abbreviated, the meaning of these abbreviations are as indicated below.

$\text{CoCl}_2(\text{g/l})$: $\text{CoCl}_2 \cdot 6\text{H}_2\text{O}$ salt concentration in the cobalt solution.

$\text{Fe}(\text{g/l})$ in composition : Concentration of the iron powder in the cobalt-coating solution.

$\text{H}_3\text{BO}_3(\text{g/l})$: Concentration of boric acid in the cobalt coating solution.

Agit. no : Dial number on the stirring motor

Co% : Cobalt percent cemented onto iron powder.

Fe g/l (solution) : Ionic iron concentration in the cobalt coating solution.

Co g/l (solution) : Ionic cobalt concentration in the solution.

E.T. : The experiment had been carried out in the mechanically stirred beaker.

E.F. : The experiment had been carried out in the fluidized bed cell.

The first experiment in the mechanically-agitated cell was carried out at room temperature, in cobalt chloride solution with additions of boric acid (see table

8); this represented a commercial plating solution. The results given in table 8 show that under these conditions virtually no cobalt deposition occurred.

After obtaining the low cobalt cementation in the first test, the experimental temperature in the second test was increased to 80°C, while attempts were made to keep the PH of the solution at its natural level (4.4).

An increased solution temperature in experiment, E.T.2 produced an improved cobalt cementation rate, and allowed the deposition of 30.2% cobalt in 90 minutes (see table 9). Iron powder dissolution in the test was about 8% more than the amount of cemented cobalt. Evaporation was not accounted for in the solution analysis.

In the experiment E.T.3 cobalt chloride concentration was increased to 300 g/l. The results of the experiment showed 28% cobalt cementation in 1½ hours which was significantly lower than the previous experiment although the iron dissolution rate was decreased to 11.43 g/l in 90 minutes (see table 10). The cemented cobalt analysis results show a rapid increase in the cementation rate after the first 40 minutes of the experiment.

After the preliminary experiments with cobalt chloride solutions, some further experiments were carried out using cobalt sulphate solutions. In the first test 100 g/l of cobalt salt was used at 80°C and a PH of about 5. The results of the experiment E.T.4 are shown in table 11.

The amount of cemented cobalt in 90 minutes was 7% while the iron powder dissolution in the experiment was 3.7% in 1½ hours. The iron powder dissolution occurred at an almost constant rate but the cobalt cementation rate showed a sharp increase after the 50th minute of the experiment.

A cobalt sulphate (0.3 M/l) and chloride (0.03 M/l) commercial solution was also employed in the study of the cobalt cementation, at various PH levels.

The results of the test in this mixture show that 7.1% cobalt cementation was produced at a PH of 4 to 5 after an hour reaction time. A considerable increase in the cobalt cementation rate appeared after 30 minutes (see table 12). In this experiment sulphuric acid was used to keep the PH of the solution between 4 and 5. Powder suspension was at a minimum even when the most vigorous stirring was used: the powder suspension was then extremely poor, and after 45 minutes the colour of the solution became darker than it was at the beginning of the test.

4.1.1 Influence of Temperature on the Deposition of Cobalt in the Mechanically Stirred Cell.

In order to determine the activation energy of the process (see the section below) the effect of temperature on the deposition process was measured at various temperatures between 80 and 30°C (see table 13). The experiments E.T.6 to E.T.11 were carried out in 100g/l cobalt chloride

solutions at a PH of 3 ± 0.3 with 50g/l iron powder concentration in the solution.

In the experiment E.T.6, which was carried out at 80°C 3.36% cobalt cementation was obtained after 60 minutes while in the same time 6.7g/l iron powder dissolved in the solution. The experiment (E.T.7) in the same solution as the above test but at a temperature of $(72 \pm 2)^{\circ}\text{C}$, gave only 1.40% cobalt deposition in the same time with 2.70% g/l iron powder dissolution in the solution. The cobalt cementation rates in the same solution but at 60°C and 50°C were 2.35 g/l and 1.30 g/l: all figures refer to the results obtained after 60 minutes.

The rates of cobalt deposition and iron dissolution at temperatures below 50°C were even lower in E.T.10 and E.T.11. It is evident that the rate of deposition was very sensitive to the temperature of the solution.

4.1.2 Prolonged Deposition of Cobalt in the Mechanically Stirred Cell

Prolonged treatment of iron powder in the cobalt chloride solution leads to the production of a powder that contained almost 70% cobalt, which suggested the process did not lead to the formation of an impervious deposit on the surface of the powder, which would inhibit any further reaction (see table 14). The amount of dissolved iron in the final solution was 62 g/l.

The solution temperature in the prolonged iron

powder treatment was reduced to $48 \pm 3^{\circ}\text{C}$ from 65°C after 7 hours on account of the high evaporation at the higher temperature. The duration of this experiment was three days.

4.2 Deposition of Cobalt in the Fluidized Bed Cell

The observation of up to 68.5% cobalt cementation onto iron powder in the mechanically agitated cell showed that a significant amount of cobalt deposition was possible when iron powder was placed in acidic solutions of certain cobalt salts. Therefore in order to obtain better control of the agitation process, further experiments were carried out in the gas agitated fluidized bed cell, which was more uniformly agitated than the mechanically agitated cell.

These experiments counted under C.F. code numbers.

4.2.1 Presence of Froth in the Fluidized Bed Cell

During the course of the experiments in the fluidized bed cell a froth layer on the top of the solution was usually present, which was caused by the nitrogen gas bubbles coming from the membrane and then rising to the surface of the solution.

The size of the bubbles and the thickness of the froth layer were affected by various factors. Usually the higher the gas flow rate the greater was the froth thickness. The bubble size in the froth, which varied from 2-3mm to about 5cm. in diameter, decreased as the temperature of the solution decreased. The temperature

of the nitrogen gas also influenced the size of the bubbles; when the gas temperature was higher than the solution temperature, the size of the bubbles varied little while they were passing through the solution. In the case when the gas temperature was lower than the solution, the bubble size increased sharply while it was passing upwards through the solution. The bubble size in solutions of low PH was a little smaller than in solutions of higher PH.

The thickness of the froth layer was an indication of the gas flow rate. It varied between 12cm. and 15cm. at the optimum rate of 5 l/min gas flow. In some experiments the froth layer thickness stayed large (15cm) even at ^{the} lower gas flow ^{rate} (2-3 l/min) some time after the beginning of the test.

The colour of the froth layer was also a good indication of the fluidization of the powder. When the froth was colourless the fluidization was poor, while a dark coloured froth was associated with good fluidization.

4.2.2 The Results in the Fluidized Bed Cell

During the first experiments in the fluidized bed cell, C.F.1 and C.F.2, a determination was made of the optimum gas flow rate which would give the maximum rate of cobalt deposition under a specific set of experimental conditions (see table 15).

In C.F.1, when the gas flow was 5 l/min, 1.84% cobalt was deposited at a PH of 3 and temperature of $68 \pm 1^{\circ}\text{C}$ in

one hour. In the case of C.F.2 only 0.90% cobalt was produced under the same conditions as C.F.1 except for the gas flow, which was 10 l/min during the first 10 minutes, but was then dropped to 8.5 l/min on account of the excessive production of the froth. Gas flow rates below 5 l/min at the beginning of experiments were not used because it was evident that under these conditions the iron powder fluidization was poor, with most of the powder settled on the base of the chamber and colourless froth.

4.2.3 Effect of Iron Powder Concentration on the Deposition of Cobalt

After these initial experiments, the effect of iron powder concentration on the cementation rate in CoCl_2 solutions was studied in experiments C.F.3 \rightarrow C.F.5. The results of these experiments are shown in table 16.

In experiment C.F.3, which included 100 g/l of cobalt chloride and 50 g/l iron powder in a solution with a PH of 4.5-5, 1.60% cobalt deposition was obtained with 1.20 g/l iron powder dissolution in one and a half hours.

Experiments C.F.4 and C.F.5 were also carried out under the same conditions as C.F.3 except for the amount of iron powder, which varied between 75 g/l and 100 g/l. The amounts of cemented cobalt in experiments C.F.4 and C.F.5 were 2.8% and 1.98% respectively while the corresponding amounts of iron dissolution were 4.95 g/l and 2.40 g/l respectively after 90 minutes.

An unacceptable amount of frothing of the solution was corrected by the addition of a few drops of silicone to the solution containing 100 g/l of iron powder 30 minutes after the start of the experiment. Although the addition of this material caused the froth to subside, it appeared to be associated with a reduction in the rate of cobalt deposition. However the results obtained in the first 30 minutes (1.44% cobalt) suggest that the best deposition rates were obtained at a powder concentration of 100 g/l (see fig. 18).

The effect of iron powder concentration on the rate of cobalt deposition from cobalt sulphate solutions was studied by using iron powder concentration between 100 g/l and 300 g/l. The results of these experiments, (C.F.6 - C.F.8) are shown on table 17 and fig. 19. During the course of the above experiments the froth became black in colour indicating that iron powder became uniformly distributed through the cell. The time at which this effect was produced varied in each experiment. Thus it was evident after 3 minutes in the case of C.F.6, after 5 minutes in C.F.7, and after 10 minutes in C.F.8.

The solution temperatures of the above experiments were $69 \pm 4^{\circ}\text{C}$, and the PH varied between 4 and 4.5. The amounts of cobalt produced after 90 minutes in these tests were 31%, 8.60%, and 0.70% respectively while the amount of iron dissolved in the solution was 72 g/l, 68.5 g/l and 34.2 g/l respectively.

The lack of association between cobalt deposition and iron dissolution is due to the poor fluidization obtained in the denser beds.

Sometime after the beginning of the experiments C.F.6, C.F.7 and C.F.8, the PH of the solutions started to vary very rapidly: the point at which these fluctuations began were: 45 minutes in C.F.6; 28 minutes in C.F.7; 30 minutes in C.F.8. In view of the results of the experiments C.F.3 → C.F.5 and C.F.6 → C.F.8, all further experiments used an iron powder concentration of 100 g/l.

4.2.4 Influence of PH on the Rate of Cobalt Deposition

An examination was made of the influence of the solution PH on the cobalt cementation rate in cobalt sulphate and chloride solutions at temperatures between 67°C and 73°C. A range of temperatures has been quoted here, since it proved very difficult to maintain a constant temperature in the cell for long periods of time on account of a temperature drop in the gas heating tube.

Fig. 20 shows that the optimum PH for cobalt deposition in solutions containing 100 g/l of cobalt sulphate in a bed containing 100 g/l of iron powder lay between 4 and 4.5. This range changed to 3.5 to 4 when the cobalt sulphate was replaced by cobalt chloride (see fig. 21). The relevant experimental conditions are shown in table 18 and table 19, which also give information about the amount of cobalt removed from, and the amount of powder

dissolved in the solution. When the PH of the solution was less than 5 the rate of solution of the iron powder was always high even when the quantity of cobalt deposition was small. In the experiment, C.F.32 concentrated H_2SO_4 , and in the C.F.15, C.F.16, C.F.17, C.F.18 and C.F.19 HCl, were used to maintain the PH of the solutions.

A froth was always produced in these experiments. It was usually colourless but turned black as the coating time increased. The point at which the froth started to appear varied considerably: after 20 minutes, 45 minutes, 12 minutes, 3 minutes, 5 minutes from the beginning of test in experiments C.F.9, C.F.10, C.F.15, C.F.16, C.F.18 respectively. In the case of experiments C.F.13, C.F.20, and C.F.22 the froth was always colourless.

During experiment C.F.16 the dark coloured froth started to lighten after 60 minutes and the powder particles agglomerated on the surface of individual bubbles: this was associated with a sudden change in the PH of the solution. The experiment C.F.22 was interrupted for 2-3 minutes at 30th minute due to malfunction of the equipment.

The amount of deposited cobalt after 90 minutes in solutions of optimum PH was 31% in the case of cobalt sulphate and 9.2% in the case of cobalt chloride (both solutions were at a concentration of 100 g/l).

In a number of experiments the amount of deposited

cobalt obtained after 90 minutes, appears less than the amount which had been deposited in 60 minutes. This is probably due to a sample taking error. Powder samples from the top of the solutions were always richer in cobalt than the samples from deeper parts of the solutions, e.g. C.F.11, C.F.15, C.F.17, and C.F.18. These samples taken from the solution during use tended to be rather higher than that obtained in the bulk material.

4.2.5 Effect of Boric Acid Addition on the Rate of Cobalt Deposition from CoCl_2 and CoSO_4 Solutions

A study was also made of the effect of boric acid on deposition in cobalt chloride solutions containing 100 g/l of this constituent. The conditions and results of these experiments are shown in table 20.

The effect of the addition of boric acid on the rate of cobalt deposition from cobalt chloride solutions was irregular, with no clear trend within the range of boric acid concentration investigated. This is probably mainly due to a variation in the solution temperature. Thus the consistently good results obtained at a concentration of 15 g/l were associated with a temperature of at least 74°C. Although boric acid had little effect on cobalt deposition rate, the addition of at least 15 g/l had a stabilizing effect on the PH of the solution which was usually within the range 3.7-4.2 (see fig. 22).

During the progress of experiment C.F.24 a layer of dark coloured froth of 18-20 cm thickness was produced.

The appearance of a dark coloured froth in these experiments started in 13, 3, and 10 minutes in C.F.25, C.F.27, and C.F.26 and C.F.28 respectively (see table 20). The PH of the solutions in C.F.24, C.F.25 and C.F.26 changed very quickly after 80, 60, 45 minutes respectively, only in C.F.26 did it become more stable after 60 minutes.

As a continuation of the above experiments a study was made of the influence of additions of 15 g/l of boric acid on the cobalt cementation rate in cobalt sulphate solutions; the results of this study are shown in the table 21, and fig. 23.

The amount of deposition, in 100 g/l of cobalt sulphate solution at $(71 \pm 2)^{\circ}\text{C}$ and PH of 4-4.5 in 90 minutes, was 31% cobalt, in experiment C.F.6. The addition of 15 g/l boric acid to this solution (experiment C.F.28) did not produce more than a 4% improvement in the rate of deposited cobalt.

The iron powder dissolution in the cobalt sulphate solutions was higher than the corresponding amount dissolved under the same conditions in cobalt chloride solutions (see table 20 and table 21). Thus the maximum and minimum amounts of iron powder dissolution in the chloride solutions were 23 g/l and 12 g/l respectively. The corresponding figures in the case of sulphate solutions were 72 g/l and 70 g/l.

Due to the relatively small improvement in the rate of

cobalt deposition from sulphate solution produced by additions of 15 g/l boric acid and the absence of any significant influence of this addition in cobalt chloride solutions, the effect of higher boric acid concentrations in the sulphate solutions were not investigated.

4.2.6 Effect of Temperature on the Cobalt Cementation Rate

The effect of temperature on the rate of deposition of cobalt was first studied using solutions containing 100 g/l of cobalt chloride with 100g/l of iron powder in the fluidized bed cell: the PH of the solution was the natural value for cobalt chloride, as no attempt was made to adjust the PH by additions of other constituents. The experimental conditions of experiments C.F.20 to C.F.22 and C.F.29 to C.F.31 are shown in table 22, and the effect of temperature on the rate of cobalt deposition is shown in fig. 24. The natural PH of the cobalt chloride is high, so the rate of deposition of cobalt was always relatively low. However as may be seen from fig. 24, the rate of deposition was markedly influenced by temperature, particularly when the time that the powder was immersed in the solution exceeded thirty minutes. The amount of iron dissolved in the solution was small and was of the same order as the amount of cobalt deposited on the powder.

At the beginning of experiment C.F.29 a layer of colourless froth 5 cm thick was produced, which began to darken after the first twenty minutes of the experiment.

Fluidization was poor, so after the first hour of the test, the gas flow rate was increased to 7 l/min.

However some of the powder still settled onto the membrane at the base of the chamber. Towards the end of the test the gas flow decreased steadily because of the pressure drop in the gas cylinder.

Likewise, the other experiments in this series produced a layer of colourless froth, which did not contain a significant amount of iron powder. The thickness of this layer varied significantly from experiment to experiment and also with time, but was approximately 5 cms in magnitude.

The study of cobalt cementation in the above mentioned experiments (see table 22) shows that the maximum amount of deposited cobalt, from a solution containing 100 g/l of cobalt chloride and 100 g/l of iron powder at 68°C, was 2.68% cobalt in 90 minutes. Table 22 also shows a reduction in the rate of cemented cobalt when the temperature was decreased (also see fig. 24) so that at temperatures below 50°C the rate of cobalt deposition became negligible. The comparatively low rates of deposition of cobalt in all the experiments in this series is almost certainly due to the high PH employed.

The amount of dissolved iron powder in the solutions of C.F.2D, C.F.29, C.F.30 and C.F.31 was rather less than the dissolved amount in the other experiments (see table 22).

A similar investigation to determine the effect of temperature on the rate of cobalt deposition was carried out with the cobalt sulphate solutions as shown by experiments C.F.13 and C.F.32 to C.F.35 in table 23 and fig. 25.

During the experiment C.F.13 a 10 cm thick dark coloured layer of froth was formed in the solution at the beginning of the test and remained there throughout the experiment. A layer of colourless froth about 8 cm thick formed on the surface of the solution during experiment C.F.32, but powder began to enter this layer after the experiment had continued for 5 minutes. The froth thickness reached a value of about 15 cm after the first half hour and the colour darkened a little but there was always a quantity of iron powder on the membrane which did not fluidize. In the experiment C.F.33 cold gas was used for the fluidization, because of malfunction of the gas heating equipment. Therefore the gas was blown directly from the gas cylinder without passing through the flowmeter. The optimum gas flow rate was estimated from the froth thickness, which was about 15 cm. All the powder fluidized well and the froth was dark coloured during the trial. The froth in the solutions used in experiments C.F.34 and C.F.35 was also colourless and the layer was about 15 cm thick. In these experiments cold nitrogen gas was also used for fluidization.

The average reaction temperatures in these experiments

were 70, 59, 51, 40 and 30°C in C.F.13, C.F.32, C.F.33, C.F. 34, and C.F.35 respectively. The amounts of cemented cobalt in these experiments, which involved solutions containing 100 g/l of cobalt sulphate and 100 g/l of iron powder, were 0.44, 0.16, 0.08 and 0.08 percent in C.F.13, C.F.32 to C.F.35 respectively after 90 minutes. These amounts of deposited cobalt are lower than the amounts obtained under the same conditions with the cobalt chloride solutions. Likewise the amount of iron dissolution in these experiments was lower than that was observed with the cobalt chloride solutions under the same conditions. The actual values of this iron dissolution was 2.93, 0.22, 0.425, 0.15 and 0.20 g/l in C.F.13, C.F.32 to C.F.72 respectively after 90 minutes reaction time.

4.2.7 Effect of Cobalt Ion Concentration on the Cobalt Deposition Rate

Table 24 shows the effect of cobalt chloride concentration in a solution of relatively high PH on the rate of deposition of cobalt on the iron powder. An increase in the concentration of this salt from 100 g/l to 200 g/l produced an increase in the rate of deposition, as shown in fig. 26. This effect was particularly marked between 100 g/l and 150 g/l.

The froth layer, in the solution of C.F.36, was about 10 cm thick, and was colourless at the beginning of the experiment. After 4 minutes the froth darkened a little, and the thickness of the froth layer reached 15-18 cm after

35 minutes, remaining at that thickness until the end of the experiment. At the beginning of C.F.37 a 15 cm thick layer of froth was produced which gradually darkened until 15 minutes had elapsed, after which the colour of the froth started to lighten; this was probably due to a drop in the gas flow rate, resulting from the development of a gas leak. A 5 to 8 cm. thick layer of froth formed in the solution at the beginning of experiment C.F.38 and the colour of the froth darkened a little after 10 minutes. Thickness of the froth layer gradually increased to 18-20cm.

The solutions used in experiments C.F.22, C.F.36, C.F.37 and C.F.38 included 100,150,200 and 250 g/l of $\text{CoCl}_2 \cdot 6\text{H}_2\text{O}$, respectively. The deposition rates of cobalt at 80°C with the natural PH of the solution (5.8-5.2) were 2.68, 4.32, 9.60, 14.08 percent in 90 minutes at concentrations of 100, 150, 200 and 250 g/l of cobalt chloride respectively. Iron dissolution rates in these experiments were very close to the corresponding rate of cobalt deposition viz; 3.75, 5.50, 11.0 and 18.15 g/l after 90 minutes in C.F.22, C.F.36 to C.F.38 respectively.

4.2.8 Effect of Sodium Sulphate on Cobalt Deposition Rate

It has been reported that Na_2SO_4 increased the electrolyte conductivity in NiSO_4 and CoSO_4 mixture solutions⁽¹⁰⁹⁾. Therefore the effect of sodium sulphate on the cobalt cementation rate was also studied. The results obtained in the two experiments C.F.39 and C.F.40 discouraged any

further work (see table 25 and fig. 28).

A thin layer of froth about 2cm thick, started at the beginning of experiment C.F.40. After 18 minutes this froth layer thickened to about 13-15cm and a black scum formed on the surface of the solution: after 25 minutes this dark coloured scum disappeared. The same thing happened during experiment C.F.39.

The amount of cobalt deposited during experiment C.F.39, which was carried out in a solution containing 100 g/l of CoSO_4 , 100 g/l of iron powder and 60 g/l of sodium sulphate was very low (1.60% cobalt in 90 minutes) although 93.5 g/l iron powder dissolved in the same period of time. In addition to C.F.39 solution 15 g/l of boric acid was added into C.F.40 solution, and the experiment was carried out at PH of 3-4.2 and $70 \pm 1^\circ\text{C}$. The result of this experiment showed that only 4.20% cobalt was deposited while 81.3 g/l of iron powder dissolved during the same period of time (see table 25).

4.2.9 Electrodeposition of Cobalt onto Iron Powder in the Fluidized Bed Cell

A limited series of experiments were carried out which involved the electrodeposition of cobalt from cobalt sulphate solutions (table 26). The experiment C.F.41, which involved the use of a cobalt sulphate solution containing 100 g/l of CoSO_4 with 100 g/l iron powder and an addition of 15 g/l boric acid, produced a very high rate of cobalt deposition (31.6% cobalt in

90 minutes), although the potential applied was relatively low (5.2 ± 0.1)V. The use of a much higher potential in experiment C.F.42 (15-10 volts) produced virtually no deposition (0.40% cobalt in 90 minutes), which was probably due to the poor fluidization characteristic obtained in this case, plus oxidation of the powder surface. The PH of the solution was also generally slightly higher (5) than in experiment C.F.41 (3.8-5). In neither case was there a significant reduction in the cobalt ion concentration in the solution. The use of a solution free from boric acid in experiment C.F.43 again produced virtually no cobalt deposition (0.60% cobalt in 90 minutes). In this case excellent fluidization conditions were obtained but the PH of the solution was as in experiment C.F.42 (5.2) rather high.

In all cases the amount of iron that dissolved in the solution was greater than the amount of cobalt deposited in the corresponding time. Thus, 24.5, 0.37, 0.57 grams of cobalt deposited in experiment C.F.41, C.F.42, C.F.43 and 51.5, 47, 4.75 grams of iron were dissolved in the solutions respectively.

After 90 minutes of the experiment C.F.43, the powder in the solution turned to rusty colour implying the oxidation of the powder.

The applied potential and the PH of the solutions in experiments C.F.41, C.F.42 and C.F.43 were 5.1, 11, and 7.5 volts and 4.5 ± 0.5 , 5, and 5.2 respectively. The

solution temperatures of these experiments were $70 \pm 1^\circ\text{C}$.

4.3 Metallographic Results

The final part of this study was an examination of the morphology of the cobalt deposits, which involved the use of scanning electron microscopy. Scanning electron microscopy studies of the cobalt deposited on iron powders showed that the deposits were irregular and had various morphologic structures.

4.3.1 Distribution of Cobalt Deposit on the Iron Powder

The photograph in fig. 29A shows the general view of several iron particles, two of which have relatively smooth surfaces (on the left hand side of the figure), while a third on the right hand side possesses a spongy structure with a large number of small pits. The smooth particles are generally deficient in cobalt as shown by the Edax X-ray analysis in figure 29B; although a small lump of cobalt is attached to the larger of the smooth particles in the 12 o'clock direction, with even smaller pieces on the edge of the same particle in the 6 o'clock direction. The spongy particle on the right hand side of the same photograph is generally rich in cobalt (see the Edax results in figure 29C) although the left hand side of this particle is not covered in cobalt. The total cobalt deposition on this powder sample is 12.32%.

Fig. 30A shows a view of powder sample C.F.36D with irregular cobalt deposits which usually appear at pro-

trusions on the original iron particles. The right hand side of the photograph contains three large rather smooth iron particles while those on the centre and left hand side possess a spongy surface. The smooth particles in the one and two o'clock directions contain no cobalt deposit while the other smooth particle on the right hand bottom corner, contains some cobalt in the form of layers particularly on the edges at the six o'clock position and as a porous lump in the 7 o'clock direction. The iron particle at the eleven o'clock position has cobalt deposits on the left hand edge although the lower part of this particle has no cobalt. The particles on the left hand side foreground of the photograph contain a large number of irregular shaped nodular-like cobalt deposits. Edax measurements were made of the cobalt content of a large number of individual deposits on these particles, which indicated that such deposits were rich in cobalt. These results have not been shown individually, although the x-ray analysis of the whole area in the photograph is given in fig. 30B.

The photograph in fig. 31A shows an example of the coating obtained in powder sample C.F.17D, which was taken from a solution containing 100 g/l of CoCl_2 at a PH of 3.5-4. The almost spherical iron particle in the right hand side of the figure contains virtually no cobalt deposit, as shown by the x-ray analysis results in fig. 31B. The smooth particle in the centre of figure 31A is also

poor in deposited cobalt. However the large irregular particle in the top left hand corner is almost completely covered in porous cobalt, as shown by the x-ray analysis in fig. 31C. Another small area of spongy cobalt deposit is to be seen slightly to the right of this particle.

Fig. 32A shows the surface of an iron particle on which cobalt has been deposited from a solution that contained 100 g/l, of CoCl_2 at a PH of 3-3.5. Although the surface contained a considerable quantity of cobalt the rims of the circular pores that covered the surface of the iron particle were not rich in deposited material, even though the rims of these pores were raised above the general level of the surface of the particle, (see fig. 32B).

4.3.2 Sections Through Cobalt Coated Iron Particles

A number of cross-sectional photographs of the cobalt deposited iron powders were taken in order to see the regularity of the deposits.

Fig. 33A shows a cross sectional view of iron powder particles containing 7.52% cobalt deposited from cobalt chloride solution, with a concentration of 150 g/l at the natural PH of the solution (5.5-5.7). The large particle on the right hand side of the figure contains discontinuous cobalt deposits at the one, seven, and ten o'clock positions. These cobalt rich regions are shown as white particles in the x-ray photograph (figure 33B). Large deposits of cobalt, such as the one shown under the cross

in figure 33A, that appear to be free from iron, are not connected with the adjacent iron particle in the plane of the section. A particularly large agglomeration of such deposits are formed in the bottom and top left hand corners of figure 33B.

The photograph in fig. 34A also shows a cross-section of several iron particles, each of which contains a few grains of ferrite. An adherent layer of cobalt is present between the six, nine and one o'clock directions on the largest particle. Identification of these areas rich in cobalt are given by the white regions in figure 34B. In some cases the cobalt appears to have sealed over some of the recesses of the iron powder surface, leaving a porous structure. Several large particles of cobalt are present that do not appear to be connected in the plane of the photograph to any iron particle. The x-ray photograph (figure 34B) shows that the cobalt layers on the iron surface are never continuous. There is no obvious correlation between the morphology of the iron particle and the sites at which cobalt deposition has occurred, but hollow parts of the iron powder are least likely to receive any cobalt deposition.

Fig. 35A, which shows a cross-section of an iron particle from C.F.28D powder sample, containing two large and two small iron particles, on the right hand top and bottom corners, each of which contains an internal grain structure. This photograph also contains a large amount

of cobalt deposit, which fills the area around the iron particles with a porous mass of material. The high cobalt content of this material is shown by the x-ray photograph, Figure 35B, which shows a uniform cobalt rich region around the iron particles. Generally the cobalt deposit does not form an adherent layer on the surface of the iron particles.

Fig. 36 shows the cross-section of an iron particle from the sample of C.F.28D. In this photograph a cobalt lump is attached to the edge of a narrow crevice (at a conjunction of the grain boundaries) which is free from any other deposit.

The cross-section of an iron particle from the sample of C.F.37C, which was obtained from a solution that contained 200 g/l of CoCl_2 at a PH of 5.5, is shown in fig. 37A. The cobalt deposits on the particle are discontinuous, as shown by the white areas in the x-ray photograph figure 37B. The deposits between the two and five o'clock direction in fig. 37A are attached only to the high points on the surface of the iron particle, although an adherent layer of cobalt appears on the protrusion in the seven o'clock direction. Some more cobalt deposits were attached onto the small protrusions in between the eight and ten o'clock positions. It is evident from figure 37A that these deposits, together with the deposits at 4 o'clock are extremely porous. The re-entrants at six, ten, one o'clock, and the bottom of the

pits between three and five o'clock are always free from any cobalt deposits (see fig. 37B).

4.3.3 Type of Morphology of Cobalt Deposits

The cobalt deposits did not possess a consistent shape, but showed several different types of morphology. In the absence of a more precise definition of deposit type the various morphologies obtained are referred to as spongy, nodular, flaky and dendritic.

The spongy cobalt deposits obtained from a solution containing 100 g/l of CoCl_2 and 60 g/l of boric acid with a PH of 3.7-4 have been described previously (see fig. 29A and page 193). In fig. 38A the left-hand side of the photograph shows several porous layers laid on top of one another. The high cobalt content of the spongy structure under the crossed lines is shown by the Edax measurements in figure 38B. The mean cobalt content of this powder is 2.96%, which was deposited from 100 g/l of CoCl_2 at a PH of 3-3.5, and a temperature 65-67°C.

The photograph of fig. 39 shows nodular deposits of cobalt on the surface of the iron powder. These tend to be arranged in an irregular fashion with considerable areas of iron surface free from any deposit. In the background of the photograph the density of nodules is very high and particles merge into one another. The x-ray analysis of the whole area in the photograph shows iron and cobalt peaks of comparable magnitude. The mean cobalt content of the powder from which this sample was taken, was 22.2%

which had been deposited from 100 g/l of cobalt sulphate solution at a PH of 4-4.5 and a temperature of $70 \pm 3^\circ\text{C}$.

Fig. 40 illustrates the morphology of the powder produced during experiment C.F.7D, which used CoSO_4 at a concentration of 100 g/l and with an iron powder concentration of 200 g/l: the PH and temperature of the solution were 4-4.5 and 72°C respectively. Flaky deposits in fig. 40A, cover all the area between the 8 and 3 o'clock direction and some further deposits of similar morphology occur in the 5 o'clock direction. The mean cobalt content of the powder was 8.60%. Fig. 40B shows the x-ray analysis peaks of the photographed area in fig. 40A, in which the smaller peak at the right hand side is produced by the cobalt in the powder.

Dendritic cobalt deposits were observed on powder treated in a solution containing 100 g/l of CoSO_4 at a PH of 3.5-4 (see fig. 41A). The structure is present in fig. 41A between the 5 and 12 o'clock directions although particles on the far left hand side in the 4 and 10 o'clock directions show a discontinuous deposit. The cobalt peak in the x-ray analysis of the whole area is a little smaller than iron peak (see fig. 41B). The amount of the deposited cobalt in the whole sample is 22.8%.

The experimental conditions and the composition of the solutions influenced the morphology of the deposits in a complex fashion and the amount of data available did not

allow any definite conclusion to be drawn about the effect of PH in the solutions studied. However deposits obtained at low PH from cobalt sulphate appeared dendritic while the corresponding deposits obtained from cobalt chloride appeared to be spongy. Deposits obtained at high PH from cobalt sulphate tended towards the nodular or flaky type of morphology.

The effect of time and an applied electric potential on the type of morphology are described below.

4.3.4 Effect of Time on the Type of Deposit

Some change in the morphology of the cobalt deposit was observed as the cobalt deposit, depending on deposition time, increased. This effect is illustrated in the photographs shown in fig. 42 which involves samples of C.F.28B and C.F.28D, which were taken after treatment for 30 and 90 minutes respectively, in a solution that contained 100 g/l CoSO_4 and 15 g/l H_3BO_3 . In 42A the cobalt deposits appeared as congregates of nodules, an example of which is indicated by crossed lines. Some more nodules are present on an adjacent particle in the 5, 7 and 11 o'clock directions. The total cobalt content of this powder was 5%. Fig. 42B indicates the presence of cobalt detected during a scan of the area shown in fig. 42A. The photograph in fig. 42C is of the same powder after treatment for 90 minutes in the same solution. The nodules shown in fig. 42A have now grown into a spongy deposit while the cobalt content of the powder after 90 minutes treatment

had reached 35%. The overall size of the individual pieces of deposit was smaller than the protrusions shown on the original iron particle (compare figures 42A and 42C).

4.3.5 Effect of Current Applications on the Deposit Morphology

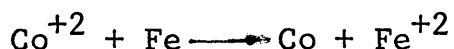
Application of a current slightly changed the morphology of the deposits (compare fig. 43A and fig. 42C). The photograph in fig. 43A was taken after electrodeposition onto iron powder had taken place for 60 minutes, using a solution consisting of 100 g/l of CoSO_4 , 100 g/l of iron powder, and 15 g/l of H_3BO_3 at a PH of 4-4.5 and a temperature 70°C . Figure 43A shows mixed morphology of sponge and flake. The sponge structure was also observed after cementation deposition only from the same solution (see fig. 42C). The spongy structure in fig. 43A, is predominant in the photograph (fig. 43A) and dispersed all over the directions (1,3,4,5,7,8,9 and 11 o'clock). The flaky deposits appear in 2 and 7 o'clock directions.

The results of the x-ray analysis of the area shown in figure 43A are given in figure 43B, the iron and cobalt peaks are approximately the same size. The mean cobalt content of this powder was 14.5%.

5. DISCUSSION

5.1.1 Cobalt Cementation in the Mechanically Agitated Cell

Theoretically, if a metal is in contact with a metal ion, which is more noble than the metal, the metal ion can be expected to deposit onto the metal, as shown in equation 1,



According to Wadsworth⁽⁶⁾; reverse reactions in cementation processes may effectively prevent the deposition of a more noble metal ion onto a less noble metal when $n_c(E_c^{\circ} - E_a^{\circ}) < 0.3$. The values of n_1, E_c° , and E_a° in the case of the cobalt iron reaction are 2, 0.277V, and 0.44V respectively, and the value of $n_c(E_c^{\circ} - E_a^{\circ}) = 0.326$. Therefore the cobalt cementation reaction should be possible according to Wadsworth's analysis, and the reverse reaction insignificant. Although cobalt cementation by iron has not been reported previously, most work of this type has used solid pieces of the cementing agent⁽¹⁰⁴⁾. However Jaiswal and Fletcher⁽²⁾ have shown that nickel deposition onto iron by means of the cementation reaction is possible when the iron is in the form of powder. The value of $n_{\text{Ni}}(E_{\text{Ni}}^{\circ} - E_{\text{Fe}}^{\circ}) = 0.42\text{V}$ which is only slightly larger than the corresponding value for cobalt. Therefore the iron-cobalt cementation reaction may also proceed at a significant rate when the iron is again in the form of relatively fine powder. Therefore preliminary investigations were carried out in a simple mechanically agitated cell, in

order to acquire some initial information about the possibility of cobalt cementation onto iron powder.

In the first experiment virtually no cobalt deposition occurred. Consequently the cobalt chloride concentration and the temperature of the solution were both increased, and the PH was lowered (see E.T.2) with the results that 30.2% cobalt was deposited in one and a half hours. This clearly indicated that cobalt cementation was possible using iron powder, and justified a more detailed investigation. The comparison between the results of E.T.2 and E.T.3 shows that a higher (cemented cobalt/dissolved iron) ratio was produced during E.T.3 than during E.T.2. It was probably due to the higher cobalt chloride concentration during E.T.3 (300g/l. as opposed to 100 g/l)^{than} during E.T.2. These results indicate that high temperature and high cobalt concentrations have a beneficial effect on the cementation process and the subsequent experiments have taken this consideration into account. Similar results were obtained with the use of cobalt sulphate solutions, as is shown by the results of experiment E.T.4. Although the rate of deposition was slightly lower than after a similar time at a similar temperature with cobalt chloride, the PH of the solution was in the range 4.5 to 5.3, which is significantly higher than that used in the earlier experiments.

A cobalt sulphate-cobalt chloride mixed solution, with

additions of KCl and H_3BO_3 , was used by Safranek⁽⁶⁰⁾ in a commercial cobalt electroplating process. In order to check the characteristic of this commercial electroplating solution in relating to the cobalt cementation reaction a single experiment was carried out, but with the cobalt concentration of this solution reduced to the same level as the previous experiments.

The cobalt deposition rate in the commercial solution (E.T.5) was greater than that obtained from either cobalt sulphate or cobalt chloride solutions of the same cobalt ion concentration (of experiments E.T.4 and E.T.6). However the PH's of these three solutions were not constant, being 4.5-5.9 in the case of cobalt sulphate and 2.6-3.0 in the case of cobalt chloride. When cobalt chloride solutions of a PH of 3.2-4.4 were used (experiment E.T.2) then the rate of cobalt cementation was markedly increased, and was markedly greater than that obtained with the commercial solution used in E.T.5. These anomalies in the early experiments indicated the PH of the solution had a significant effect on the rate of cementation, and pointed the way to a further study in the next stage of the investigation. There was no definite evidence that the KCl and the H_3BO_3 present in the commercial solution had any significant effect on the rate of the cementation reaction.

The experiments E.T.6 to E.T.11 were carried out at a PH of about 3 and at various temperatures in order to determine the effect of temperature on the rate of cobalt

deposition and so to determine the activation energy of the process. The results of this series of experiments showed a sharp drop in the cementation rate as the temperature fell below 45°C (see fig. 44). The Arrhenius analysis, shown in fig. 44, indicates that the activation energy of the reaction was 91.51 kJ mol⁻¹ at temperatures above 45°C, but a change in the slope of the Arrhenius curve at 45°C suggested that the activation energy of the process was not constant but that two different mechanisms were involved. The results obtained at temperatures below 45°C showed a wide degree of scatter and it was not possible to obtain a meaningful activation energy from them. However the activation energy obtained at higher temperatures suggests that the deposition process is a charge transfer controlled reaction, since Bockris and Conway⁽¹⁰³⁾ have reported that a charge transfer controlled reaction has an activation energy in excess of about 25 kJ mol⁻¹. Annamalai and Murr⁽¹⁰⁴⁾ also found a change in the activation energy for the cementation of copper on iron, but the transition temperature was slightly lower, at 35°C. The activation energies in this case were 33.22 kJ mol⁻¹ in the 30-60°C range and 95.77 kJ mol⁻¹ in the 10-30°C range.

This series of experiments was concluded with a prolonged experiment (E.T.12) to obtain an indication of whether a high degree of replacement of the iron powder by cobalt was possible. The rate of deposition remained

approximately constant for three days of treatment (20.5 hours total treatment time) at PH of 3.5 and temperature of $60 \pm 10^{\circ}\text{C}$, after which almost 70% of the iron had been replaced by cobalt. Thus there was no indication that a continuous layer of cobalt had formed on the surface of the iron, this preventing further iron dissolution. In addition to the dissolution of iron as a consequence of the process, some of the iron powder was consumed by other reactions, as shown by the presence of a red coloured deposit on the surface of the powder.

5.1.2 Influence of Boric Acid on Cobalt Deposition in the Mechanically Stirred Cell.

Boric acid is frequently used in commercial cobalt plating solutions, in order to maintain the PH of the solution in the required range. Therefore 60gl^{-1} of H_3BO_3 was added to the solution used in experiment E.T.2. The rate of deposition obtained $7.76\text{ gl}^{-1}\text{ h}^{-1}$ in E.T.2, whereas the closest comparable solution (used in E.T.6) gave a deposition rate of $1.5\text{ gl}^{-1}\text{ h}^{-1}$. Therefore there was some indication that boric acid might have to be added with benefit to the solutions used to produce cementation reaction.

5.2.1 Cobalt Cementation in the Fluidized Bed Cell

The preliminary experiments clearly indicated that the reaction being studied was worthy of further investigation. However, the original cell was crude and did not allow sufficiently good contact between all particles

of powder and the solution, since a considerable quantity of the powder lay on the floor of the chamber. Therefore a fluidized bed cell was constructed to a design similar to that used by Jaiswal, which ensured that all particles of iron used were in equally good contact with the solution.

The results of the first six experiments in the new cell, C.F.1 to C.F.6, revealed that the optimum gas flow rate in solutions that contained 100g/l of cobalt chloride at a PH in the range 3 ± 0.5 was 5 l/min (see table 21). However in some cases in the following experiments, it was observed that the optimum powder fluidization was obtained at a lower gas flow rate, in some cases as low as 3 l/min, some time after the beginning of the experiments. A major indication of the quality of the state of fluidization was the colour of the froth in the solutions, since a black colour was only produced by the even distribution of the iron powder through the bed. When the gas flow rate was fixed at 5 l/min the layer of froth was usually about 15-18 cm thick which was the maximum that could be conveniently accommodated in the glass vessel. Provided no gas leakages were present these conditions usually gave a dark coloured bed that indicated good fluidization.

5.2.2 Influence of Iron Powder Concentration on the Rate of Cobalt Deposition

Tables 16, 17 and figures 18, 19 showed the effect of iron powder concentration on the cobalt cementation rate in cobalt chloride and sulphate solutions, at PH's of

4.5-4.9 and 4-4.5 respectively. The results of these experiments showed that the optimum iron powder concentration, for the maximum amount of cobalt deposition, was 100 g/l. In the case where the concentration of iron powder was 100 g/l or less, a sharp increase in the rate of cobalt deposition occurred after about 15 minutes (see fig. 18 and 19). Thus the cementation process appears to be autocatalytic since the existing cobalt deposit aids the deposition of the material later in the reaction.

In experiments C.F.7 and C.F.8, which contained 200 and 300 g/l of iron powder respectively, the rate of deposition was low. This was, probably, mainly due to very poor fluidization at these powder concentrations. Thus a significant amount of iron powder settled on the base of the chamber during the two experiments. However it is possible that side reactions in competition with the cementation reaction, are associated with the poor deposition rate. For example the PH of the solutions in these cases increased rapidly during the course of these experiments, which could have been due to evolution of hydrogen. However, there is not any obvious explanation why such side reactions should be particularly prominent in very concentrated beds.

An abrupt change occurred in the slope of the curve showing the relationship between time and the amount of cobalt deposited at the point where a few drops of silicone anti-foaming agent were added during experiment C.F.5

(see fig. 18) to control the generation of froth in the bed. No such change in the slope of the corresponding curve occurred during experiment C.F.6 which did not require the addition of silicone. Thus there appears to be a relationship between the use of this reagent and a reduction in the deposition rate.

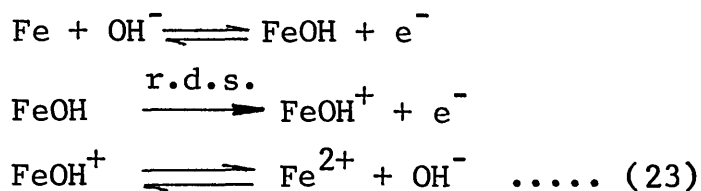
5.2.3 The Influence of PH on the Cobalt Cementation Rate

The investigation of the influence of PH on the cementation process shows that the maximum rate of cobalt deposition occurred in solutions containing 100 g/l cobalt sulphate with 100 g/l of iron powder, with PH in the range 4 to 4.5 (see fig. 20). This range changes to between 3.5 to 4 when the cobalt sulphate is replaced by cobalt chloride of the same concentration (see fig. 21). The details, on which these conclusions are based, are shown in tables 18 and 19.

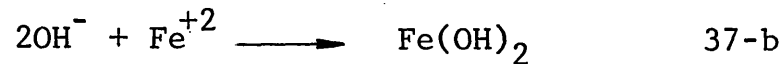
It is possible that the maximum rate of the cobalt deposition within the optimum PH range was associated with equation 1, viz.



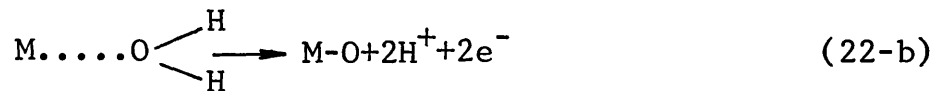
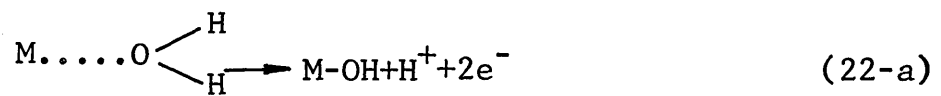
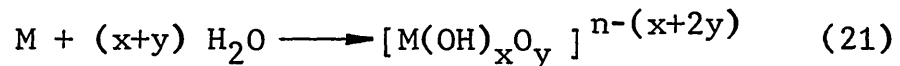
At higher PH values the reactions are probably as shown by equation 23, viz.



or as has been suggested by Fletcher and Cifentes⁽¹⁰⁵⁾,



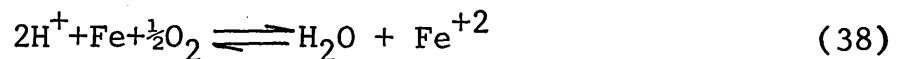
On the other hand low iron powder dissolution at high PH values may be due to formation of a passive layer (as indicated by reaction 21 and 22),



In the case of PH's below the optimum level the reaction shown by equation 32 may facilitate the evolution of hydrogen



Rickard and Fuerstenau⁽¹⁰⁶⁾ have suggested in the case of Cu^{++}/Fe cementation another reaction involving hydrogen



In the present instance it is possible that this last reaction will not be significant on account of limited oxygen availability in the solution: absorption of this element would be hindered by the presence of the nitrogen fluidizing gas.

The high rate of iron powder dissolution at low PH values in experiments C.F.10, C.F.39 and C.F.40 combined

with small amounts of cobalt deposition clearly indicates the significance of the side reactions at low PH values. Likewise importance of side reactions was observed at high PH values, where again the ratio of (dissolved iron/deposited cobalt) was high (6.65 in C.F.13). On the other hand the high cobalt deposition rates at the optimum PH levels was associated with low (dissolved iron/deposited cobalt) ratio (2.87 in C.F.11 and 2.32 in C.F.6). This clearly indicates that the consumption of iron by side reactions was minimised in solutions at the optimum PH. Under these circumstances the cementation reaction will be predominant.

At the optimum PH the rate of deposition of cobalt from cobalt sulphate was significantly greater than that obtained from the corresponding solution of cobalt chloride. However the rate of cobalt deposition to iron dissolution was significantly greater when the latter solution was used. Thus the side-reactions that lead to the excessive consumption of iron powder are reduced by the presence of chloride ions. However, it is not clear why this does not lead to a simultaneous improvement in the rate of cobalt deposition as a consequence of the cementation reaction.

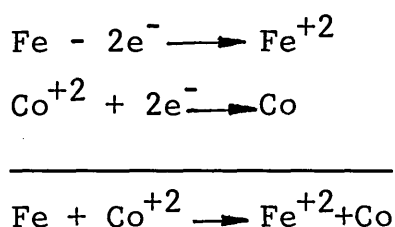
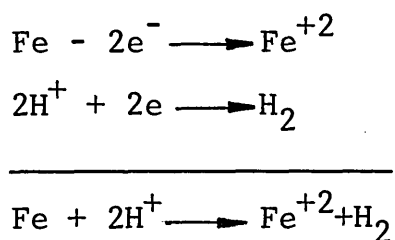
5.2.4 Effect of Boric Acid on the Cobalt Cementation

The effect of boric acid on the rate of cobalt cementation in the fluidized bed cell was not very large

(see tables 21 and 22). These results support those obtained in the mechanically stirred cell. The maximum rate of the cementation for cobalt chloride was obtained from a solution that contained 15 g/l of boric acid, 14.4% cobalt in ninety minutes in experiment C.F.24. The corresponding quantities of cobalt of the cementation in solutions containing nought g/l and 30g/l boric acid were 9.2 and 10.56% respectively. Further addition of boric acid to 60g/l produced some improvement but not enough to restore the amount recovered to 14.4%. The rather irregular variation in the results are probably due to fluctuations in the temperature and the PH of the solutions (see tables 20 and 21).

The addition of 15g/l boric acid had little effect on the rate of the cementation reaction in cobalt sulphate solutions (compare C.F.6 and C.F.28 in 21). Although this amount of boric acid produced a small increase in the percentage of cobalt contained in the powder the recovery of cobalt, as measured by the quantity of this element cemented from a constant volume of solution was less than that obtained from a solution free from boric acid (19.45 g/l and 17.06 g/l in C.F.6 and C.F.28 respectively). Thus the use of boric acid does not have a very significant effect on cobalt deposition except in the control of the PH of the solution. This leads to the reduction in the amount of hydrogen generated by means of a side reaction. Although it is not possible to make an accurate quantitative

assessment of this effect some indication of the reduction in the quantity of hydrogen evolved may be obtained from consideration of quantities of cobalt and iron involved in two experiments, one of which used 15 g/l boric acid while the other used none of this constituent. Thus;



If we call the current, generated by dissolution of iron i_{Fe} , and ^{that} consumed by deposition of cobalt and evolution of hydrogen are i_{Co} and i_{H} respectively. The mass of the dissolved iron can be expressed by the Faraday's law as;

$$\begin{aligned} W_{\text{Fe}} &= \frac{i_{\text{Fe}} \cdot t \cdot A'_{\text{Fe}}}{n_{\text{Fe}} \cdot F} \\ W_{\text{Fe}} &= \frac{i_{\text{H}} \cdot t \cdot A'_{\text{H}}}{n_{\text{H}} \cdot F} + \frac{i_{\text{Co}} \cdot t \cdot A'_{\text{Co}}}{n_{\text{H}} \cdot F} \end{aligned} \quad (39)$$

consideration of the amounts of cobalt deposited and iron dissolved in a solution containing 15 g/l boric acid (experiment C.F.24) suggests that;

$$\begin{aligned}
i_{\text{Fe}} &= \frac{W_{\text{Fe}} \cdot n_{\text{Fe}} \cdot F}{t \cdot A} \\
&= \frac{22.73 \times 2 \times 96493}{5400 \times 55.847} \\
i_{\text{Fe}} &= 14.548 \text{ mA} \\
i_{\text{Co}} &= \frac{13 \times 2 \times 96493}{5400 \times 58.933} \\
i_{\text{Co}} &= 7.88346 \\
i_{\text{H}} &= i_{\text{Fe}} - i_{\text{Co}} \\
i_{\text{H}} &= 6.6614 \text{ mA} \\
W_{\text{H}} &= \frac{6.6614 \times 5400 \times 1}{96493} \\
W_{\text{H}} &= 0.1864 \text{ g.} \\
V_{\text{H}} &= \frac{W_{\text{H}} \cdot 2}{22.4} \\
V_{\text{H}} &= 2.0876 \text{ l.}
\end{aligned}$$

The corresponding amount of hydrogen evolved during experiment C.F.17 was 6.9l. Thus the absence of boric acid in this latter case is likely to be associated with a greater quantity of hydrogen evolution.

5.2.5 Effect of Temperature on the Cobalt Cementation

One of the most important factors that affected the rate of cobalt cementation was temperature. The investigation of this effect was carried out in solutions that contained either 100 g/l of cobalt chloride or 100 g/l of cobalt sulphate (see tables 22 and 23).

There was usually an abrupt increase in the cementation

rate as the temperature rose above 50°C (see figures 24 and 25). However the magnitude of this effect was greater in the case of cobalt chloride solutions than it was in the case of those containing cobalt sulphate (see fig. 26). After 30 minutes there was a significant increase in the amount of cobalt deposited from the cobalt chloride solution at temperatures above 50°C. The corresponding increase in cobalt sulphate solutions began after 15 minutes at temperatures above 60°C.

The relatively low rate of deposition at the start of the cementation process may indicate that an auto-catalytic reaction is involved, as suggested in the discussion of the results obtained in the mechanically agitated cell. The rate of deposition of cobalt is probably enhanced by the existence of previously deposited cobalt at cathodic sites. Another possibility is that during the course of the reaction, the area available for iron dissolution is increased. Annamalai et al⁽¹⁰⁴⁾ found an increase in the rate of cementation of copper onto iron, and attributed it to the enhancing effect of the surface deposit. Cornet et al⁽¹⁰⁷⁾ suggested that an enhanced cementation rate, during a deposition reaction, is associated with an increase in the effective cathodic area. Fletcher and Cifuentes, have found a similar change in the energy of Ni⁺⁺/Fe cementation reaction, which changed at 50 and 70°C, from 28.2 to 64.5 kJ/mol and from 68.9 to 144.4 kJ/mol from the Watt's type and nickel chloride

spectively.⁽¹⁰⁵⁾
 solutions respectively.⁽¹⁰⁵⁾ However these activation energies were obtained from measurements of the change in the amount of material deposited on the powder rather than changes in the concentration of the solution. The two methods are equivalent provided a significant change in the solute concentration in the solution has not occurred.

The activation energies of the reactions occurring above 50°C, after taking the evaporation factor into account, are 107.77KJ/mol for 100 g/l cobalt chloride (fig. 45) and 49.207 KJ/mol for 100 g/l cobalt sulphate solutions (fig. 46) which were calculated as follows;

$$\log \left(\frac{C_i}{C_o} \right) = -k_o A_s t / \bar{V} \quad (40)$$

$$\text{where } \bar{V} = \frac{V_i + V_r}{2} \quad (41)$$

where \bar{V} , V_i and V_r are mean, initial and final solutions volumes respectively, and $A = 1.4302 \text{ dm}^2/\text{g}$ iron powder.

E , the activation energy, is then obtained from the Arrhenius equation

$$\log \frac{K_2}{K_1} = \frac{\Delta G^*(T_2 - T_1)}{2.302 \cdot R \cdot T_2 \times T_1} \quad (42)$$

where $T_2 > T_1$, and K_2 and K_1 are corresponding to values on the curve of $\log K_o$ against $(1/T)10^3$ diagram.

It was, in practice, difficult to measure the volume of the solution remaining at the end of the experiment since extra liquid was introduced while extracting the

powder. It was therefore necessary to obtain the final volume of the solution indirectly from measurements of the dissolution of iron and cobalt in the solution and in the powder. Thus,

$$\begin{aligned} & \text{Final mass of powder (U)} \\ & = \frac{\text{Mass of cobalt in final powder (D)}}{\% \text{ of cobalt in the final powder (E)}} \end{aligned}$$

But,

$$D = \text{Initial mass of cobalt in solution (C)} - \text{Mass of cobalt in final solution (S)}$$

Therefore,

$$U = \frac{C-S}{E} \quad (43)$$

Also

$$S = \text{Final volume of the solution (V}_r) \times \text{Final cobalt concentration (l)}$$

Therefore,

$$U = \frac{C-V_r l}{E} \quad (44)$$

By consideration of a mass balance for iron, and a similar analysis the final mass of powder (U) may be shown to be given by the equation

$$U = \frac{F-V_r k}{G} \quad (45)$$

where F = initial mass of iron powder

k = concentration of dissolved iron in the final solution.

G = % of iron in the final powder.

Eliminating U in equations 44 and 45

$$\frac{C-V_r l}{E} = \frac{F-V_r k}{G}$$

$$V_r = \frac{EF-GC}{Ek-Gl} \quad (46)$$

Then the mean volume \bar{V} required in equation 41 was then obtained for $\bar{V} = \frac{V_i + V_r}{2}$.

The values of the activation energy obtained by these calculations are within the range that Bockris and Conway⁽¹⁰³⁾ suggest is associated with charge transfer control.

5.2.6 Effect of Cobalt Salt Concentration on the Rate of Cobalt Deposition.

Table 24 shows the effect of cobalt chloride concentration in the solution on the rate of deposition of cobalt on the iron powder. An increase in the concentration of this salt from 100 g/l to 250 g/l produced an increase in the rate of deposition, as shown in fig. 27. This two and a half times increase in the solute concentration gave a five fold increase in the rate of cobalt deposition. It is possible that this increased deposition rate is due to a rise in the overall mass transport under the influence of a higher initial concentration gradient. However in that case it is expected a first order reaction increase will occur relative to the metal ion concentration in the solution,

i.e.

$$k = - \frac{\bar{V}}{A_s t_i} \cdot \log \left(\frac{C_i}{C_o} \right) \quad (47)$$

The relationship between concentration of cobalt ions and k obtained from three of the four results shown in table 27 are consistent with equation 47, indicating that the results can be explained in terms of a first order reaction. The one result, obtained in 150 g/l is rather lower than this equation would indicate.

5.2.7 Effect of Additions of Sodium Sulphate on Cobalt Cementation

Sherwood et al⁽⁹⁶⁾ have reported that the addition of sodium sulphate to cobalt and nickel electroplating solutions used in fluidized beds. The purpose of such additions was to increase the conductivity of the electrolyte, which they considered would increase the rate of deposition. Copper recovery by cementation has also been improved by the use of this constituent⁽¹⁰⁸⁾.

The addition of 60 gl⁻¹ Na₂SO₄ in experiment C.F.39 of the present work gave a poor rate of cobalt deposition (1.6% in 90 minutes, see table 25 and fig. 28). Although this value was higher than that obtained from a corresponding solution free of sodium sulphate used under similar conditions (see experiment C.F.9, table 18). At the low PH values involved very high rates of iron dissolution were obtained, probably on account of side reactions that involved hydrogen evolution. The use of

sodium sulphate slightly reduced this iron dissolution, but the magnitude of this effect was still very high.

5.3 Electrodeposition in the Fluidized Bed Cell

A limited series of experiments were carried out which involved the electrodeposition of cobalt from acidic cobalt sulphate solutions (see table 26).

Comparison of the results of the electroplating experiment C.F.41 with the corresponding result obtained under electroless conditions (C.F.28) shows that the amount of deposition of cobalt was greater in the former case. There was virtually no net loss of cobalt from the solution in the electroplating case, although the amount of iron that dissolved in the solution was substantial in both experiments.

The total quantity of cobalt deposited in experiment C.F.41 was 43.6% higher than that obtained in the electroless case (C.F.28). Thus the increased amount of deposition that resulted from the use of an electric current was smaller in proportion than the amount obtained by cementation. Furthermore the iron dissolution process continued throughout the experiment from which it may be concluded that the original iron particle did not become completely coated by electrodeposit. Thus the situation was very complex, since these sites that were anodic during the electroless deposition case, and at which iron dissolution occurred during the cementation reaction,

remained free of cobalt deposit when an electric potential was applied to the cell. Since cobalt deposition should then occur at all points on the powder when it was in contact with the cathode, it would appear that the cementation reaction which maintains some anodic points on the powder at other times, dominates the process and prevents the build up of cobalt at such portions. Alternatively, the electrodeposition process when the powder is in contact with the cathode is selective, and is concentrated at those points where cobalt is also deposited by cementation.

A marked change in the morphology of the deposit was not produced by the use of an electric current. The mixed cemented and electrodeposited material shown in fig. 42-C showed both flakes and a spongy structure, whereas the electroless deposit was predominantly spongy. However, there is insufficient evidence to show that these flakes are electrodeposits.

Experiment C.F.43 used a PH of 5.2, which is known to be associated with poor cementation rates. However, the use of electrodeposition did not lead to a marked increase in the rate of deposition relative to that obtained by cementation alone. Therefore, a deposition process dominated by electrodeposition was not produced.

5.4 Morphology of the Layer of Cobalt Deposited on the Iron Powder

An even coating of cobalt onto iron powder was never

observed. The edges of the non-circular pits and the protrusions on the non spherical particles appeared the most favoured positions to receive the first cobalt deposits. This can be seen in five and eleven o'clock directions in the centre of fig. 30-A and seven o'clock direction of figure 32-A. These positions appeared to be rich in anodic sites. In addition, general views of coated particles suggest that irregularly shaped and highly pitted particles are more likely to provide suitable deposition sites than the smooth surfaced particles (figures 29-A, 30-A and 31-A).

The shape of the pits also effects the cobalt deposition process; if the pits are circular, it does not appear to receive a significant amount of cobalt (see figure 32-A). Thus the mean cobalt content of the powder in this figure was 2.96%, but this element was not detected on the edge of these pits with circular morphology. Further evidence of such anodic sites is shown in sections of iron particles (figures 33-37); these figures also clearly show the irregular nature of the cobalt deposit. The absence of a continuous layer is important with respect to the cementation process, since the separation of all the iron portions of the particles from the solution would prevent the formation of Fe^{++} ions in the solution, and so bring the cementation reaction to an end. With this irregular morphology the continuation of the cementation process is not dependent on an abrasion process

that constantly removes deposited material, as suggested by Fisher⁽¹⁰⁸⁾ with respect to copper cementation.

If the whole surface of a pit remains anodic and the continuation of the cementation process causes the pit to become deeper there will be an effective increase in the anodic surface area of the particle. At the same time continued deposition on the first sites to be covered in cobalt will cause the cathodic surface to also be increased. Thus both anodic and cathodic surface areas are likely to change in size as the deposition process continues, although the ratio between the two surfaces may be relatively unchanged.

In some instances, where the quantity of cobalt was substantial (e.g. 35% as in fig. 35-A) the iron particle was, it appeared, surrounded by a large number of smaller cobalt particles with highly irregular morphology. It is not clear whether these sections represent particles that are joined together and form a continuous whole with the iron particle or whether each is quite separate. The continuous nature of the cobalt image in figure 35-B suggests the former, as do the small necks of solid material that occasionally connect the highly porous cobalt particles in the plane of the section. However generation of individual cobalt particles by an abrasion technique similar to that suggested by Fisher⁽¹⁰⁸⁾ cannot be completely ruled out. Figure 35-B also shows that the

iron particle remains in contact with the solution even when the cementation process is far advanced.

The S.E.M. photographs of the iron particles show a variety of deposit morphologies. There is not a clear relationship between the morphology of the cobalt deposit and PH, although most of the deposits obtained from cobalt chloride solutions with a PH of 3-4 were spongy (e.g. see figures 29-A, 31-A, 38-A). The morphology of the deposits, from cobalt sulphate solutions, differ from those produced from the chloride solutions. The former show both dendritic and flaky structures (see fig. 40-A) at a PH of 4-4.5, and a spongy structure at a PH of 4-5 (see fig. 42-A). The observation of a nodular structure in figures 39-A and 42-A may be due to the short deposition time relative to that used in the other experiments. Annamalai and Murr⁽¹⁰⁴⁾ related the spongy structure in the deposits to the use of a stationary electrode while nodular deposits were associated with the use of a rapidly rotating electrode.

A change in the deposit morphology was observed as the reaction time increased from 30 to 90 minutes (see figures 42-A and 42-C respectively). Thus the nodular deposit observed in the early stages of the process was replaced by the spongy morphology characteristic of the later stages. It is not clear whether this change was a normal progression during growth or whether a small increase in PH towards the end of the process was respon-

sible.

When a potential was applied across the cell containing a cobalt sulphate solution at a PH between 4 and 4.5 the deposit consisted of a mixture of spongy and flaky morphology (see fig. 43-A), while that produced under equivalent conditions, but without an electric potential was spongy (see fig. 42-C).

Since the rate of deposition was greater than can be maintained by electro-deposition alone and that the rate of deposition did not fall significantly with time the "anodic" sites on the powder must remain in contact with the solution, to allow the cementation process to continue. Fig. 43-A clearly shows that the electro-deposition component of ^{the} process has in fact not covered these "anodic" sites with electrodeposit.

6. CONCLUSIONS

1) Replacement of iron powder by cobalt takes place by means of the cementation reaction



in a three phase fluidized bed: under optimum conditions 35% of the iron could be replaced in 90 minutes. Furthermore almost complete removal of the cobalt ions in the solution was possible by means of this reaction.

2) The experimental variables that had the greatest effect on this process were the PH of the solution and the solution temperature. The temperature of the solution should be as high as is practically possible and its PH should be approximately 4 although the optimum range varied slightly with the type of solution used.

3) Optimum fluidization was obtained when the iron powder concentration was 100 g/l of solution and the gas flow rate was 5 l/min. At higher powder concentrations and lower flow rates a significant amount of powder lay on the base of the cell.

4) An increase in the cobalt ion concentration generally increased the rate of cobalt deposition in accordance with the rate equation of a first order reaction.

5) The cobalt cementation reaction proceeded autocatalytically.

6) Simultaneous deposition of cobalt electrolytically

and by cementation did not lead to the formation of a complete layer of cobalt, since iron at anodic sites remained in contact with the solution.

7) The morphology of the layer of cemented cobalt was very irregular, with anodic sites remaining in contact with the solution until at least 70% of the iron had been replaced by cobalt. A variety of morphologies were observed. Although an attempt at a classification of these morphologies has been made a mixture of structures was frequently found on the same particle, which made such classification very difficult.

8) The effect of process variables on the deposit morphology was not clear although this deposit was always irregular.

7. Recommendations

1) The fluidization process in the cell was sometimes rather irregular: improvements in design, e.g. by the use of glass blattoni in the lower section, might be possible.

2) The process should be used with commercial waste cobalt solutions, to see whether constituents other than cobalt affect either the cementation reaction or the purity of the product.

3) The cementation process should be continued until the maximum amount of replacement of iron by cobalt has occurred, in order to ensure the maximum purity obtained in the product.

4) Both coarser and finer iron particles should be studied to investigate the effect of this variable on the cementation reaction and the fluidization process.

REFERENCES

1. H. Dixon, A.J. Fletcher & R.T. Cundill, Powder Met. 1978, No. 3, 131-140.
2. S. Jaiswal, A.J. Fletcher & R.T. Cundill, PH.D. thesis of H. Dixon 1980, Sheffield City Polytechnic.
3. L. Cifuentes, Private Communication.
4. D.R. Gabe, Principles of metal surface treatment and Protection, Pergamon Press.
5. D.R. Crow, Principles and Application of Electrochemistry, Pub. by Chapman and Hall, London, 1974.
6. M.E. Wadsworth, Reduction of metals in Solution, Trans. Met. Soc. AIME, Vol. 245, July, 1969, 1381-1394.
7. C. Wagner, Corrosion Science, 5.751. 1965.
8. N.D. Tomashow and G.P. Chernowa, Passivity and Protection of Metals, Pub. Plenum Press, N.Y. 1967.
9. K.J. Vetter, Electrochemical Kinetics, Theoretical and Experimental Aspects, Academic Press, N.Y. 1967.
10. J.W. Diggle, Oxides and Oxide films. Pub. Marcel Dekker Inc. N.Y. 1972.
11. J.M. Bockris et al. Electrochem. Acta. 4, 325, 1961.
12. D.W. Rice et al. Atmospheric Corrosion of Cobalt, J. El. Chem. Soc. Elec. Chem. Sci. and Tech. Sept. 1979 (1159-1166).
13. T. Ohtsuko and N. Sato. 27th Meeting of Int. Soc. of Elec. Chem. 1976.
14. B.D. Drozdov. Zhur Priklad Khim, 1958.
15. B. Meddings, J.A. Lund. Can. Min. and Met. Bul. July, 1963.
16. Wasyl Kunda. Hydromet. 7, (1981), 77-97.
17. B. Meddings and V.N. Mackiv. The Gaseous Reduction of Metals from Aqueous solutions. Unit Proc. In Hydromet. Met. Soc. Conf. Dallas, Texas 1963.

18. A.R. Burkin. Metallurgical Reviews 1967, Vol. 12. (1-10).
19. F.A. Shaufelberger and T.K. Roy. Bul. Ins. Min and Met. 1955, 64, (375-93) (500-14).
20. R. Hitesman and W. Kunda. Hydromet. 4, 1979, 345-375.
21. H. Narkus. Metallizing of Plastics. Pub. by Reinhold Pub. Inc. N. Y. 1960.
22. F. Pearlstain. Metal Finishing, August 1955, Vol. 53, (08), 59.
23. D.J. Levy. Electrochem. Technol. 1963, 1.38.
24. E.A. Sullivan. Metal Plating by Chemical Reduction with Borohydrates, U.S. Pat. No. 2,942, 990, August 1960.
25. McLeod, H. Chemically Reduced Co-B alloy, U.S. Pat. No. 3,063,666.
26. W.H. Safranek. The properties of Electrodeposited metals and alloys. Pub. Elsevier, 1974, p.439.
27. H. Zeilmaker. Reducing agents for Ni and Co plating. 27th Meeting of Inter. Soc. of Elect. Chem. Amsterdam, Oct. 1976.
28. F. Pearlstain and R.F. Weightman. J. El. Chem. Soc. Elec. Chem. Sci. and Technology, August, 1974, 1023-1028.
29. G.A. Sadakow and E.A. Sullivan. The Progress of Electroless cobalt deposition, Met. Abs. 1979, 12. 35. 1843.
30. B.V. Rao, Y.V. Rao and Y.L. Saha. Trans. Indian Ins. Metals, Feb. 1973, 26(1), 1-5.
31. J.R. De Pew. J. El. Chem. Soc. El. Chem. Sci. and Tech. Sep. 1973, 1187-1192.
32. I.M. Ivanov et al. Hydromet. 4. 1979. 377-387.
33. J.L. Sabot and D. Bauer. J. Inor. Nucl. Chem. Vol. 41, p.767-769.
34. A.W. Ashbrook. Inor. Nuc. Chem. 1972, Vol. 34, 1721-1737.
35. A.J. Van der Zeeuw. Hydromet. 4. 1979, 21-50.

36. J. Shibata and S. Nishimura. Trans. Japan. Ins. Met. Nov. 1977, 18.11. 794-802.
37. E.P. Zhelibo and T.V. Chubar. Poroskovaya Met. 1974, Oct. 10, 1-7.
38. Yu. I. Kimechenko et al. Sov. Pow. Metall. Met. Ceram. April 1975, 14. 266-268.
39. S. Harada et al. J. Jpn. Soc. Pow. Metall. April 1978, 25(3), 80-85.
40. M.R. Edwards and D.G. Lovering. Electrowinning and Refining, Int. Metals Reviews, Sep. 1976.
41. G.S. Victorovich and A.P. Serikov, V.V. Waumov. Sov. J. of Non-Ferrous Metall. 1971, 44.10. 12-16.
42. A. Filmer, A.J. Parker, M. Ruone, and L.G.B. Wadley, Proc. Aust. Inst. Min and Met. 1978, Dec. 2.68. 39-46.
43. F.R. Morral. Met. Finish, June, July 1964, 59-64.
44. G.R. Lakshrimarayanan, E.S. Chen and J.S. Sadak, J. El. Chem. Soc. Ele. Chem. Sci and Tech. 11. 1976. 1612-1616.
45. R. Walker. Met. Finish. May-June 1978.
46. M. Yamamoto, T. Sato and Y. Shimazaki. Mem. Fac. Eng. Hokaida Univ. Dec. 1976, (3), 45-54.
47. R. Sard, R. Weil and C.E. Schwartz. J. Elec. Chem. Soc. May 1966, 424-428.
48. F.R. Morral. Plating, Sept. 1965 (879-888).
49. F.R. Morral. Plating, June 1967, (693-701).
50. S. Armyanav, S. Vitkova. Surf. Tech. 7, 1978, (319-329).
51. A.E. Fallicheva, B.A. Spiridonau, Y.N. Salimov and S.V. Zhernokleova. Zashchita Metallov. 11. 662, 1975.
52. R. Sivakumar and T.L. Rama Char. Plating, Sept. 1972, (861-867).
53. L.A. Kukoz and V.V. Terenteva. Trudy Novoherkes Politekhn. Ins. 287. 62. 1974.

54. C.H. Chisholm. El. Dep. and Surf. Treatm. 3. 1975. 321-333.
55. F.A. Still and J.K. Dennis. Metallurgia and Metal Forming, Jan. 1977. 10-21.
56. M.E. Browning and E.W. Turns. A.S.T.M. Spec. paper No. 318. 107, 1962.
57. M.E. Browning and F.J. Dunkerly. A.S.T.M. Spec. paper No. 64. M.53.
58. S.K. Narang and T.L. Rama Char. Met. Finish. Sept. 1971, 52-53.
59. V.P. Greco. Plating. Feb. 1972, 115-125.
60. W.H. Safranek. Modern Electroplating. Ed. F.A. Lovenhaim. Pub. John Wiley and Sons. Inc. N.Y. 1975.
61. S.C. Sirivastav. Surf. Tech. 10. 1980. 237-257.
62. M. Sarojamma and T.L. Rama Char. Met. Finish. Oct. 1971.
63. K.E. Heusler and L. Fischer. 27th Meeting of Int. Soc. of El. Chem. 1976.
64. L. Holt, J. Stanyer and R.J. Ellis. Plating, Sept. 1973, (918-921).
65. Y.N. Sadama and S. Yajima. Surf. Tech. 4. 1976, 331-338.
66. V.B. Singh and P.K. Tikoo. Surf. Tech. 7. 1978, 225-237.
67. W.R. Wearmouth and K.C. Belt. Trans. Inst. Met. Finish. 1974, V.52, 114-118.
68. M.J. Wilkinson and E. Jackson. Br. Corr. J. 1976, Vol. 11, No. 4, 208-211.
69. M.A. Schluger, I.F. Ponomorenko and A.I. Saimanova, Protection of Metals, 1972, V.8, 56-59.
70. V.E. Carter. Trans. Ins. Met. Finish. 1973, V.51, 103-107.
71. T. Takei. Surf. Tech. 8. 1979, 543-552.
72. R. Walker. Met. Finish. Nov. 1972, (334-336).

73. J.H. Lindsay and H.J. Read. Plating, May 1970, 497-503.
74. D.H. Buckley. Nasa Tech. Paper, NASA, T.M.-X-52246, Mar. 1968.
75. R.D. Sirivastava and S.G. Nigam. Surf. Tech. 10, 1980, 343-348.
76. D.B. Subrahmanyam and T.L. Rama Char. Met. Finish. Dec. 1976.
77. T.R. Ingraham and R. Kerby. Trans. Met. Soc. AIME, Vol. 245, Jan. 1969, 17-19.
78. G. Van der Heiden, C.M. Raats, and H.F. Boon. Chem. and Ind. 1 July 1978, 465-468.
79. B.J. Sabacky and J.W. Evans. Met. Trans. Vol. 8-B, March 1977
80. M. Fleischmann and J.W. Oldfield. J. Elec. Anal. Chem. 29, 1971, 211-230.
81. F. Goodridge and C.J. Vance. Electrochem. Acta. Vol. 24. 12. 1979. 1237-1242.
82. S. Germain and F. Goodridge. Elec. Chem. Acta. August 1976, 21(8), 545-550.
83. F. Goodridge, J.R. Backhurst and M. Fleischman. J. El. Chem. Soc. Nov., 1969, 1600-1607.
84. F. Couret and D. Hutin. J. Appl. El. Chem. 7. 1977, 463-471.
85. Tangappan and H.K.V. Udupa. Trans. of East V. 9. April, 1974.
86. M. Fleischman, L. Tennakon, and J.W. Oldfield, J. Appl. Elec. Chem. 1, 1977, 103-112.
87. D.C. Garbin and D.R. Gabe, J. Appl. Elec. Chem. 5. 1975. 129-143.
88. R. Tanyappan and B. Krishnamurty. Met. Finish. Dec. 1979. 69.(12), 43-44.
89. J.A. Wilkinson and K.P. Haines. Trans. Inst. Min. and Metall. 9. 1972, C.157.
90. M.I. Alkatsev et al. M.A. 74.12.44.80 (Izvest. V.U.Z. Tsvetnaya. Met. 1974. (3) 25-26).

91. M.I. Alkatsev et al. M.A.76.12.58.0768. (Izv. V.U.Z. Tsvetn. Metall. 1976. 1. 49-53).
92. P.G. Alferdson and I.D. Doig. Trans. Inst. Chem. Engrs. Vol. 51, 1973.
93. R.S. Wenger and D.N. Bennion. J. Appl. Elec. Chem. 6. 1976. 385-396.
94. C. Simson and J. Clifford. J. Met. July 1977. 29. (7), 6-10.
95. D.S. Flett. Chem. and Ind. Mar. 1971, 300-302.
96. W.G. Sherwood, C. Nicolic and P.B. Quenau. Met. Trans. B. Vol. 10-B (12). 1979, 659-666.
97. G. Asti and P. Cavalotti. Ceramurgia Int. 2. 1977. Vol. 3. 70-77.
98. R.D. Sirivastava and S.K. Nigam. Surf. Tech. 8. 1979. 371-384.
99. W.T. McFarlon. Plating. Jan. 1970.
100. J. Foster and M. Cameron. Trans. Ins. Met. Finish. 1976. Vol. 54. 178-184.
101. J. Foster and N.M.J. Karalpper. Trans. Ins. Met. Finish. 1973. Vol. 51. 27-31.
102. D.W. Smith and P.D. Groves. Trans. Ins. Met. Finish. 1977. Vol. 55. 136-140.
103. J. O'M Bockris and B.E. Conway. Modern Aspects of Electrochemistry. V.11. pub. by Plenum Press.
104. V. Annamalai and L.E. Murr. Hydrometallurgy. 4. 1979, 57-82.
105. A.J. Fletcher and L. Cifentus. To be Published.
106. Rickard and Fuerstenau. Trans. T.M.S. AIME, 1968. vol. 239, p.1487-93.
107. I. Cornet, W.N. Liwin, and R. Kappesser. Trans. Inst. Chem. Eng. 1969, 47, T 222-226.
108. W.W. Fisher. U.S. Bu. Mines, C.F.R. 40-79, Jul. 1978.

TABLE I

Change of Electrode Potential with Ion Concentration
(at 25°C)

Concentration	1M	10^{-2} M	10^{-7} M	10^{-20} M
Potential (volts)	E°	$(E^{\circ}-0.059)$	$(E^{\circ}-0.21)$	$(E^{\circ}-0.59)$

TABLE 2

Standard Electrode Potentials (reduction at 25°C)

Metal Couple	E° (volts)	Metal Couple	E° (volts)
Li^+/Li	-3.01	$2\text{H}^+/\text{H}_2$	0.00
Ca^{2+}/Ca	-2.87	Cu^{2+}/Cu	0.337
Na^+/Na	-2.713	O_2/OH^-	0.401
Mg^{2+}/Mg	-2.37	Cu^+/Cu	+0.52
Be^{2+}/Be	-1.85	$\text{Hg}_2^{2+}/\text{Hg}$	+0.798
U^{3+}/U	-1.80	Ag^+/Ag	+0.799
Al^{3+}/Al	-1.66	Rh^{3+}/Rh	+0.8
Ti^{2+}/Ti	-1.63	Hg^{2+}/Hg	+0.854
Zr^{4+}/Zr	-1.53	Pt^{2+}/Pt	+1.2
Mn^{2+}/Mn	-1.18	Cl_2/Cl^-	+1.358
Zn^{2+}/Zn	-0.763	Au^{3+}/Au	+1.50
Cr^{3+}/Cr	-0.74	Au^+/Au	+1.70
Fe^{2+}/Fe	-0.44	$\text{Cr}^{3+}/\text{Cr}^{2+}$	-0.41
Cd^{2+}/Cd	-0.403	$\text{Sn}^{4+}/\text{Sn}^{2+}$	+0.15
Co^{2+}/Co	-0.277	$\text{Cu}^{2+}/\text{Cu}^+$	+0.153
$\text{Co}(\text{OH})_2^{+2}/\text{Co}$	-0.73	$\text{Fe}^{3+}/\text{Fe}^{2+}$	+0.77
Ni^{2+}/Ni	-0.25	$\text{Co}^{3+}/\text{Co}^{2+} (3\text{fHNO}_3)$	+1.842

TABLE 3

Cobalt Plating Bath and Relevant Data (104)

No	Bath Composition (g/l)	Temp °C	Current Density amp/cm ²	PH	Cobalt	
					CPH	FCC
1	504 CoSO ₄ ·7H ₂ O.17NaCl.45H ₃ BO ₃	30	100	6.5	X	
2	CoSO ₄	30	0.005-1	1.5 1.2-7	X	X
3	CoSO ₄ ·Co(NH ₄) ₂ (SO ₄) ₂	30	0.01-1	1.7-5		
4	350 CoCl ₂ ·20H ₃ BO ₃		0.006			
5	300 CoSO ₄ ·7H ₂ O.3NaCl, 6H ₃ BO ₃		2-8.10 ⁻⁵			
6	300 CoSO ₄ ·7H ₂ O.3NaCl.6H ₃ BO ₃		16.10 ⁻⁵		X	X
	" " " "		(4-0.32)10 ⁻³		X	X
7	20-40 CoCl ₂ ·6H ₂ O	25	0.016	2	X	X
8	40-125 " "			2	X	
9	40-125 " " + saccharin			2	X	X
10	1-1.8M CoSO ₄ ·0.5M H ₃ BO ₃	20-80	0.001-0.08	1.3-6.2		
11	140-500 CoSO ₄ 7H ₂ O. 0-40 H ₃ BO ₃	0-80	0.005-0.03	1.3-1.9	X	X
12	140-500 CoSO ₄ ·7H ₂ O. 0-40 H ₃ BO ₃			1.9-6.2	X	
13	300 CoSO ₄ ·7H ₂ O.3NaCl.6H ₃ BO ₃			4.10 ⁻⁶		X

TABLE 3 - II

(continued from previous page)

No	Bath Composition (g/l)	Temp °C	Current Density amp/cm ²	PH	Cobalt	
					CPH	FCC
14	175 CoSO ₄ ·(NH ₄) ₂ ·6H ₂ O·17NaCl·50H ₃ BO ₃	20-50	100			
15	17,5 CoSO ₄ (NH ₄) ₂ SO ₄ ·6H ₂ O, 17NaCl, 45H ₃ BO ₃	20, 50	0.0061			
16	200 CoSO ₄ (NH ₄) ₂ SO ₄ ·6H ₂ O, 17NaCl, 30H ₃ BO ₃	20	2.5		X	X
17	300 CoSO ₄ ·7H ₂ O·30H ₃ BO ₃	25-55	50-500	1.4	X	X
18	298 CoCl ₂ ·6H ₂ O, 30H ₃ BO ₃	"	"	1.4	X	X
19	319 CoSO ₄ ·7H ₂ O 45 CoCl ₂ 6H ₂ O, 30H ₃ BO ₃	"	"	1.4	X	X
20	250 CoSO ₄ ·7H ₂ O 25KCl. 25H ₃ BO ₃		100	5.4-7		
21	CoSO ₄ ·7H ₂ O	30-50	50-800	2.5-5.3		
22	282 CoSO ₄ ·7H ₂ O·15KCl, 65Na ₂ SO ₄ · 10H ₂ O·12H ₃ BO ₃	50				
23	500 CoSO ₄ ·7H ₂ O·17NaCl 45H ₃ BO ₃	30	0.008-0.5	5.41	X	
	"	45	0.094		X	X
	"	70	0.094			X

TABLE 3-- III

(continued from previous page)

No	Bath Composition (g/l)	Temp °C	Current Density amp/cm ²	PH
24	565 CoSO ₄ ·7H ₂ O.25KCl.9H ₃ BO ₃	20	900-3600	3-5.7
25	3n.Co fluoborate, 8H ₃ BO ₃	25	41	3.15
26	N Co fluoborate 0.4 naphthol, 8H ₃ BO ₃	25	418	3.6
27	450 Co sulfamate, 30ml. formate, 375 antipit agent	40	328	2.5-5.5
28	100-500 CoSO ₄ ·7H ₂ O	50	500	1.5-2.5
29	165 CoSO ₄ ·7H ₂ O.85Na ₂ SO ₄ ·17.5MgSO ₄ 35H ₃ BO ₃	65-70	100	4.5
30	400 CoCl ₂ ·6H ₂ O.25 H ₃ BO ₃	25-70	540-2700	5
31	312 CoSO ₄ ·7H ₂ O.20 NaCl.30 H ₃ BO ₃		D.C/A.C	

subs: substrate
 sxtl: single crystals

TABLE 4

Results of Plating Conditions on Structure of Electroplated Cobalt

Lath No.	Cathode	Operation Condition	CPH	FCC	Orientation		Remarks
					C.P.H.	F.C.C.	
1	St. steel	PH:6.5-4.5	X				Decreasing to 1.5 increases F.C.C
2,3	Cu, Fe, Co	PH 3.5	X	X	(001)Co//((111)Cu		At 4mA/cm ² increase randomly oriented Co. At high PH only C.P.H.
4	Cu		X	X			
5,6	sxtl. Cu		X	X			
	Cu	PH 1.3-1.9	X	X	(1010)//subs		
17	(100) Cu Cu	0.6 A/cm ² - 20 min		X		(110)//((100)C	But at 50°C (100)Co// (100)Cu
15	Pt.(110) [001]	20°C		X	(1120)Co//subs.	Same as subs.	20,000-50,000A deposits are crystalline
18	Au(110) [001] Brass		X	X			
21,22	Co(electroly)					(011)	

TABLE 5

Cobalt-molybdenum and cobalt-tungsten solutions, which were used for die plating

Cobalt sulphate	Sodium Chloride	Boric Acid	Composition g/l				pH	Temp °C	c.d. A/dm ²
			Heptonate	Molybdate	Tungstate				
150	28	40	200	-	-	1.5-2.0	55	4	
150	28	40	100	-	-	1.5-2.0	55	4	
150	28	40	200	3.15	-	1.5-2.0	55	4	
150	28	40	200	6.30	-	1.5-2.0	55	4	
100	28	40	200	12.60	-	1.5-2.0	55	4	
150	28	40	100	3.15	-	1.5-2.0	55	4	
150	28	40	100	6.30	-	1.5-2.0	55	4	
150	28	40	100	12.60	-	1.5-2.0	55	4	
150	28	40	100	-	15.75	1.5-2.0	55	4	
150	28	40	100	-	31.50	1.5-2.0	55	4	
150	28	40	100	-	47.25	1.5-2.0	55	4	
150	28	40	200	-	47.25	1.5-2.0	55	4	

TABLE 6

Chemical Analysis of the Atomet 25 Iron Powder

Components	C	Ni	Mn	Si	S	P	O
Amount %	0.063	0.090	0.008	0.0107	0.006	0.50	0.41-0.680

TABLE 7

Sieve analysis of the Atomet 25 Iron Powder

Mesh Size (μm)	%
+150	8.31
-150+125	7.46
-125+90	27.45
-90+75	14.41
-75+53	19.51
-53+45	3.40
-45	19.42

TABLE 8

Results of Cobalt Deposition Experiment E.T.1 in a Mechanically Stirred Solution.

Test No. E.T.1.	Time (min)	Composition			Conditions			Results		
		CoCl ₂ (g/l)	Fe (g/l)	H ₂ BO ₃ (g/l)	Temp. (°C)	PH	Agit. No.	Powder Co%	Solution Fe(g/l)	Co(g/l)
A	14	100	66	60	18	4.30	4	0.10	0.44	21.6
B	21				18.5	4.55	4	0.15	0.63	21.84
C	31				19	4.6	4	0.10	0.80	22.28
D	40				18.5	4.65	4	0.09	0.97	22.22
E	50				20	4.72	4	0.08	1.11	23.16
F	60				20	4.71	4	0.10	1.26	21.80
G	90				21		4	0.10	1.48	22.30

TABLE 9

Experimental Conditions and Results of the Experiment E.T.2

Test No	Time (min)	Composition			Conditions		Results			
		CoCl ₂ (g/l)	Fe (g/l)	H ₃ BO ₃ (g/l)	Temp. (°C)	PH	Conductivity * (104)	Powder Co%	Solution Co(g/l) Fe(g/l)	
A	11	100	50	60	80	4.4	61	1.56	29.60	3.28
B	20				80	3.3	87	5.00	27.41	6.15
C	30				83	3.4	61	10.03	26.40	10.56
D	40				80	3.85	83	13.8	25.45	13.64
E	50				80	3.3	62	18.6	25.26	17.68
F	60				82	3.2	90	21.6	24.61	22.15
G	90				75	4.3	95	30.2	24.60	38.77

Note: Agitation no: at the beginning of the test was 3.5,

after 10 minutes it was increased to 4. The heating

of the solution being used, so far, was maintained by a hot plate.

* : Unit of conductivity, here and in the following tables, is umho cm^{-1} .

TABLE 10

The Conditions and Results of Experiment E.T.3

Test No. E.T.3	Time (min)	Composition		Conditions			Results		
		CoCl ₂ (g/l)	Fe H ₃ BO ₃ (g/l)	Temp. (°C)	PH	Conductivity (10 ⁴)	Powder Co%	Solution Co(g/l) Fe(g/l)	
A	10	300	50	40	3	10.5	2.34	70.4	1.08
B	20				4	100	2.44	70.34	1.22
C	30				2.25	110	4.14	73.60	2.04
D	40				3.7	100	4.41	79.38	2.63
E	50				2.55	115	30.6	86.66	3.41
F	60				2.7	125	31.8	85.93	4.15
G	90				3.3	100	28.8	95.00	11.43

TABLE 11

Experimental Conditions and Results of the Experiment E.T.4

Test No. E.T.4	Time (min)	Composition		Conditions			Results	
		CoSO ₄ (g/l)	Fe (g/l)	Temp. °C	PH	Agit. No	Powder Co%	Solution Co(g/l) Fe(g/l)
A	10	100	50	79	4.9	3	0.14	22.25 0.43
B	20			79	5.3	"	0.58	22.40 0.63
C	30			79	5.1	"	0.32	22.25 0.95
D	40			78	4.8	"	0.58	25.25 1.40
E	50			77	4.69	3.5	0.88	26.25 1.60
F	60			80	4.71	4	2.26	29.25 1.98
G	90			81	4.53	"	7.00	32.75 3.70

Notes: the PH of the solution was kept below 5 by H₂SO₄ addition.
The solution evaporation rate was 53ml/10min, at 70-80°C.

TABLE 12

Experimental Conditions and Results of the Experiment E.T.5

Test No.	Time (min)	Composition			Conditions		Results					
		CoSO ₄ (g/l)	CoCl ₂ (g/l)	H ₃ BO ₃ (g/l)	KCl (g/l)	Fe (g/l)	Temp. (°C)	PH	Agit. No	Powder Co%	Co(g/l)	Fe (g/l)
A	10	90.55	8	30	20	50	75	4.9	3	0.22	23.75	0.40
B	20						76	4.9	3	0.52	23.50	0.50
C	30						75	5.0	3.5	0.80	24.75	0.75
D	40						75	4.5	"	2.80	25.00	1.50
E	50						75	4.43	"	4.40	25.00	2.21
F	60						73	4.42	"	7.10	25.25	3.00

TABLE 13 - I

The conditions and Results of the Experiments E.T.6 and E.T.7.

Test No.	Time (min)	Composition		Conditions			Results			
		CoCl ₂ (g/l)	Fe (g/l)	Temp (°C)	PH	Agit. No.	Conductivity (10 ⁴)	Powder Co%	Solution Co (g/l)	Solution Fe (g/l)
E.T.6	A	100	50	80	3	3.75	8.1	0.52	39.5	1.25
	B			81	2.6	"	9	0.74	40.5	2.65
	C			80	2.9	"	9.5	1.48	40.5	3.65
	D			80	"	"	9.5	1.94	40.0	4.75
	E			81	"	"	10.5	4.08	43.0	5.80
	F			80	"	"	10	3.36	43.0	6.70
E.T.7	A	100	50	75	3	3.5	9	0.24	40.0	0.55
	B			72	3.1	"	9	0.46	40.5	0.85
	C			70	3.2	"	8.5	0.50	41.25	1.35
	D			74	3.5	"	8.4	1.0	40.0	1.70
	E			72	3.3	"	8.6	1.10	42.0	2.25
	F			70	3.2	"	8.6	1.40	40.5	2.70

Note: The experiments were carried out in the hot water bath.

TABLE 13 - II

The Conditions and Results of the E.T.8 and E.T.9

Test No.	Time (min)	Composition		Conditions				Results		
		CoCl ₂ (g/l)	Fe (g/l)	Temp (°C)	PH	Agit. (No)	Conductivity 10 ⁴	Powder Co%	Solution Co (g/l)	Fe (g/l)
E.T.8		100	50							
A	10			61	3	3.5	6.8	0.13	30.75	0.60
B	20			60	2.8	"	7.1	0.135	31.00	0.90
C	30			61	2.9	"	7.1	0.170	30.85	1.20
D	40			60	3	"	7.45	0.27	31.50	1.50
E	50			60	2.9	"	7.5	0.42	32.00	1.80
F	60			60	3	"	8	0.40	32.20	2.35
E.T.9		100	50							
A	10			50	3	3.5	6	0.08	30.75	0.45
B	20			50	"	"	6.1	0.085	30.75	0.65
C	30			51.5	"	"	6.2	0.096	30.90	0.80
D	40			52	"	"	6.4	0.110	30.10	1.00
E	50			51	"	"	6.5	0.140	31.70	1.15
F	60			50	"	"		0.170	33.00	1.30

TABLE - 13 - III

The Experimental Conditions and Results of the E.T.10 and E.T.11

Test No	Time min.	Composition		Conditions			Conductivity		Results	
		CoCl ₂ (g/l)	Fe (g/l)	Temp (°C)	PH	Agit. No.	Conduc-tivity 10 ⁴	Powder Co%	Co (g/l)	Fe (g/l)
E.T.10		100	50							
A	10			43	3	3.5	5.75	0.080	52.0	0.25
B	20			42	"	"	5.5	0.095	55.0	0.45
C	30			42	"	"	5.4	0.100	54.0	0.45
D	40			40	2.85	"	5.25	0.110	53.5	0.525
E	50			40	3	"	5.3	0.100	56.5	0.65
F	60			42	"	"	5.5	0.094	56.0	0.785
E.T.11		100	50							
A	10			30	2.9	3.5	4.5	0.135	33.0	0.235
B	20			"	2.95	"	4.5	0.166	58.75	0.30
C	31			"	3.0	"	4.55	0.133	56.00	0.35
D	40			"	"	"	4.7	0.100	57.00	0.425
E	50			"	2.9	"	"	0.80	58.00	0.525
F	60			31	2.85	"	"	0.094	56.00	0.55

TABLE 14

Conditions and Results of E.T.12

Test No.	Time (h)	Composition Conditions							Results		
		CoCl ₂ (g/l)	Fe (g/l)	Temp. (°C)		PH	Agit No.	Powder Co%	Solution Co Fe (g/l) (g/l)		
A	7	100	50	78	65	3.4	4	3	13.2	32	16.75
B	14.5				45		4	4	22.0	30	29
C	20.5				50		4	4.5	68.0	27.5	62

TABLE 15

Conditions and Results of the C.F.3 and 4.

Test No.	Time (min)	Composition		Conditions			Results			
		CoCl ₂ (g/l)	Fe (g/l)	Temp (°C)	PH	Gas Flow (l/min)	Conductivity 10 ⁴	Powder Co%	Solution Co (g/l)	Fe (g/l)
C.F.1		100	50							
A	11			69	3	5	2.1	0.22	29.95	0.60
B	20			68	"	"	3	0.44	29.50	1.00
C	30			67	"	"	3.2	0.76	29.50	1.50
D	40			67	"	"	2.6	0.42	30.50	1.95
E	50			68	"	"	3.45	1.10	26.0*	2.80
F	60			68	"	"		1.84	32.5	4.30
C.F.2		100	50							
A	10			75	3	10	1.4	0.22		
B	20			66	3	8.5	1.3	0.26		
C	30			68	3.2	"	1.05	0.48		
D	40			68	3	"	3	0.68		
E	50			68	3	"	1.5	0.90		

* Small amount of distilled water mixed into the sample accidentally.

TABLE 16

Effect of Iron Powder Concentration on the Cobalt
Cementation Rate

Test No.	Time (min)	Compo- sition		Conditions			Results		
		CoCl ₂ (g/l)	Fe (g/l)	Temp (°C)	PH	Conduc- tivity 10 ⁴	Powder Co%	Solution Co (g/l)	Fe (g/l)
* C.F.3		100	50						
A	15			70	4.71	1.8	0.22	40.75	0.10
B	30			67	4.73	2.7	0.30	40.75	0.20
C	60			69	4.65	4	0.84	42.75	0.60
D	90			65	4.5	2.6	1.60	36.25	1.20
C.F.4		100	75						
A	15			78	4.63	4.4	0.3	36.75	0.30
B	30			"	4.64	4.45	1.20	36.0	1.10
C	60			"	4.63	4.63	3.9	33.50	3.2
D	90			70	4.8	4.8	2.8	33.50	4.95
C.F.5		100	100						
A	15			77	4.77	5.2	0.24	43.5	0.30
B	30			75	4.71	0.66	1.44	42.25	1.45
C	60			71	"	1.2	1.76	47.75	2.10
D	90			71	"	1.55	1.98	51.5	2.40

* An accurate gas flow measurement was not possible because of a gas leakage from the heater tube.

TABLE 17

Relation Between the Iron Powder Concentration and Rate of Cobalt Deposition

Test No	Time (min)	Composition		Conditions			Results		
		CoSO ₄ (g/l)	Fe (g/l)	Temp (°C)	PH	Gas Flow (l/min)	Powder Co%	Co (g/l)	Fe (g/l)
C.F.6	15	100	100	68	4.1-4.5	5.5	2.48	22.5	7.5
	30			70	"	4.5	10.0	16.3	20
	60			73	4-4.5	3	22.2	3.84	46.5
	90			73	4-5	2.5	31.0	1.92	72
C.F.7	15	100	200	69	4-4.5	5.5	0.46	21.0	1.25
	30			71	"	4.5	1.40	21.5	10.7
	60			72	"	3.5-3	9.16	17.7	62.5
	90			72	"	"	8.60	6.0	68.5
C.F.8	15	100	300	66	4-4.5	6.5	0.24	21.0	6.50
	30			67	4.5-5	"	0.30	22.0	9.70
	60			70	"	6.5-4	0.52	23.2	18.7
	90			75	5-5.5	3.5-1.5	0.70	10.0	34.2

TABLE 18 - I

Influence of the PH of the solution on the Rate of Cementation of Cobalt onto Iron Powder

Test No	Time (min)	Composition		Conditions		Results			
		CoSO ₄ (g/l)	Fe (g/l)	Temp (°C)	PH	Gas Flow (l/min)	Powder Co%	Solution Co (g/l)	Fe (g/l)
C.F.9	15	100	100	69	3.2-3.5	6.5	1.8	24.5	22.5
	30			73	3-3.5	6.5 5	3.0	24.0	105
	60			73	3-3.5	5 4.5	1.0	27.5	125
	90			70	3.1	4.5	0.0	30.5	"
C.F.10	15	100	100	69	3.7-4	6.5	5.20	23.5	14.0
	30			69	3.6-4	"	10.40	20.0	26.75
	60			71	3.5-4	"	22.8	17.25	75.0
	90			73	"	4.5	2.66	26.25	120.0
	120			68	"	"	6.00	31.50	130.0
C.F.11	15	100	100	67	4-4.5	6.5	1.3	20.0	3.13
	30			68	4-4.2	"	13.6	17.0	10.7
	60			65	4.2-4.4	"	19.6	14.1	22.0
	90			63	4-4.5	"	10.6	14.75	34.5
C.F.6	15	100	100	68	4.1-4.5	5.5	2.48	22.5	7.5
	30			70	"	10.0	16.3	20	
	60			73	4-4.5	22.2	3.84	46.5	
	90			73	4-5	31.0	1.92	72	

TABLE 18 - II

(continued from the previous page).

Test No	Time (min)	Composition		Conditions			Results		
		CoSO ₄ (g/l)	Fe (g/l)	Temp (°C)	PH	Gas Flow (l/min)	Powder Co%	Co (g/l)	Fe (g/l)
C.F.12	15	100	100	69	4.5-5	5	0.54	23.5	1.4
	30			"	3	1.28	25.5	3.85	
	60			4.5-4.7	2.5	4.24	24.0	13.0	
	90			4.5-5	2	8.16	20.5	25.0	
C.F.13	15	100	100	68	5.6	5	0.26	21.28	0.45
	30			5.5-5.6	4.5	0.30	22.0	0.75	
	60			5.4-5.6	4	0.36	24.75	1.93	
	90			5.4-5.6	3.5	0.44	27.0	2.93	
C.F.14	15	100	100	67	5.8	5.5	0.19	22.5	0.32
	30			5.75	"	0.17	23.75	0.25	
	46			5.78	"	0.14	20.50	0.375	
	*								

* At the beginning of the experiment, C.F.14, there was some gas leakage in between the membrane and the lower section of the fluidized bed cell. During the experiment the leakage increased and finally the membrane slipped to one side and the experiment was stopped at the 46th minute.

TABLE 19 - 1

Effect of PH on the Rate of Cobalt Cementation onto Iron Powder from 100g/l
CoCl₂ Solution

Test No	Time (min)	Composition		Conditions			Results		
		CoCl ₂ (g/l)	Fe (g/l)	Temp (°C)	PH	Gas Flow (l/min)	Powder Co%	Solution Co (g/l)	Solution Fe (g/l)
C.F.15	15	100	100	65	2.5-3	7	0.56	28.75	4.25
	30			"	"	2.80	29.00	7.50	
	60			"	6.5	10.24	27.00	16.25	
	90			"	5 4.5	7.52	25.00	27.0	
C.F.16	15	100	100	68	3.3-3.5	5.5	0.6	25.0	2.38
	30			"	"	2.68	"	4.95	
	60			3-3.5	5.5-5	6.0	"	12.0	
	90			"	4.5	6.72	20.75	20.20	
C.F.17	15	100	100	66	3.5-4	6.5	0.54	37.5	2.5
	30			"	"	3.20	36.0	5.5	
	60			"	5	13.20	32.5	14.0	
	90			"	4.5	8.90	29.5	24.0	

TABLE 19 - II

(continued from previous page)

Test No	Time (min)	Composition		Conditions			Results		
		CoCl ₂ (g/l)	Fe (g/l)	Temp (°C)	PH	Gas Flow l/min	Powder Co%	Solutions Co (g/l)	Fe (g/l)
C.F.18		100	100						
A	15			68	3.5-4	5.5	1.08	25.5	1.85
B	30			69	"	"	3.96	29.38	3.60
C	60			68	"	"	12.80	26.5	9.10
D	90			"	3.5-4.4	4.5	9.20	24.5	12.0
C.F.19		100	100						
A	15			65	4-4.5	6.5	0.2	18.0	0.53
B	30			"	"	"	0.3	18.5	1.05
C	60			"	"	"	3.4	19.75	2.10
D	90			"	"	"	3.3	22.05	3.8
C.F.20		100	100						
A	15			63	5.6	5.5	0.2	27.0	0.4
B	30			62	5.53	"	"	29.0	0.25
C	59			64	5.45	"	1.34	29.0	1.80
C.F.21		100	100						
A	15			61	5.67	5.5	0.26	22.0	0.25
B	30			60	5.68	"	0.18	24.5	0.2
C	60			59	5.36	6	0.64	"	0.625
D	90			60	5.43	5.8	1.88	"	2.70
C.F.22		100	100						
A	16			68	5.8	5.5	0.22	23.25	0.125
B	30			66	5.73	"	0.26	25.0	0.175
C	63			68	5.6	"	1.46	25.5	2.05
D	90			68	5.7	"	2.68	27.73	3.75

TABLE 20 - I

Effect of Boric Acid on Rate of Cobalt Deposition from Cobalt Chloride Solutions at 69-76°C

Test No	Time (min)	Composition			Conditions		Gas Flow (l/min)	Results	
		CoCl ₂ (g/l)	Fe (g/l)	H ₃ BO ₃ (g/l)	Temp (°C)	PH		Powder Co%	Solution Co(g/l) Fe(g/l)
C.F.18		100	100	-					
A	15				68	3.5-4	5.5	1.08	25.5 1.85
B	30				69	"	"	3.96	29.38 3.60
C	60				68	"	"	12.80	26.5 9.10
D	90				68	3-4.4	4.5	9.20	4.5 12.0
C.F.23		100	100	12.5					
A	15				69	2.6-3.5	4.5	0.65	26.0 1.25
B	30				70	3-3.5	4.5	2.70	26.50 3.00
C	60				70	3-4	4	6.20	24.0 6.82
D	90				73	"	3	9.40	20.25 12.25
E	120				72	3-4.1	3	11.60	20.70 17.50

TABLE 20-II - Continued from previous page.

Test No.	Time (min)	Composition				Conditions			Results				
		CoCl ₂ (g/l)	Fe (g/l)	H ₃ BO ₃ (g/l)	Temp °C	PH	Gas Flow (l/min)	Powder Co%	Solution Co (g/l)	Solution Fe (g/l)			
C.F.24		100	100	15									
A	16				74	3.7-4	2.5	1.60	21.2	3.85			
B	31				76	"	"	4.08	19.0	9.0			
C	60				"	"	2.3	10.56	15.0	13.5			
D	90				"	"	"	14.40	12.3	23.75			
C.F.25		100	100	30									
A	15				69	3.8-4	5.5	0.80	20.0	2.08			
B	30				71	3.8-4.2	4.8	2.80	21.0	4.10			
C	60				71	"	4.8	12.0	18.5	13.5			
D	92				72	3.5-4.5	3.7	10.56	16.0	23.9			
C.F.26		100	100	45									
A	15				69	3.8-4.2	5	0.64	22.7	2.4			
B	30				70	"	3.5	1.84	21.2	5.0			
C	45				73	"	2.5	4.48	19.2	8.5			
D	60				73	3.8-4.5	2	6.72	16.7	11.1			
E	90				71	3.7-4	2	12.72	12.5	18.0			
C.F.27		100	100	60									
A	15				69	3.7-4	5.5	0.46	21.2	3.0			
B	30				71	"	3	1.60	"	6.0			
C	60				74	3.6-4	2.5	6.36	17.2	12.50			
D	90				74	3.7-4	2	12.32	13.2	19.0			

TABLE 21

Effect of Boric Acid on the Cobalt Cementation Rate, using CoSO_4 at 100g/l of Iron Powder at 100g/l.

Test No	Time (min)	Composition			Conditions			Results		
		CoSO_4 (g/l)	Fe (g/l)	H_3BO_3 (g/l)	Temp ($^{\circ}\text{C}$)	PH	Gas Flow (l/min)	Powder Co%	Solution Co (g/l)	Fe (g/l)
C.F.6		100	100	-						
A	15				68	4.1-4.5	5.5	2.48	22.5	7.5
B	30				70	"	4.5	10.0	16.3	20
C	60				73	4-4.5	3	22.2	3.84	46.5
D	90				73	4-5	2.5	31.0	1.92	72
C.F.28		100	100	15						
A	15				69	4.1-4.6	5	1.2	18.5	3.48
B	30				71	4-4.5	4	5.0	17.5	11.8
C	60				73-74	4-5	3-2.5	22.5	5.0	49.0
D	90				74	4-5	2.5	35.0	4.0	70.0

TABLE 22 - I

The Effect of Temperature on the Cobalt Cementation Rate using CoCl_2 100g/l and Iron Powder 100g/l

Test No	Time (min)	Composition		Conditions			Results		
		CoCl_2 (g/l)	Fe (g/l)	Temp ($^{\circ}\text{C}$)	PH	Gas Flow (l/min)	Powder Co%	Solution Co (g/l)	Fe (g/l)
C.F.22	16	100	100	68	5.8	5.5	0.22	23.25	0.125
	30			66	5.73	"	0.26	25.0	0.175
	63			68	5.6	"	1.46	25.5	2.05
	90			68	5.7	"	2.68	27.73	3.75
C.F.20	15	100	100	63	5.6	5.5	0.2	27.0	0.4
	30			62	5.53	"	"	29.0	0.24
	59			64	5.45	"	1.34	29.0	1.80
C.F.21	15	100	100	61	5.67	5.5	0.26	22.0	0.25
	30			60	5.68	"	0.18	24.5	0.2
	60			59	5.36	6	0.64	"	0.625
	90			60	5.43	5.8	1.88	"	2.70

TABLE 22 - II

(continued from the previous page)

Test No	Time (min)	Composition		Conditions			Results		
		CoCl ₂ (g/l)	Fe (g/l)	Temp (°C)	PH	Gas Flow (l/min)	Powder Co%	Co (g/l)	Fe (g/l)
C.F.29	15	100	100	58	5.65	6	0.16	21.5	0.175
	30			56	5.6	6.5	0.32	22.75	0.3
	60			53	5.83	6.5	0.52	23.75	0.45
	90			53	5.83	7	0.66	23.75	0.675
C.F.30	15	100	100	45	6	6.5	0.24	22.5	0.1
	30			44	6.2	7	0.16	23.75	"
	60			43	6.15	"	0.18	23.25	"
	90			44	6.07	"	0.14	23.75	"
C.F.31	15	100	100	37	6.27	7	0.16	22.5	0.075
	30			38	6.26	"	"	23.25	"
	60			37	6.27	"	"	23.25	"
	90			36	6.27	"	0.12	19.25	0.050

TABLE 23-I

The Influence of Temperature on the Cobalt Cementation Rate

Test No	Time (min)	Composition		Conditions			Results		
		CoSO ₄ (g/l)	Fe (g/l)	Temp (°C)	PH	Gas Flow (l/min)	Powder Co%	Solution Co (g/l)	Fe (g/l)
C.F.13		100	100						
A	15			68	5.6	5	0.26	21.28	0.45
B	30			69	5.6	4.5	0.30	22.0	0.75
C	60			70	5.5	4	0.36	24.75	1.93
D	90			70	5.5	3.5	0.44	27.0	2.93
C.F.32		100	100						
A	15			60	6.5	6	0.16	20.0	0.12
B	30			59	6.6	"	"	22.0	0.10
C	60			"	"	6.5	"	24.25	0.15
D	90			"	"	"	"	26.0	0.22

TABLE 23 - II

(continued from the previous page)

Test No	Time (min)	Composition		Conditions		Results		
		CoSO ₄ (g/l)	Fe (g/l)	Temp (°C)	PH	Powder Co%	Solution Co (g/l) Fe (g/l)	
C.F. 33	16	100	100	52	6.2	0.16	20.5	0.33
	30			53	6.54	0.24	21.25	0.375
	60			51	6.7	0.20	"	0.40
	90			50	6.75	0.16	21.5	0.425
C.F. 34	15	100	100	42	6.8	0.10	21.25	0.075
	30			40	6.85	0.09	23.25	0.125
	60			41	6.92	0.10	24.0	0.125
	90			40	6.95	0.08	25.0	0.150
C.F. 35	15	100	100	30	6.88	0.10	21.5	0.125
	30			"	7.05	0.07	22.75	"
	60			"	7.1	0.11	21.5	0.150
	90			"	7.13	0.08	21.5	0.20

TABLE 24

The Effect of CoCl_2 concentration on the Rate of Cobalt Cementation onto Iron Powder

Test No	Time (min)	Composition		Conditions			Results		
		CoCl_2 (g/l)	Fe (g/l)	Temp ($^{\circ}\text{C}$)	PH	Gas Flow (l/min)	Powder Co%	Co (g/l)	Fe (g/l)
C.F.22	15	100	100	68	5.8	5.5	0.22	23.25	0.125
	30			68	5.73	"	0.26	25.0	0.175
	60			68	5.6	"	1.46	25.5	2.05
	90			68	5.7	"	2.68	27.73	3.75
C.F.36	15	150	100	68	5.52	5.5	1.0	31.25	0.78
	30			67	5.7	"	4.20	35.0	2.85
	60			"	5.58	4.5	7.52	36.5	4.40
	90			"	5.5	4	4.32	38.0	5.50
C.F.37	15	200	100	70	5.05	4.5	3.84	44.5	2.20
	30			69	5.51	4	3.76	46.25	3.53
	60			67	5.56	"	7.04	37.25	6.25
	90			68	5.38	"	9.60	49.5	11.0
C.F.38	15	250	100	68	5.45	5	1.04	50.0	0.31
	30			"	5.47	"	6.48	55.0	3.12
	60			"	5.37	"	14.08	55.0	9.25
	90			"	5.2	4.5	14.08	53.75	18.15

TABLE 25

The Cobalt Cementation Rate onto Iron Powder using Na_2SO_4 and H_3BO_3 in CoSO_4 solutions

Test No	Time (min)	Composition			Conditions			Results			
		CoSO_4 (g/l)	Fe (g/l)	Na_2SO_4 (g/l)	H_3BO_3 (g/l)	Temp ($^{\circ}\text{C}$)	PH	Gas Flow (l/min)	Powder Co%	Co (g/l)	Fe (g/l)
C.F.39		100	100	60	-						
A	20					67	3-4	6.4	0.20	20.0	10.0
B	30					64	"	6.4	0.26	20.0	12.5
C	60					63	3.5-4	6.3	0.34	16.50	32.5
D	90					70	3.2-3.5	5	1.60	18.3	93.5
C.F.40		100	100	60	15						
A	15					70	3-3.3	6.6	0.68	18.3	8.8
B	30					69	"	"	2.76	18.3	25.0
C	60					71	"	"	4.50	18.8	62.50
D	90					70	3.3-4.2	4.5	4.20	21.5	81.3

TABLE 26

Effect of Current Application on the Cobalt Deposition Rate in 100g/l of $\text{CoSO}_4 \cdot 7\text{H}_2\text{O}$

Test No	Time (min)	Composition		Conditions			Results					
		CoSO_4 (g/l)	Fe (g/l)	H_3BO_3 (g/l)	Temp ($^{\circ}\text{C}$)	PH	Gas Flow (l/min)	Current A	Potential V	Powder Co%	Solution Co (g/l)	Fe (g/l)
C.F.41	15	100	100	15	70	4.2-4.4	5-3.5	-*	5.1	4.0	26.5	8.13
	30				70	4.2-4.5	3	-	"	8.8	26.5	15.0
	60				69	4-5	3.4	-	5.3	14.8	25.5	30.0
	90				70	3.8-5	"	-	5.1	31.6	25.0	47.0
C.F.42	15	100	100	15	71	5	5	15	11	0.30	21.7	1.8
	30				71	"	8.5	12	"	0.60	20.0	3.3
	60				69	"	7	10	"	0.40	21.25	7.1
C.F.43	15	100	100	-	69	5.2	5	5	6.2	0.2	26.3	1.10
	30				67	5.21	"	"	7.3	0.44	27.5	1.95
	60				67	5.1	"	"	7.5	0.42	28.5	3.55
	90				65	5.2	"	"	7.5	0.60	28.5	4.75

*Malfunction of galvanometer.

TABLE 27

Variation of first order reaction constant with cobalt ion concentration.

Cobalt ion concentration (g/l)	K (cm/sec)
100	$5.1139 * 10^{-10}$
150	$5.98 * 10^{-10}$
200	$9.843 * 10^{-10}$
250	$1.279 * 10^{-9}$

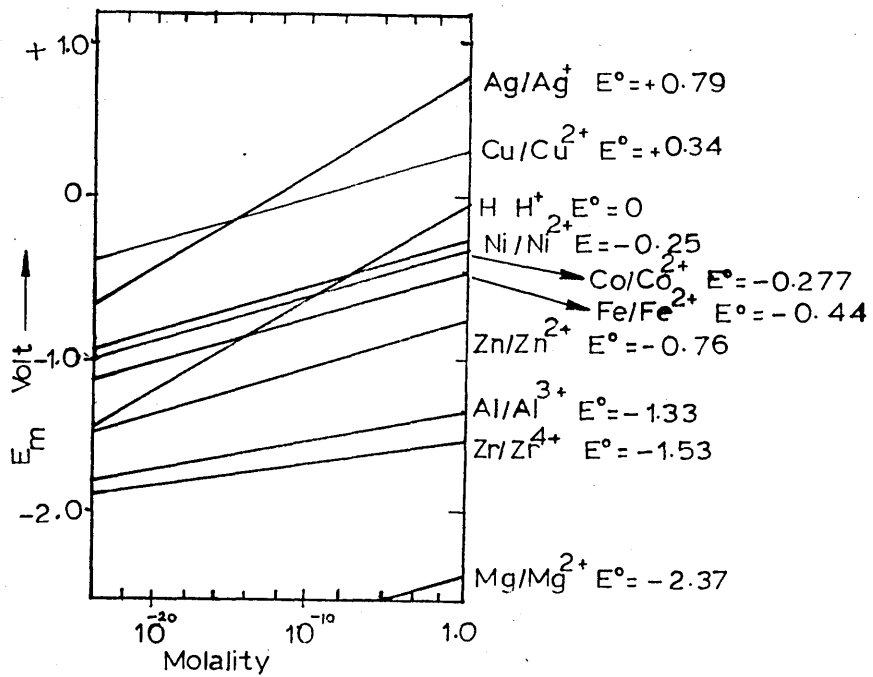


Fig.1: Variation of ion concentration with electrode potential for various metals⁽⁴⁾.

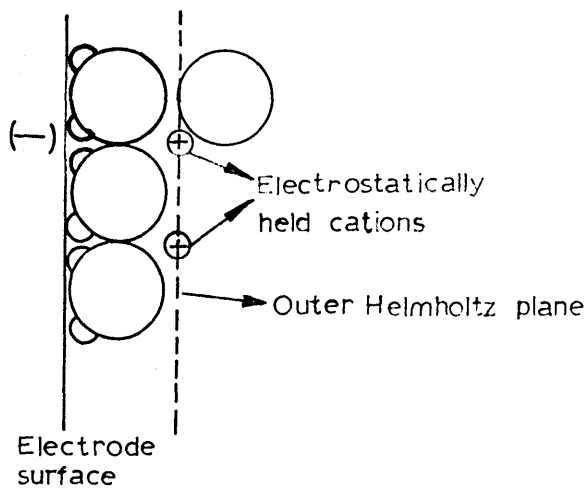


Fig.2: The Helmholtz double layer⁽⁵⁾.

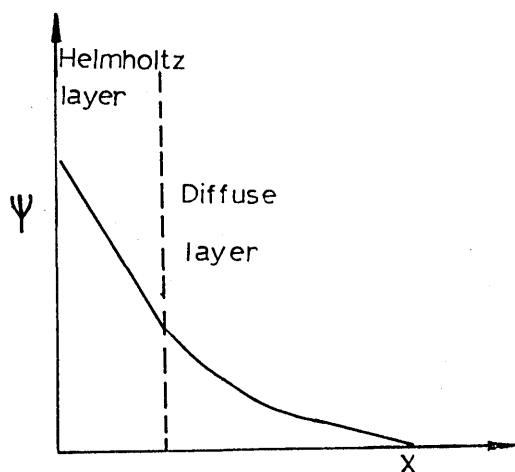


Fig. 3: Variation of potential with distance from electrode surface⁽⁵⁾.

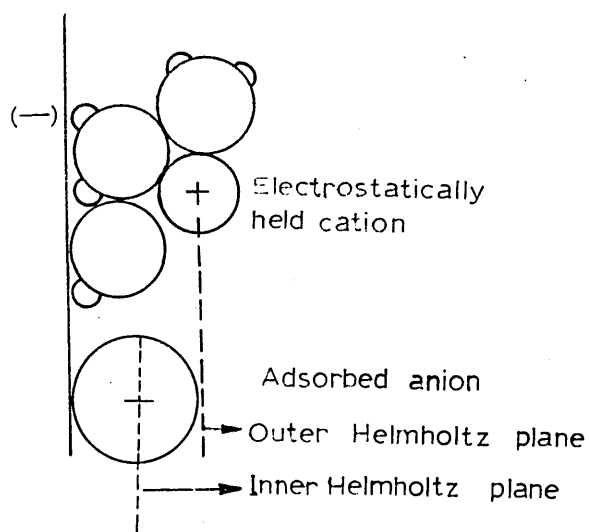


Fig. 4: Relative positions of inner and outer Helmholtz planes of electrode double layer⁽⁴⁾

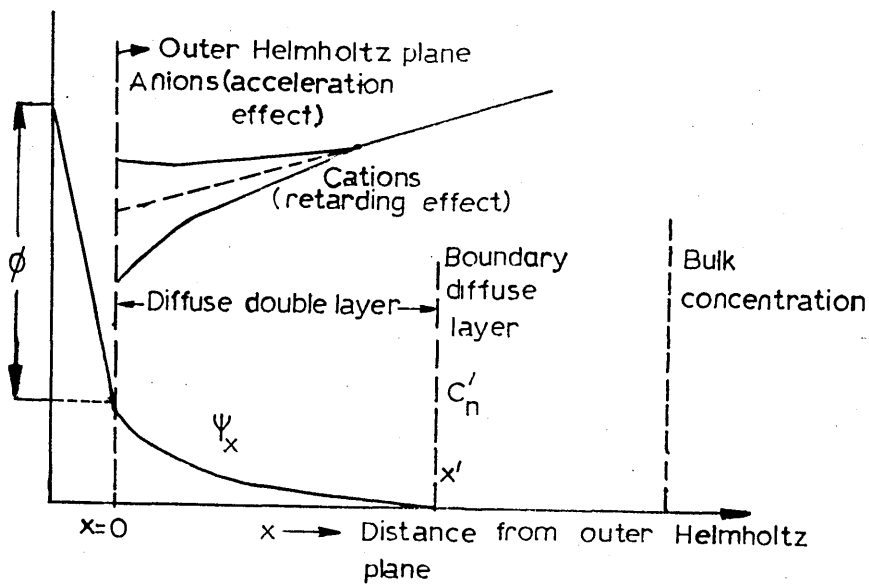


Fig.5:Electrical double layer showing variations of concentration of anions and cations in the diffuse double layer resulting from positive ψ_x values⁽⁶⁾

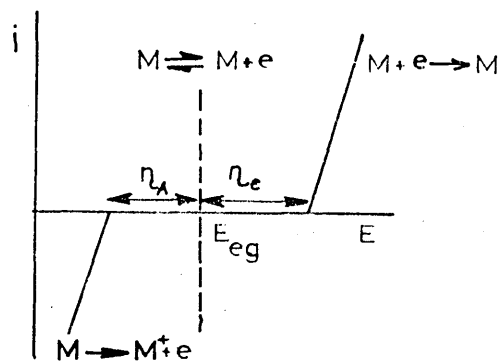


Fig.6: Current-potential relationship for a slow or irreversible system requiring an over voltage η_c for the process $M^+ + e \rightarrow M$ and η_A for $M \rightarrow M^+ + e$. In such cases the equilibrium condition $M \rightarrow M^+ + e$ is not established and E_{eq} is hypothetical⁽⁵⁾.

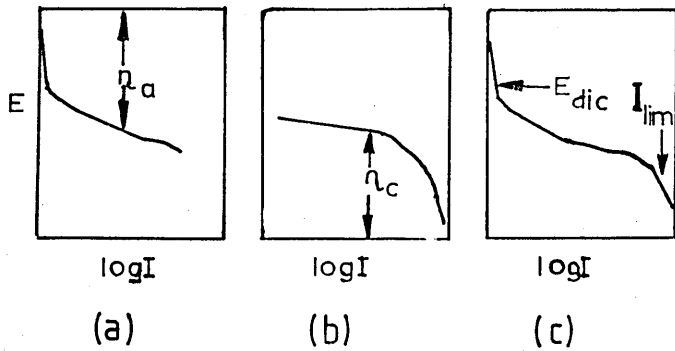


Fig.7: Components of polarisation or overpotential: (a) Activation polarisation, (b) Concentration polarisation, (c) Net polarisation curve⁽⁴⁾.

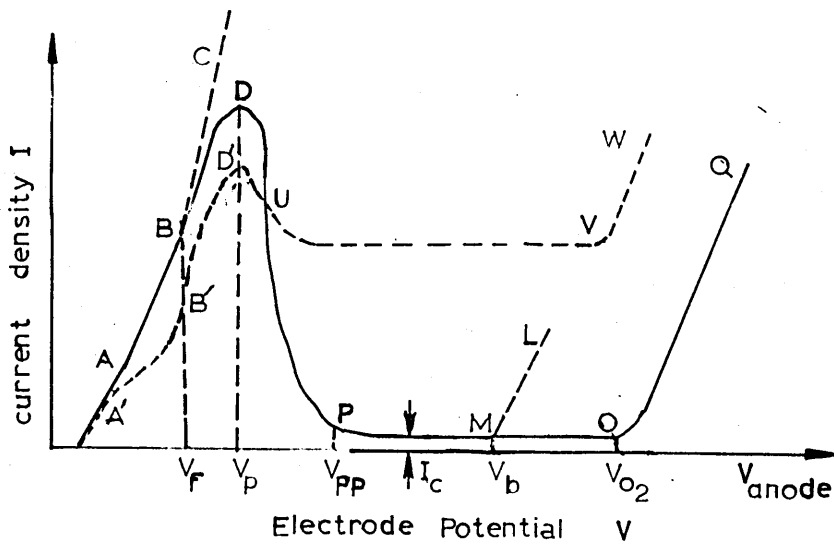


Fig.8: Schematic representation of anodic processes on metals. Curve ABDPOQ: typical active, passive and transpassive I-V curve for metal in water (Fe, Ni); curve ABC: free dissolution (Fe in alkali); curve ABDML: I-V curve in the presence of active anions, with possible salt formation in the active region (Fe in chloride solutions); curve ABDUVW or A'B'D'UVW I-V curve for metals forming less protective film (Cu, Zn) or iron in electropolishing solutions⁽¹⁰⁾.

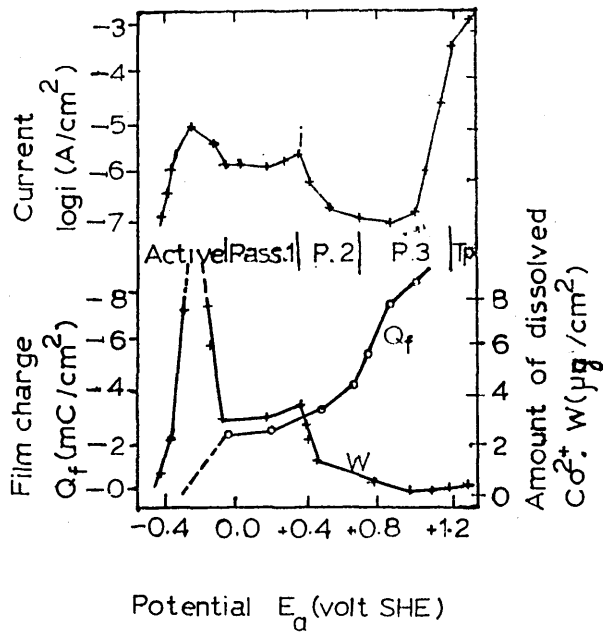


Fig.9: Polarisation curve as well as cobalt dissolution v.s. potential and film charge v.s. potential relationships in borate buffer solution at PH of 8.42⁽¹³⁾.

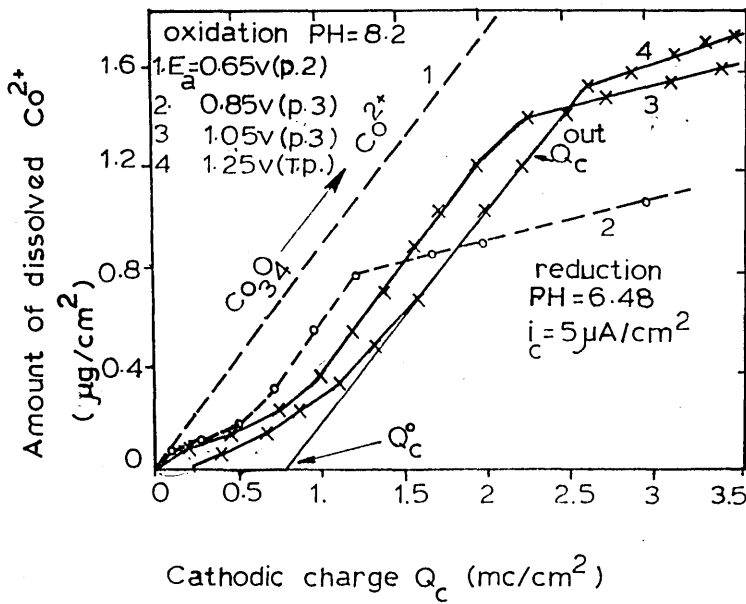


Fig.10: Dissolution curve of the film formed in the potential region, passive 2 and passive 3, during cathodic reduction, which gives the amount of dissolved Co^{2+} against the cathodic charge passed⁽¹³⁾.

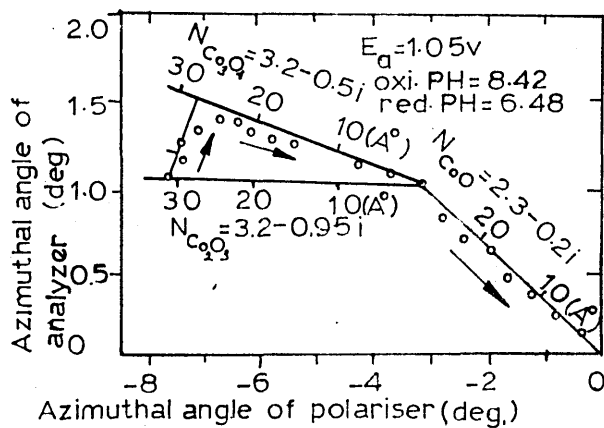


Fig.11: The film formation in passive 3 region, and the film reduction with three stages. In the first stage the outer Co_2O_3 layer changes to CoO with little decrease in the film thickness, and the Co_3O_4 film is then reduced⁽¹³⁾

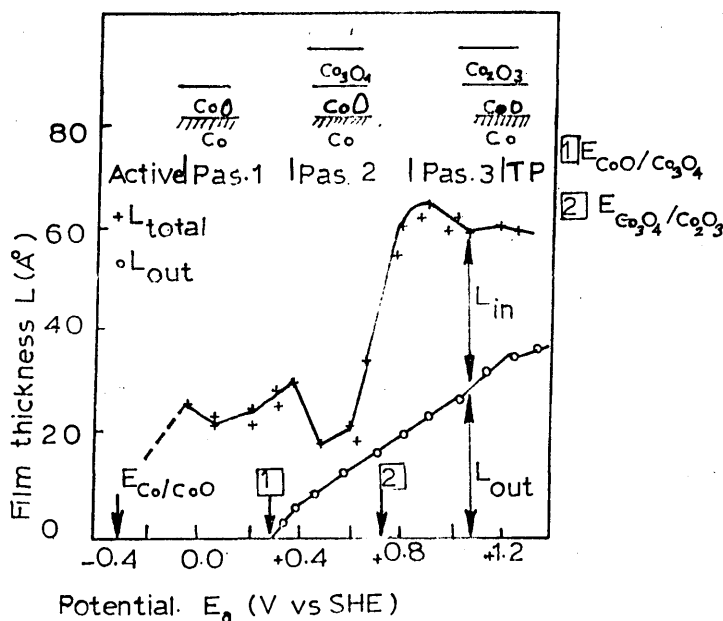


Fig.12: The thickness of the film estimated by ellipsometry as a function of potential. The outer layer thickness increased nearly linearly with the potential, but the inner layer thickness changed independently of the potential⁽¹³⁾

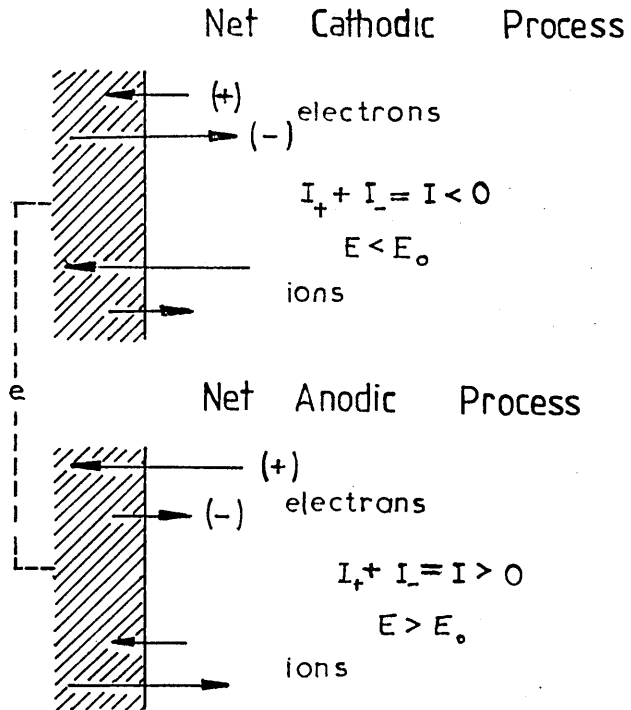


Fig.13: Flow of electrons and ions between electrode and the electrolyte for net cathodic and net anodic processes⁽⁶⁾

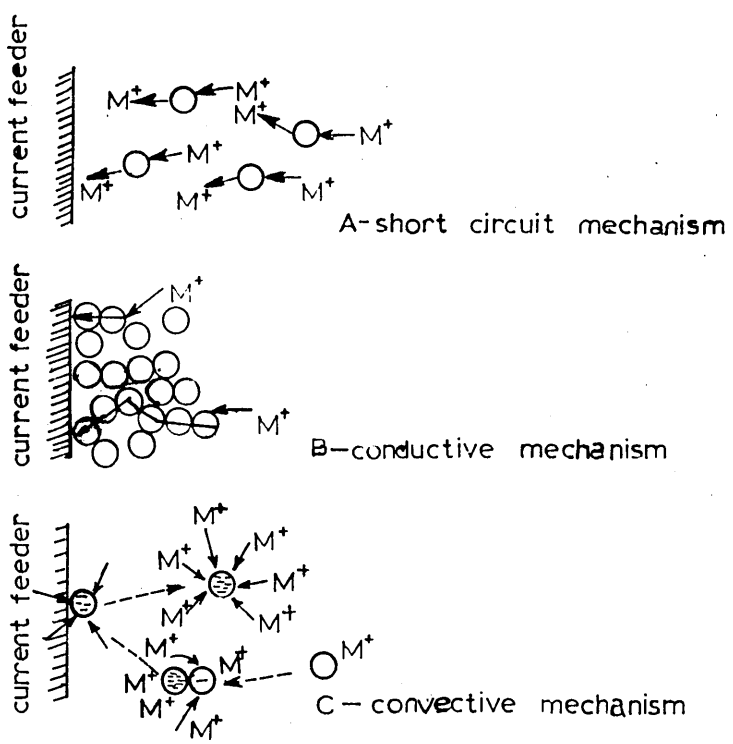


Fig.14: Possible mechanism for current conduction in fluidised electrodes⁽⁷⁹⁾



Fig.15: Mechanically stirred cell. The diameter and the height of the beaker are 13 cm and 19 cm respectively.

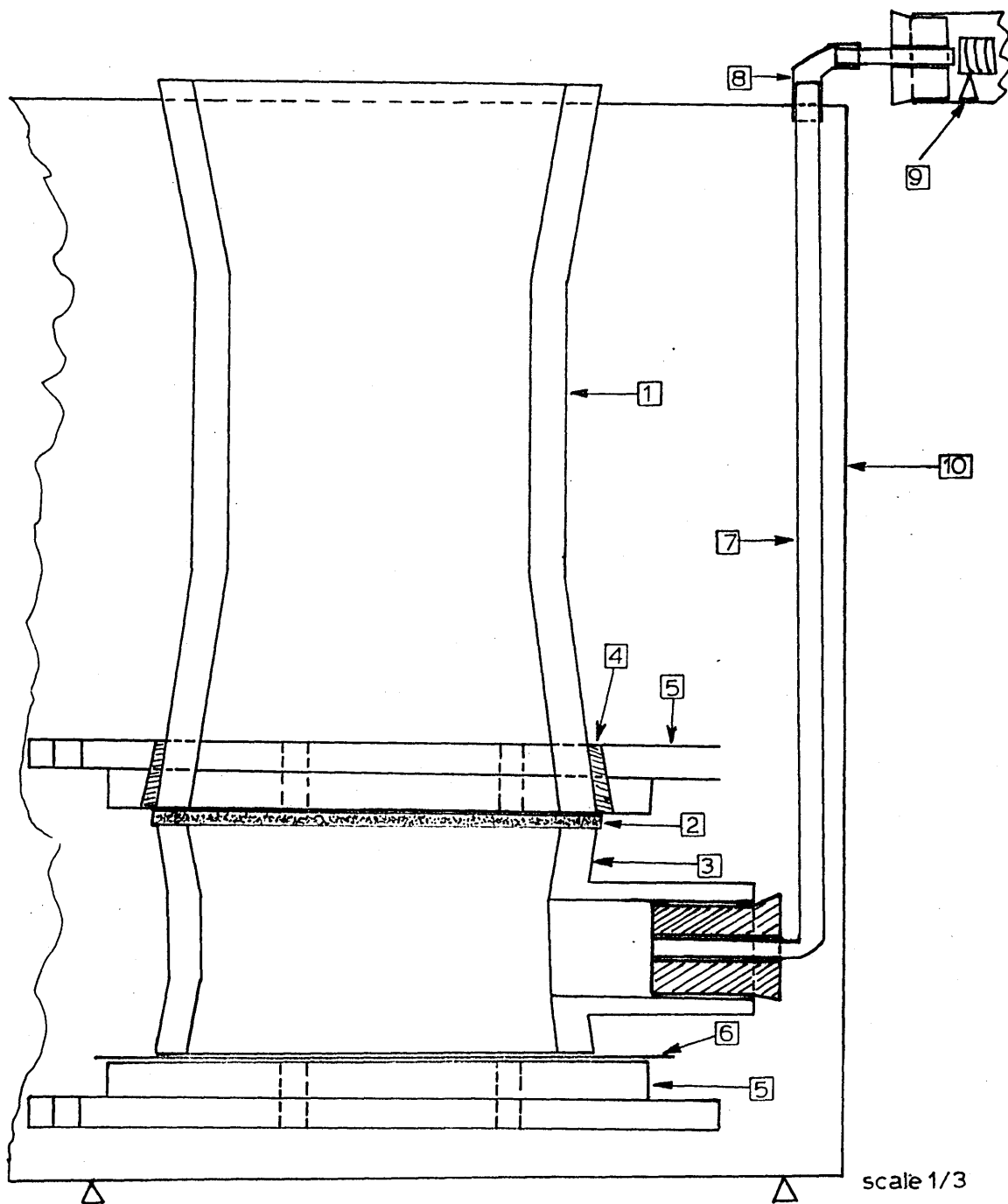


Fig.16: Fluidised bed cell: 1) Top of the cell. 2) Membrane. 3) Bottom section. 4) Rubber gasket. 5) Joining assembly. 6) Stainless steel bottom enclosing sheet. 7) Copper pipe. 8) Hard plastic pipe. 9) Heating tube. 10) Hot water bath.

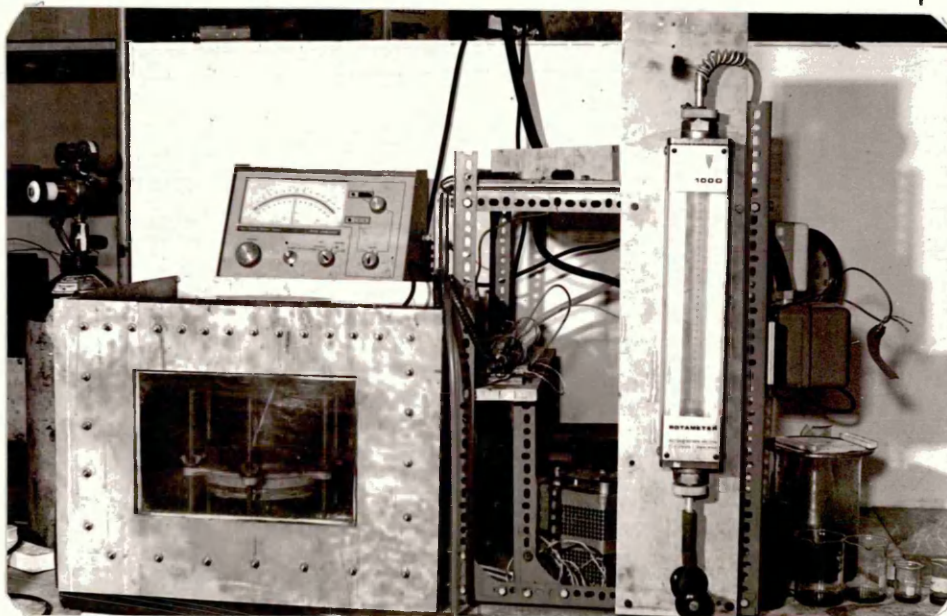
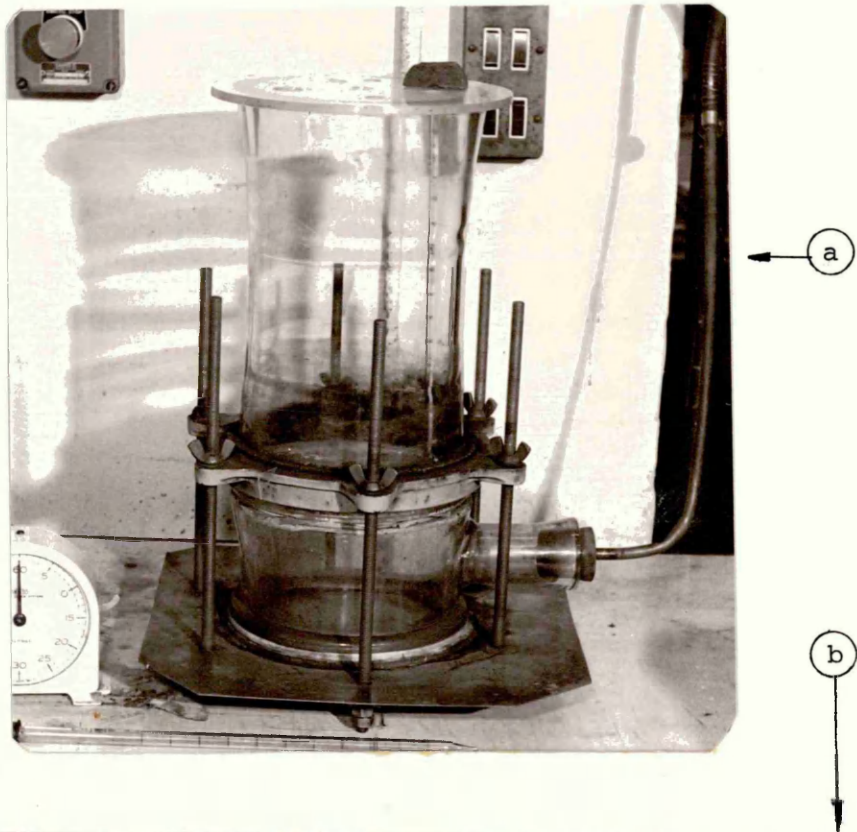


Fig.17: Two general views of the fluidised bed cell; a) on its own, b) in hot water tank.

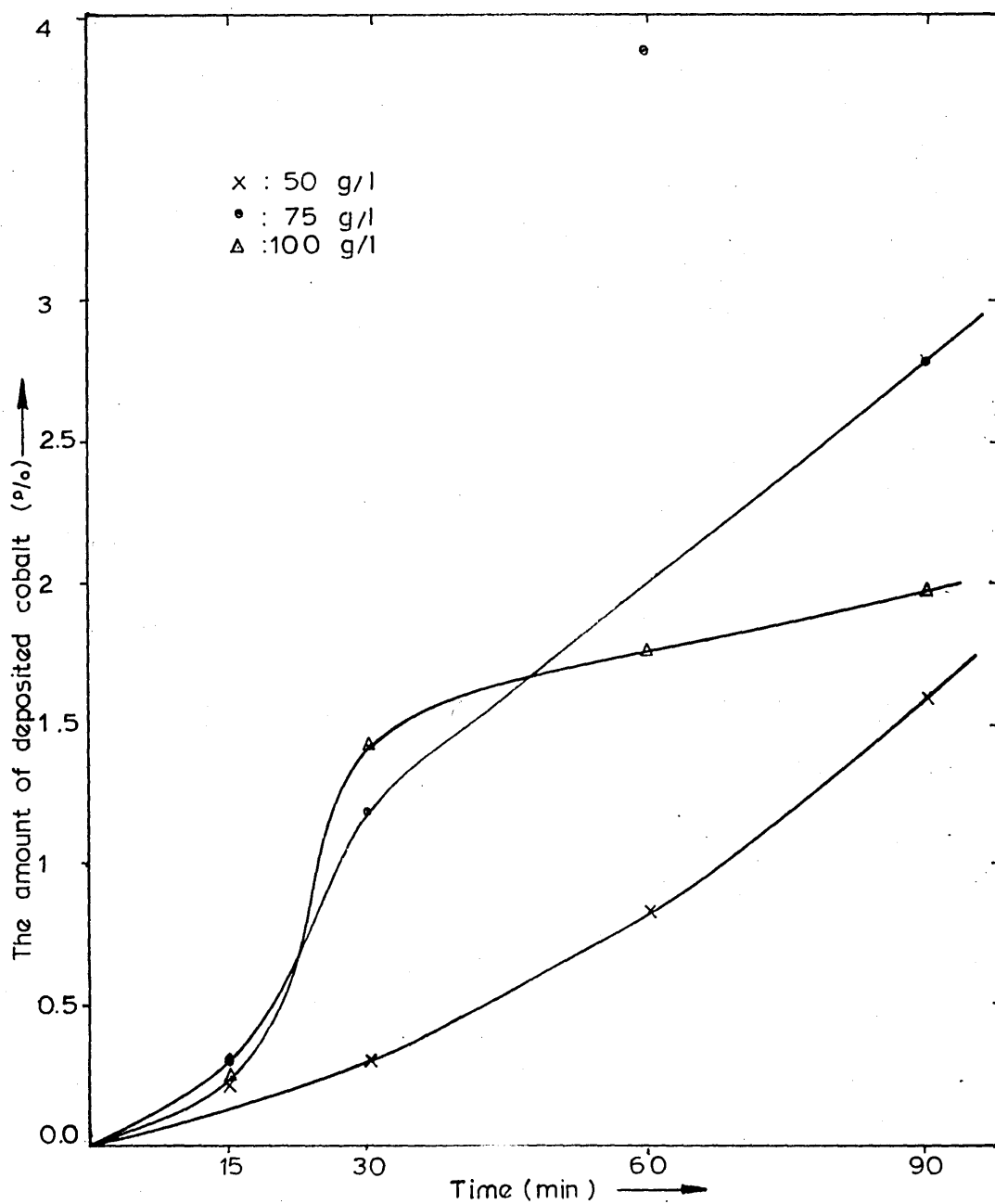


Fig.18-a: Variation of the cobalt cementation rate, at various iron powder concentrations and at PH of 4.5-5, temperature of 69 ± 3 °C, relative to time.

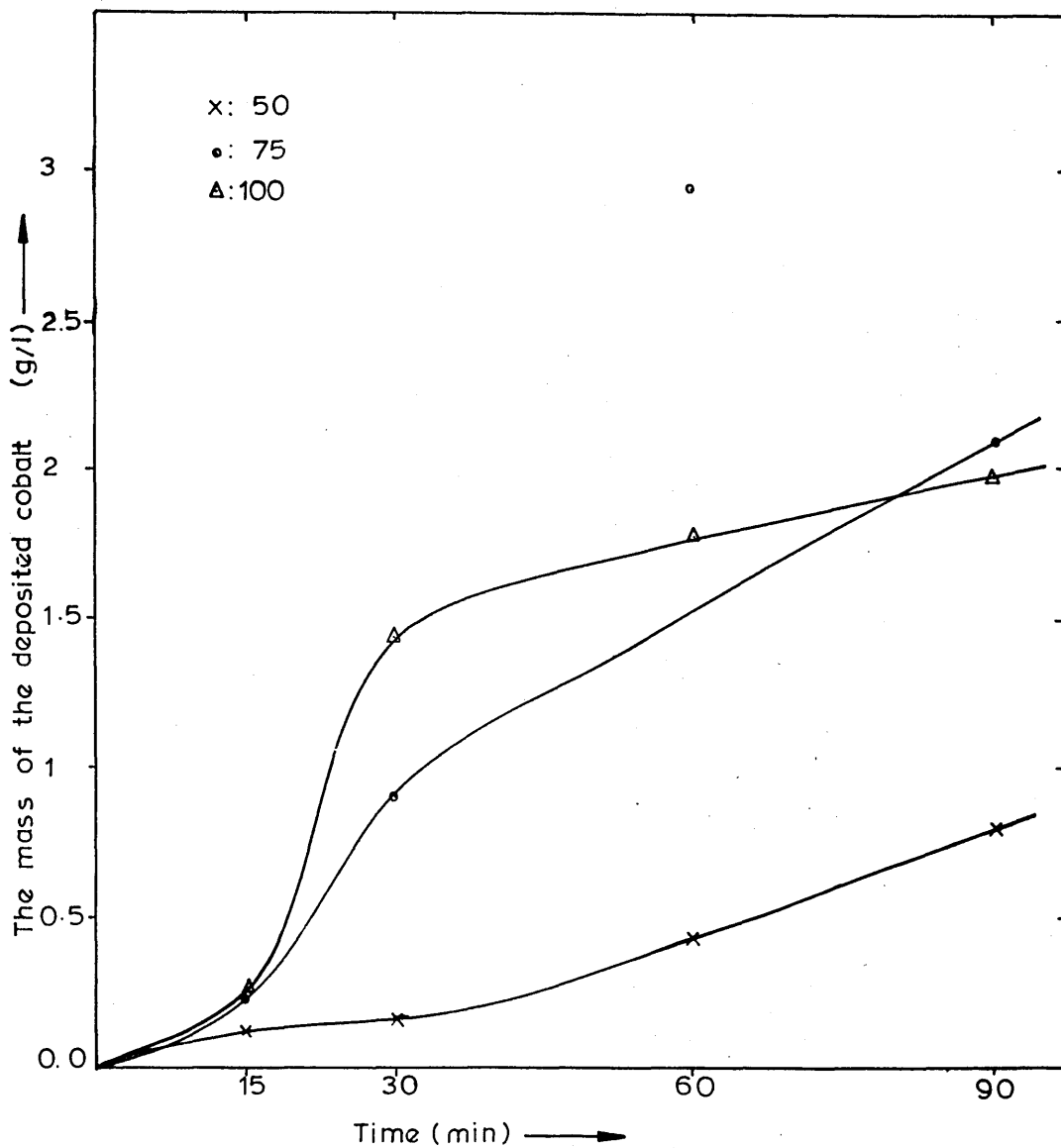


Fig.18-b: Variation of the mass of the deposited cobalt at various iron powder concentrations and at PH of 4.5-5, temperature of $69 \pm 3^\circ\text{C}$, relative to time.

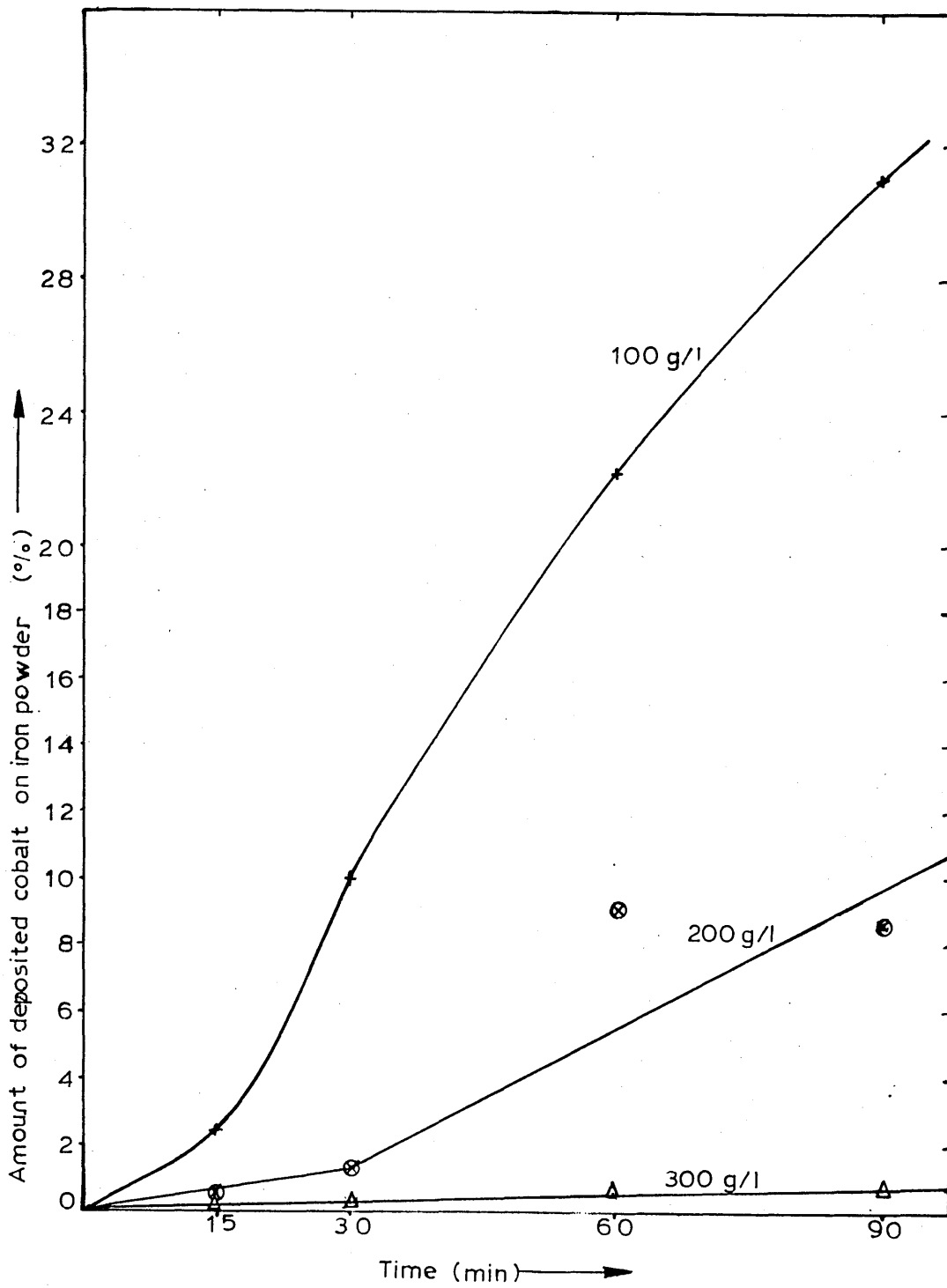


Fig.19: Cobalt deposition at various iron powder concentrations in the solutions of 100 g/l cobalt sulphate.

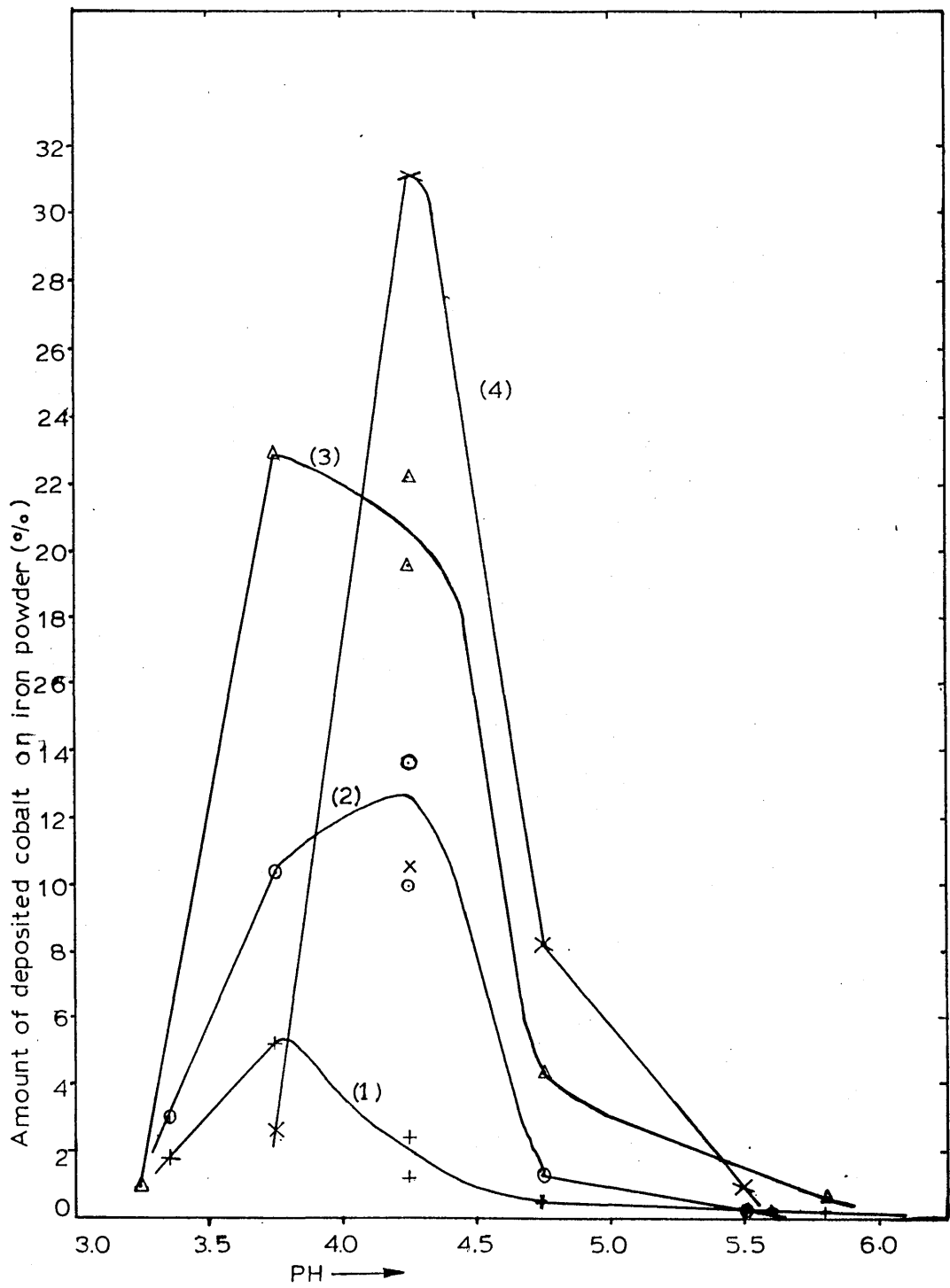


Fig.20: Effect of PH on cobalt deposition rate using 100 g/l of cobalt sulphate and 100 g/l of iron powder at various times: 1) 15 min, 2) 30 min, 3) 60 min, 4) 90 min.

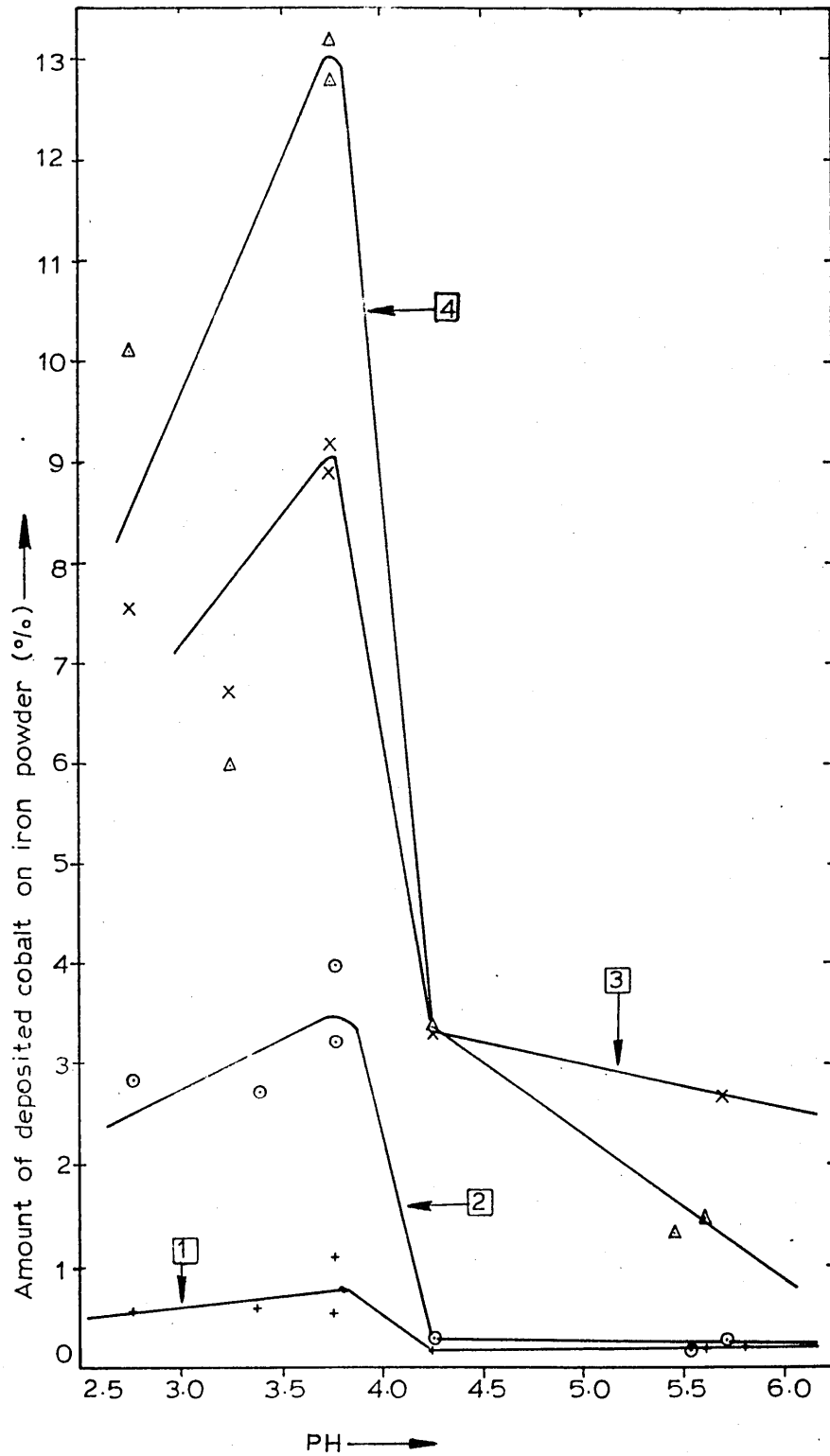


Fig.21: Effect of PH on cobalt cementation rate using 100 g/l of cobalt chloride and 100 g/l of iron powder at various times: 1) 15 min, 2) 30, 3) 60, 4) 90 min.

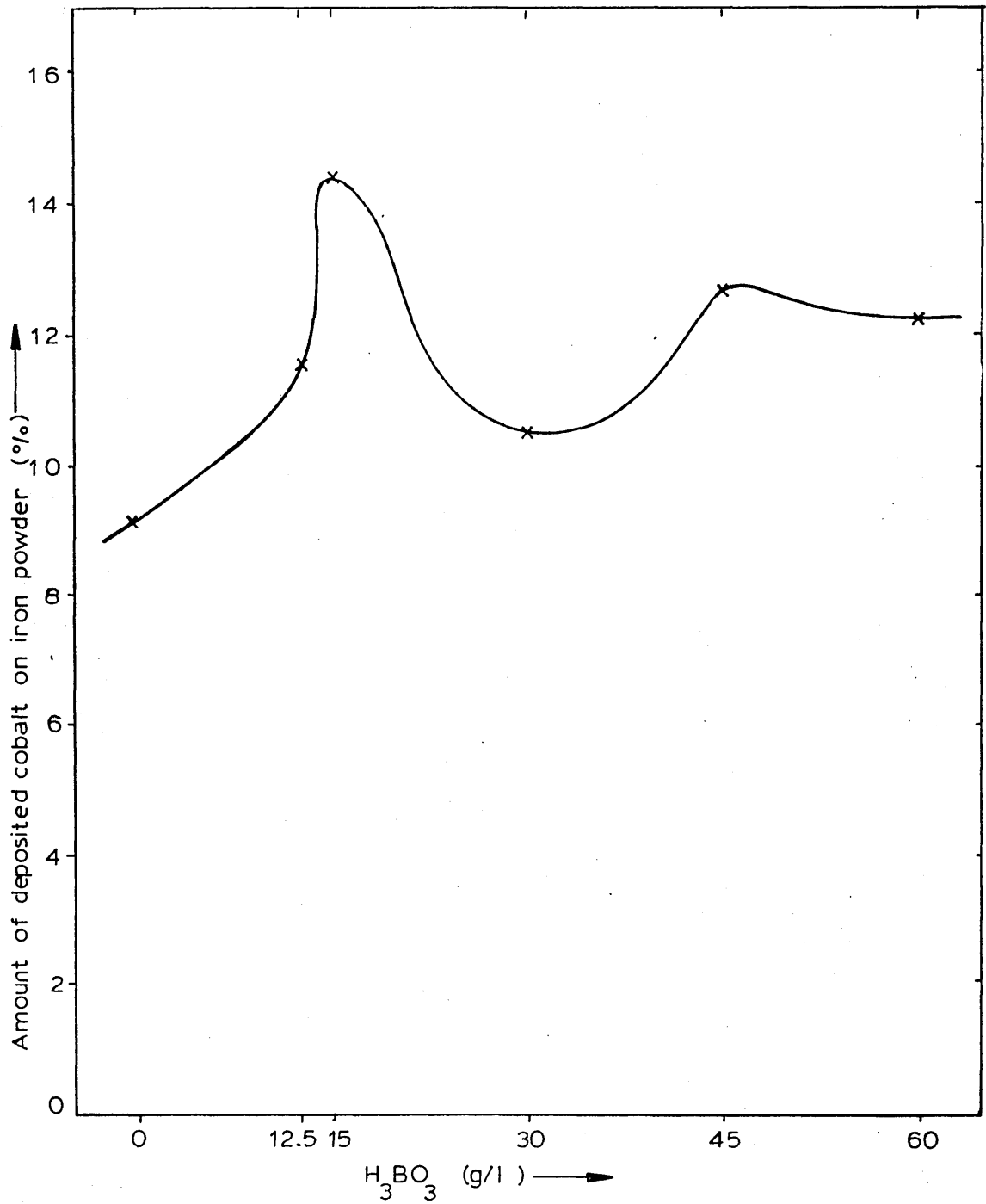


Fig.22: Effect of boric acid concentration on cobalt deposition rate using solutions of 100 g/l of cobalt chloride and 100 g/l of iron powder in 90 minutes.

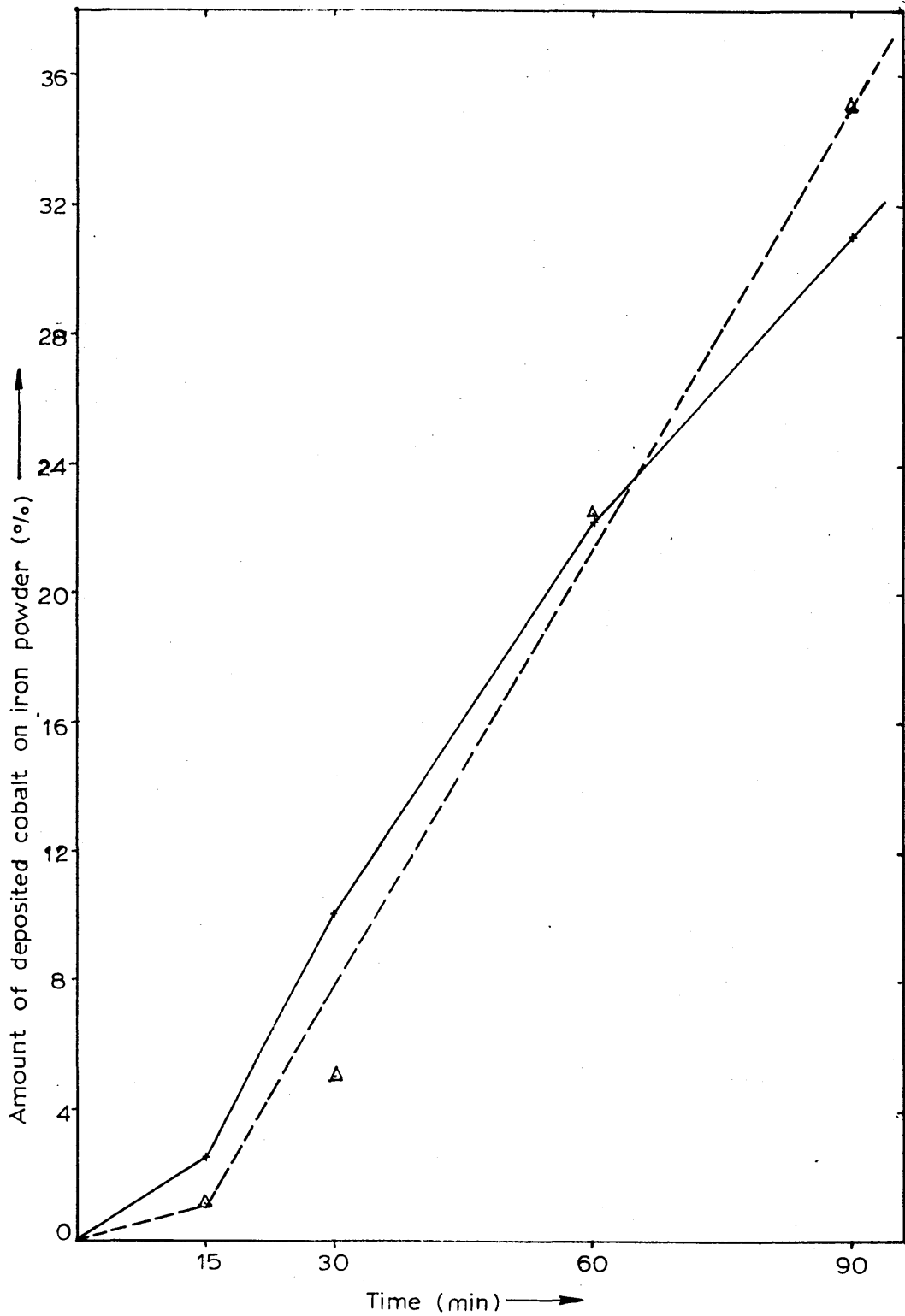


Fig.23: Effect of boric acid on cobalt deposition rate with 100 g/l of cobalt sulphate and 100 g/l of iron powder including solution,
 (—) without boric acid,
 (----) with 15 g/l of boric acid.

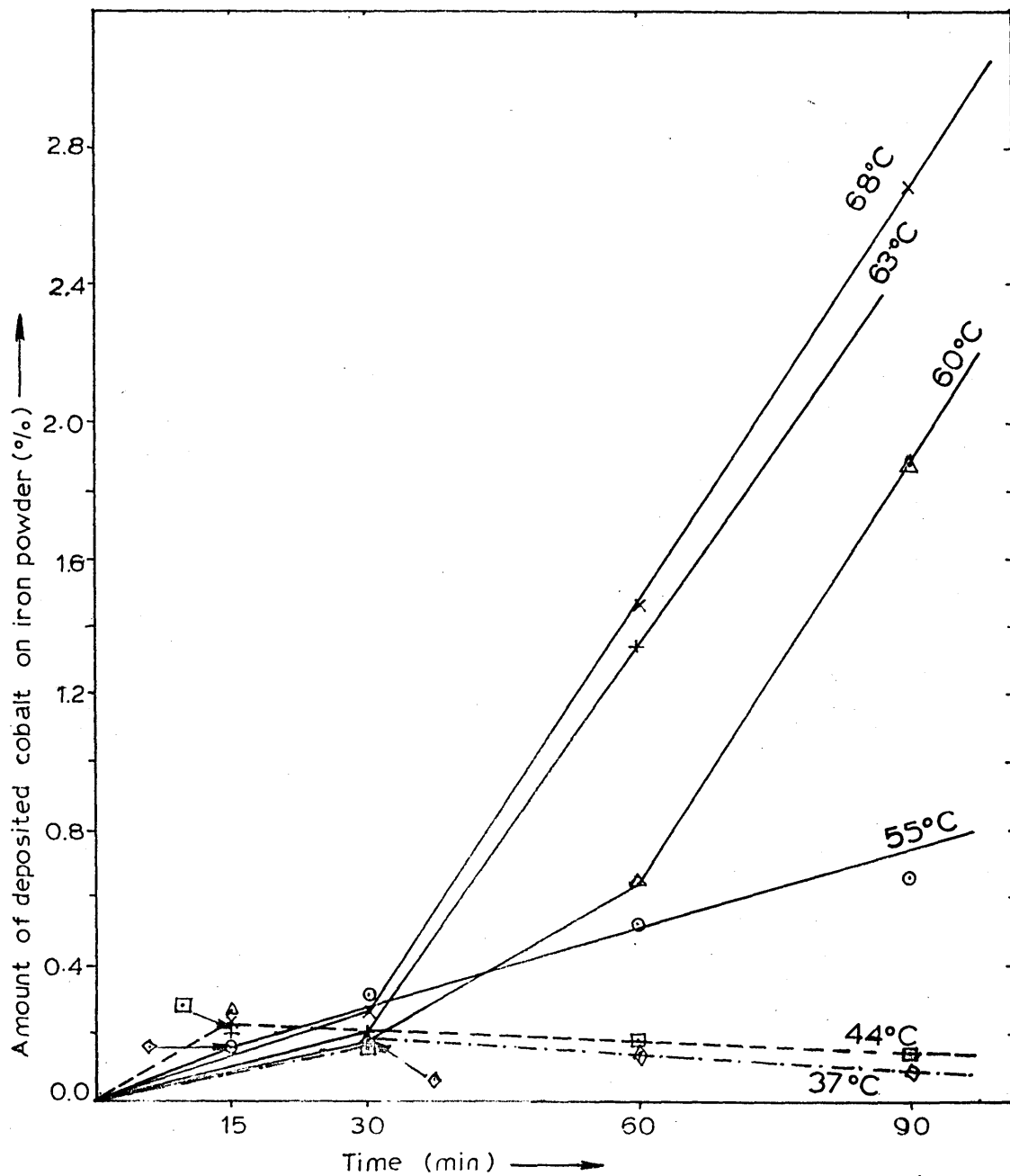


Fig.24: Effect of temperature on cobalt deposition rate using 100 g/l of cobalt chloride and 100 g/l of iron powder at natural PH (5.5–6.2)

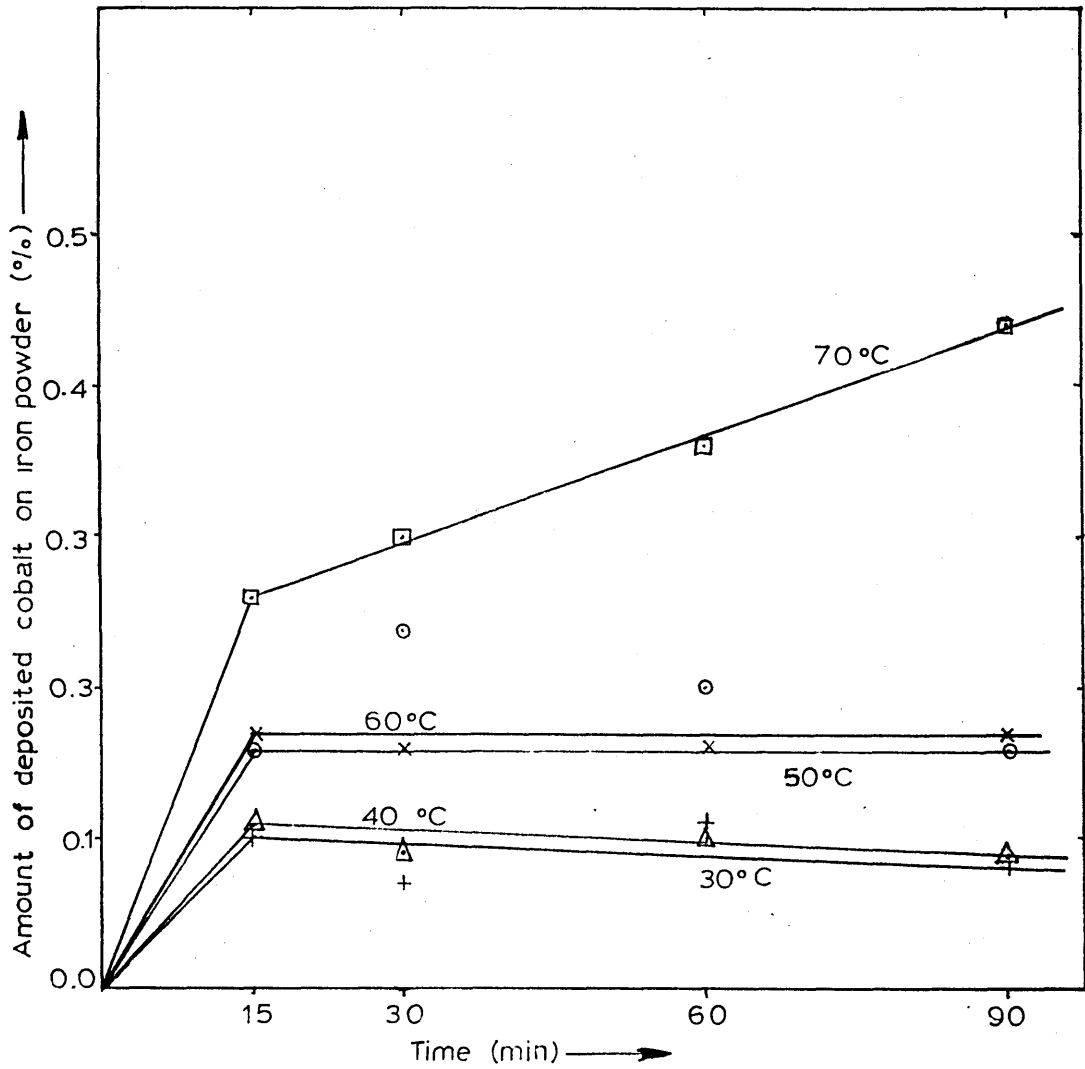


Fig.25: Cobalt deposition onto iron powder in a solution of 100 g/l cobalt sulphate and 100 g/l iron powder at various temperatures.

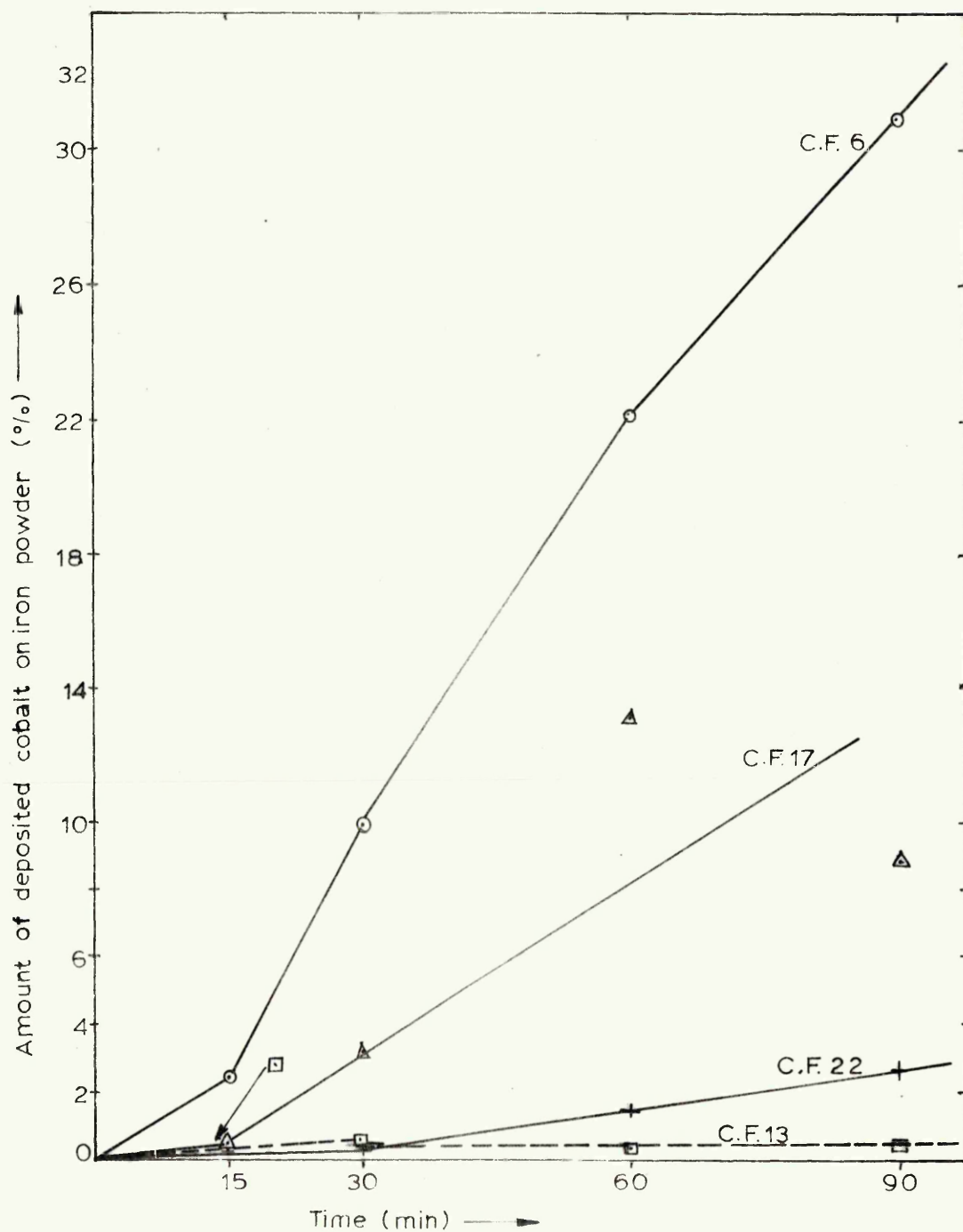


Fig. 26: Comparison of the influence of temperature and PH on cobalt deposition from cobalt sulphate (C.F. 6,13) and cobalt chloride (C.F.17, 22) solutions.

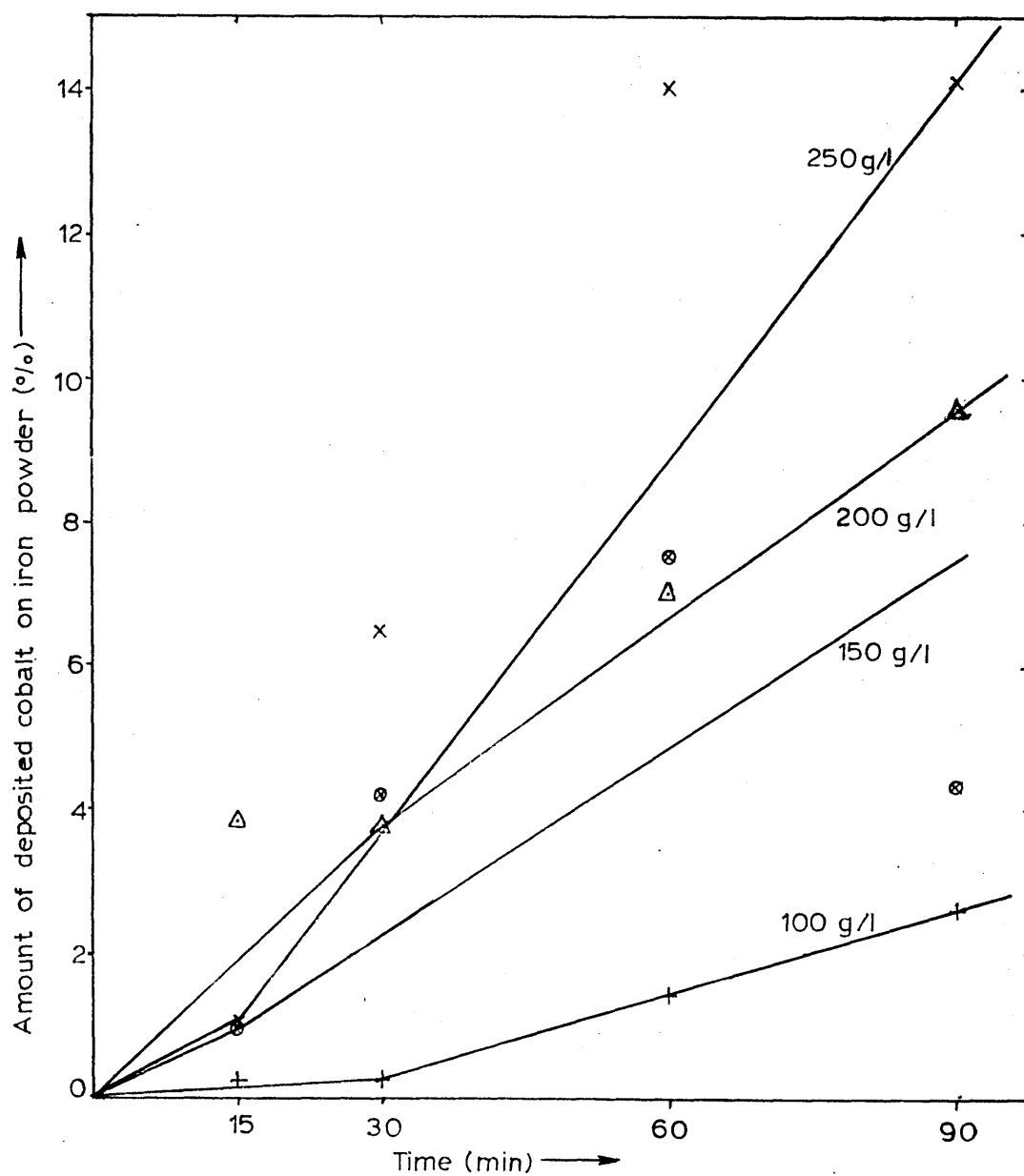


Fig.27: Effect of cobalt chloride concentration on the deposition rate in 100 g/l iron powder involving solutions at natural PH(5.8-5.2) and at a temperature of $68 \pm 1^\circ\text{C}$

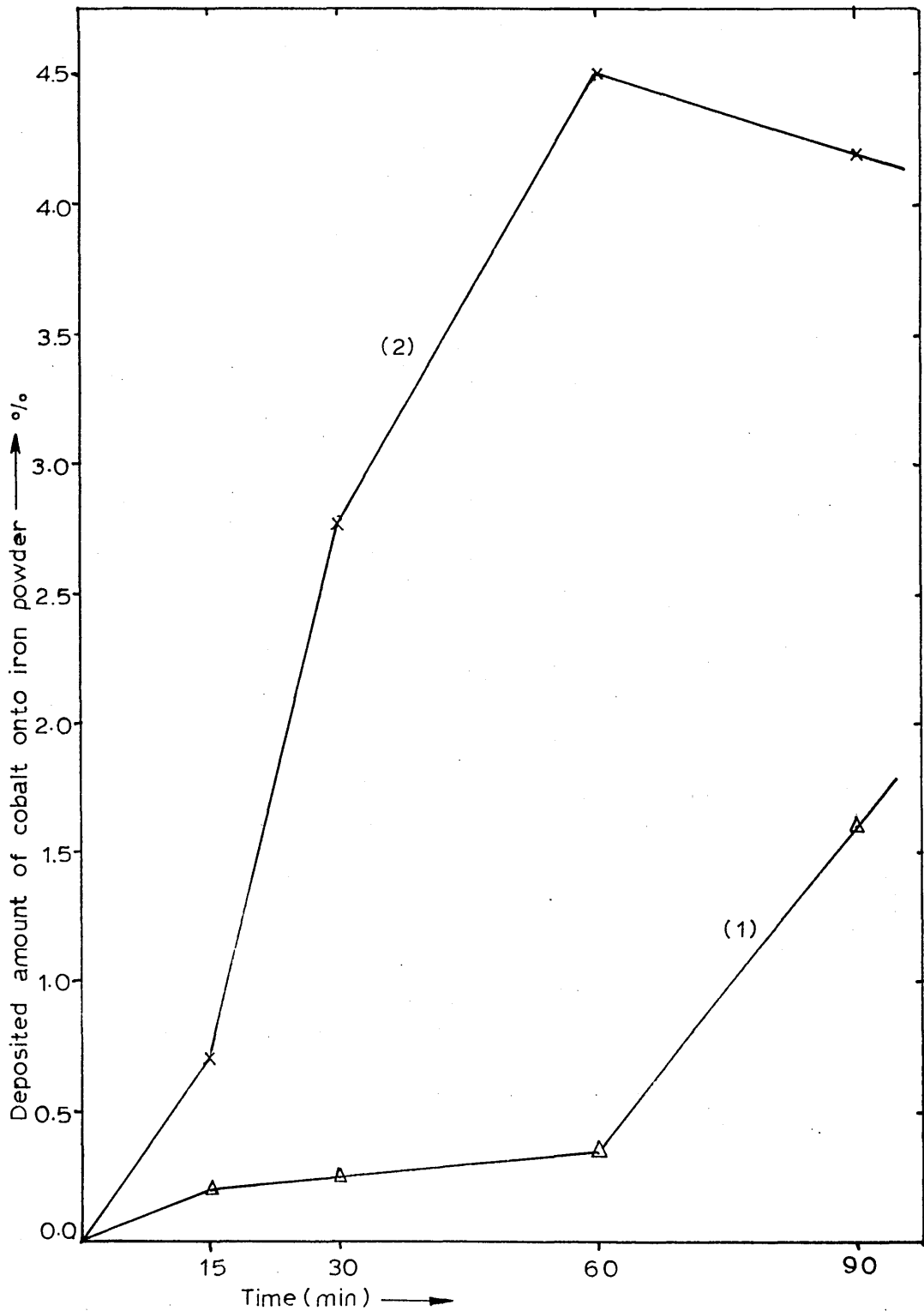


Fig.28: Effect of Na_2SO_4 (curve 1) and $\text{Na}_2\text{SO}_4 + \text{H}_3\text{BO}_3$ (curve 2) on the rate of cobalt cementation onto iron powder in 100 g/l of CoSO_4 and 100 g/l of iron powder involving solution at PH of 3-4 and at a temperature of $67 \pm 3^\circ\text{C}$.

FIG. 29

- a) Spongy deposit of cobalt on iron powder at a magnification X 1120. Composition of powder Fe-12.5%Co. Deposit obtained from 100 g/l of CoCl_2 +60 g/l of H_3BO_3 at a PH of 3.5-4.

X 1120

- b) X-ray analysis of iron concentration in surface area shown in fig. 29-a.
- c) X-ray analysis of cobalt concentration in surface area shown in fig. 29-a.

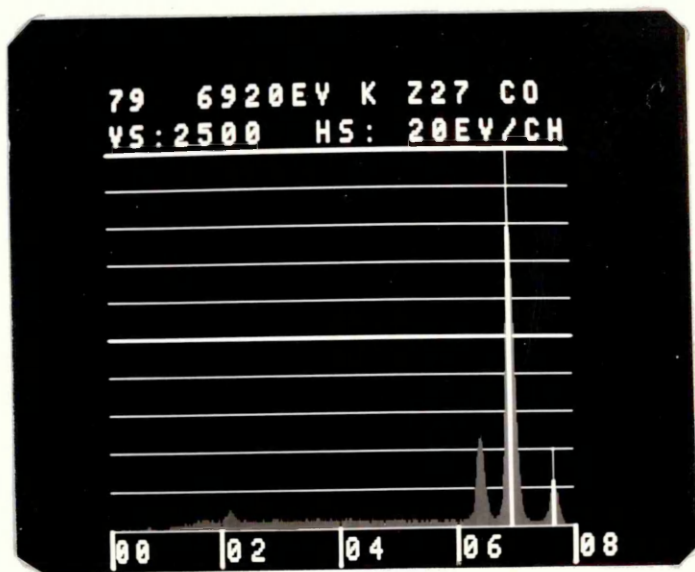
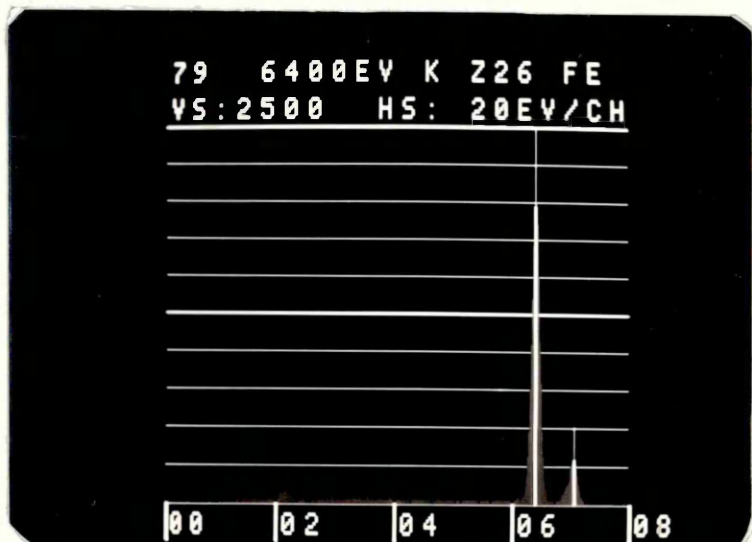
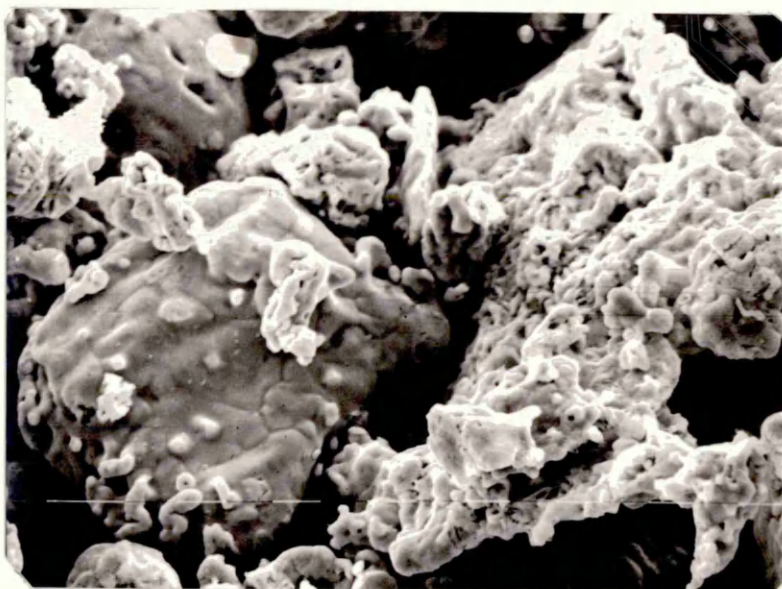


FIG. 30

- a) Deposits of cobalt on protrusions of the iron particles. Composition of powder Fe-14.4%Co. Deposition obtained from solution containing 100 g/l CoCl_2 +15g/l H_3BO_3 at a PH of 3.7-4.

X 480

- b) Edax analysis iron and cobalt (on left) peaks of the area in the above photograph.



cobalt
deposits
on the
protrusions

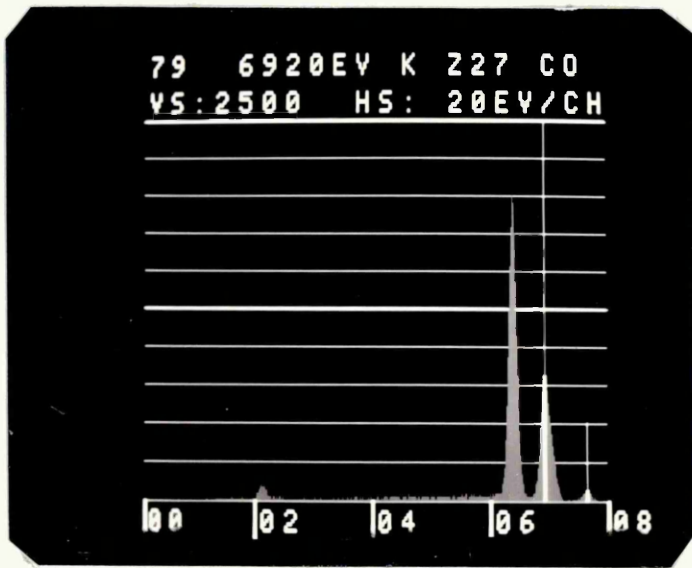


FIG. 31

- a) Spongy deposit of cobalt on iron powder and the spherical particle is free from any deposit. Composition of powder Fe-8.90%Co. Deposition obtained from solution containing 100 g/l CoCl_2 at a PH of 3.5-4.

X 1120

- b) Edax analysis iron peak of the particle in the right hand side in the above photograph.

- c) Edax analysis cobalt peak of the crossed point in the above photograph.

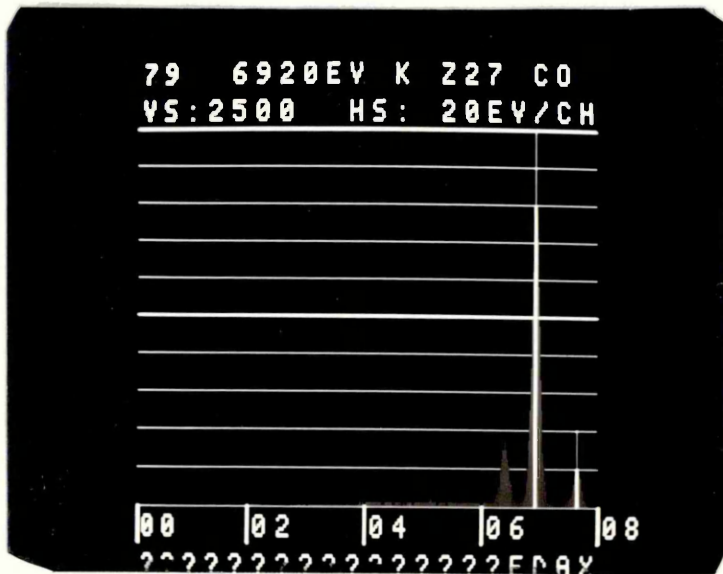
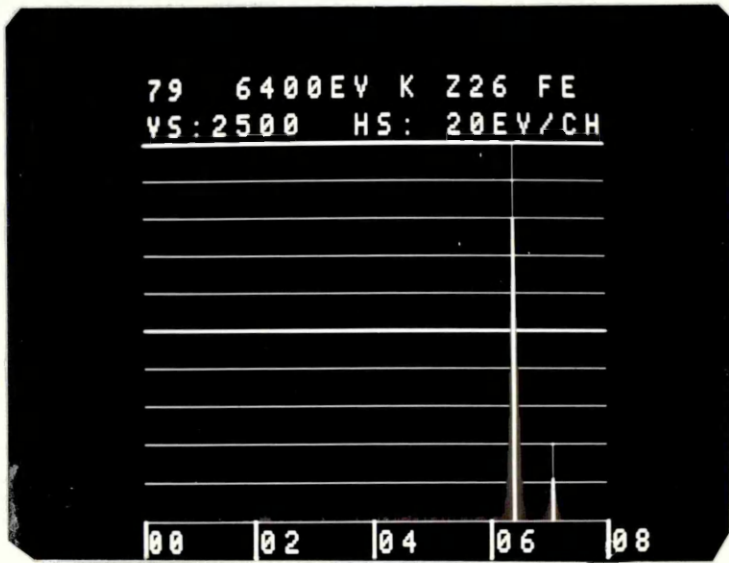
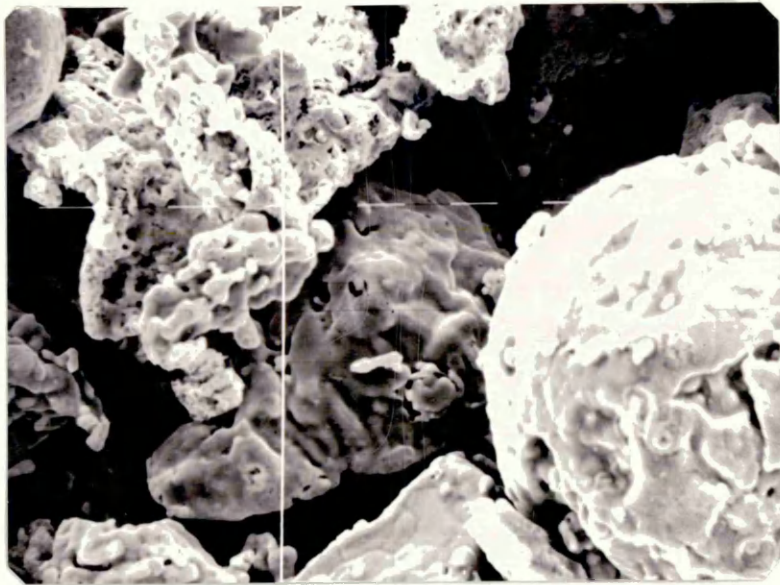


FIG. 32

- a) Cobalt free circular pits on an iron particle. Composition of powder Fe-2.96%Co
Deposit obtained from solution containing 100 g/l. CoCl_2 at a PH of 3.2-3.5.

X 2080

- b) Edax analysis iron peak of the crossed point in the fig. 32-a.

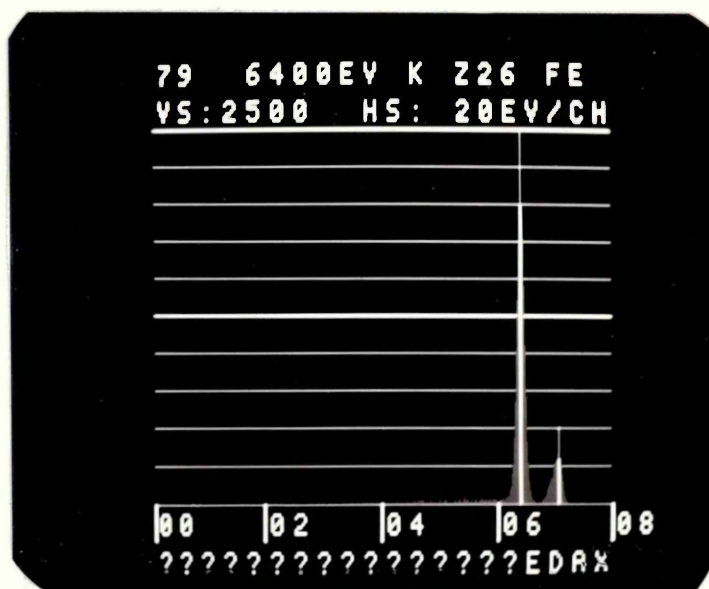
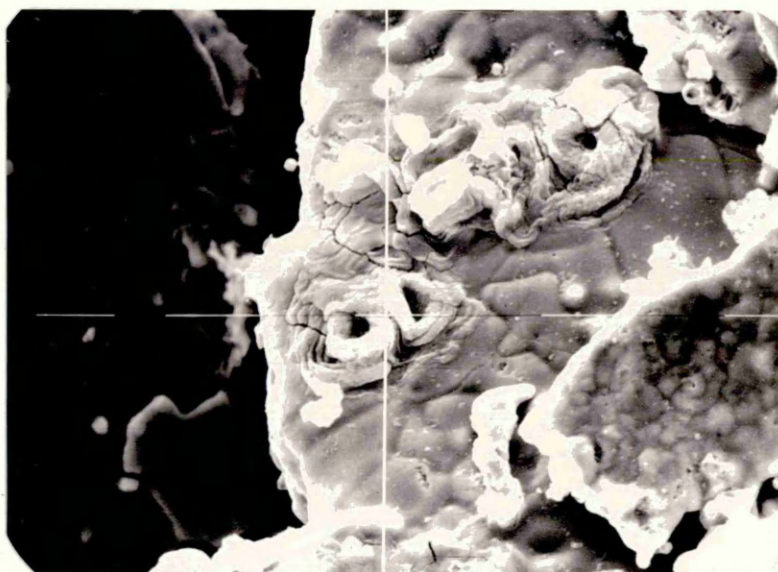
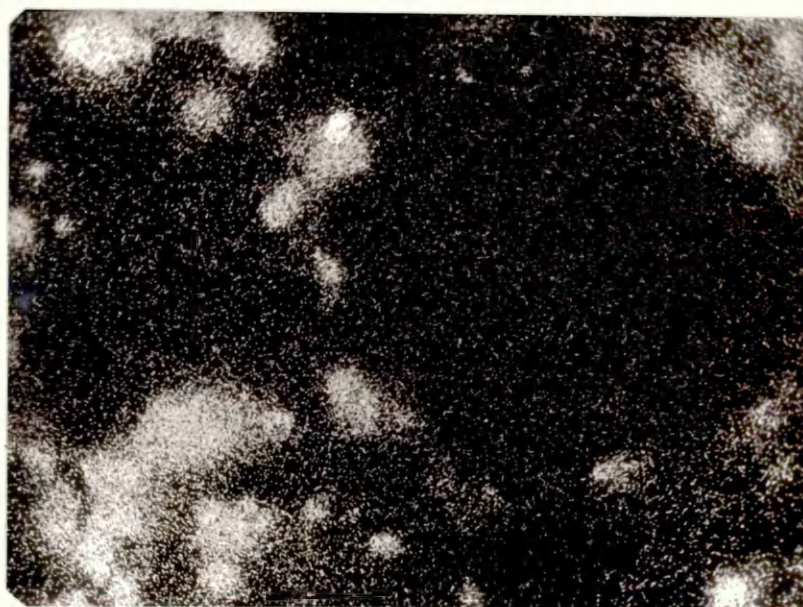
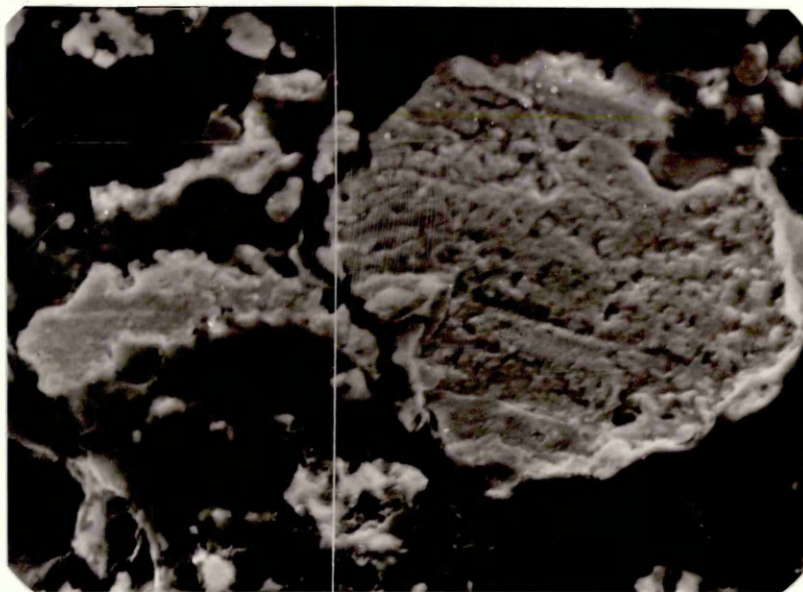


FIG. 33.

- a) Cross section of an iron powder particle
composition of powder Fe-7.52%Co.
Deposit obtained from solution containing
150 g/l. CoCl_2 at a PH of 5.5

X 1600

- b) Map of the photograph in (a), white spots
indicate the cobalt deposits.



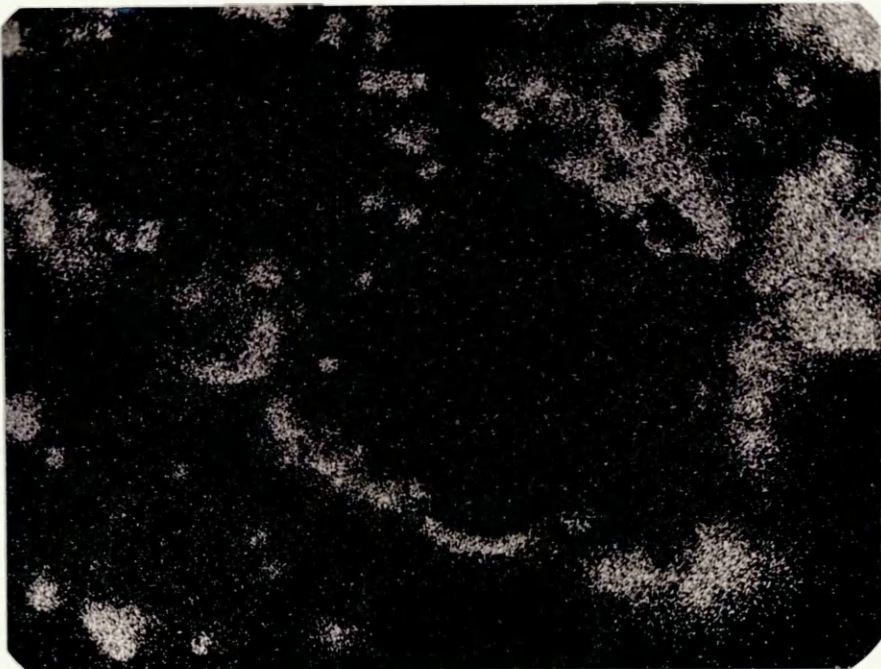
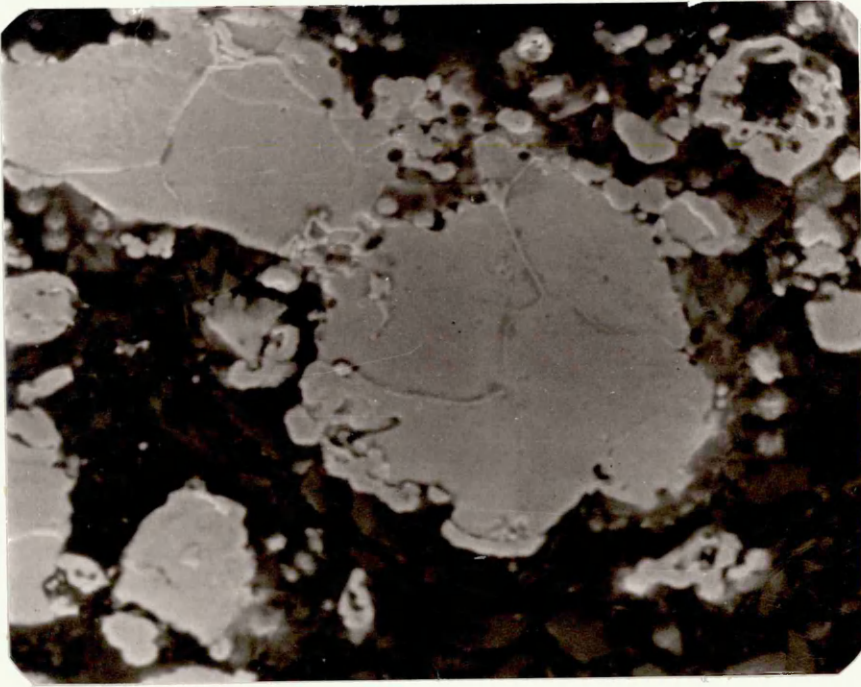
197-B

FIG. 34.

- a) Cross section of an iron particle.
Composition of powder Fe-14.08%Co.
Deposit obtained from solution containing
250 g/l CoCl_2 at a PH of 5.3

X 1200

- b) X-ray photograph of the area in the above
photograph, white colour stands for cobalt
deposit.



198-B

FIG. 35.

Cross section of C.F.28-D powder sample.

- a) iron particles (with grain boundary) and spongy cobalt deposits. The mean cobalt amount 35%. Deposit obtained from solution containing 100 g/l CoSO_4 +15 g/l H_3BO_3 at a PH of 4-4.5.

X 560

- b) Map of the area in the above (fig. 35-a) photograph, white colour indicates iron, dark colour indicates cobalt.

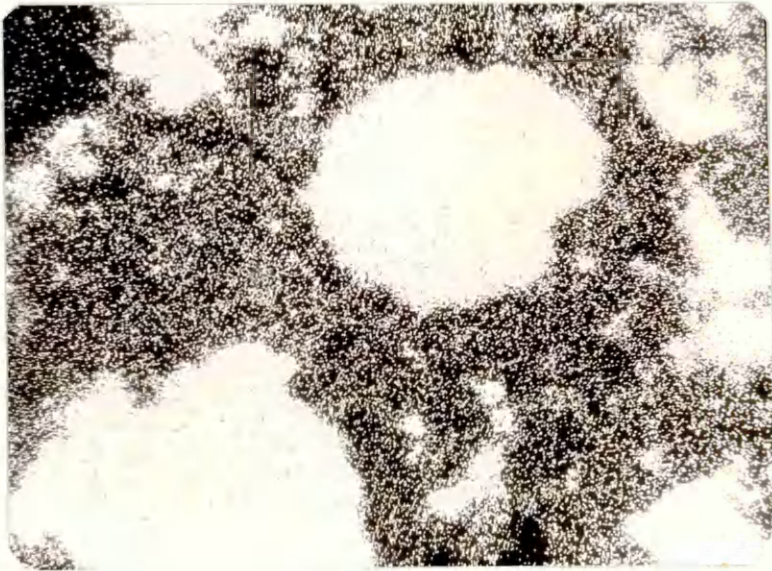


FIG. 36.

Cross section of a pit in an iron particle
of C.F.28-D and a cobalt deposit on the
edge of the pit.

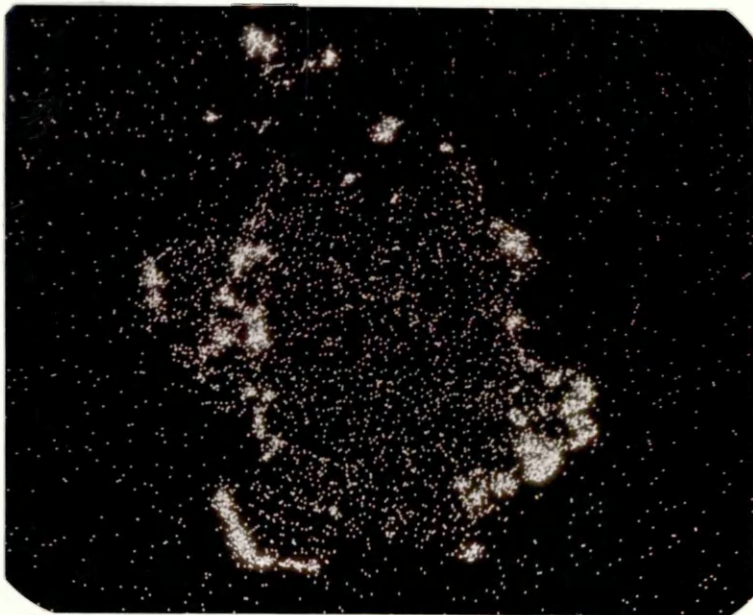
X 1600

FIG. 37.

- a) Cross section of an iron particle with cemented cobalt, which was cemented from 200 g/l CoCl_2 including solution at a PH of 5.7. Composition of powder Fe-7.04%Co.

X 560

- b) Map of the photograph in fig. 37-a.
White colour stands for cobalt deposit.



201-B

FIG. 38.

- a) Spongy cobalt deposit layers on iron particles which were deposited in 100 g/l CoCl_2 including solution, at a PH of 3-3.5. Composition of powder Fe-2.96%Co.

X 1040

- b) Edax analysis iron and cobalt (on right) peaks of the crossed point in the above photograph.

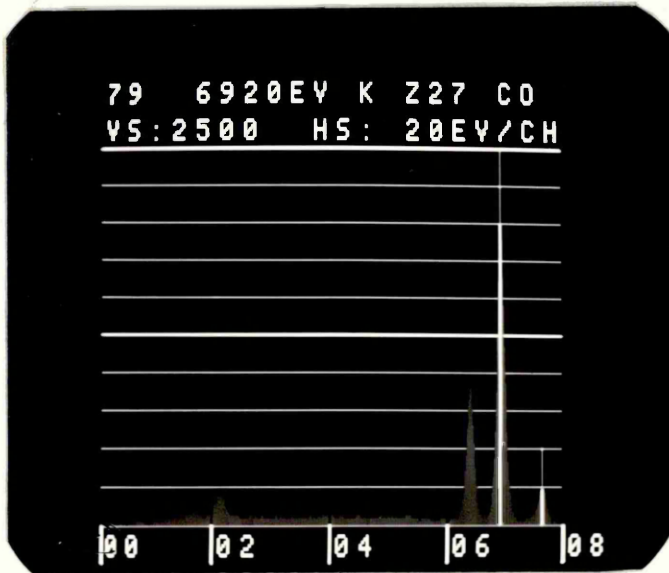
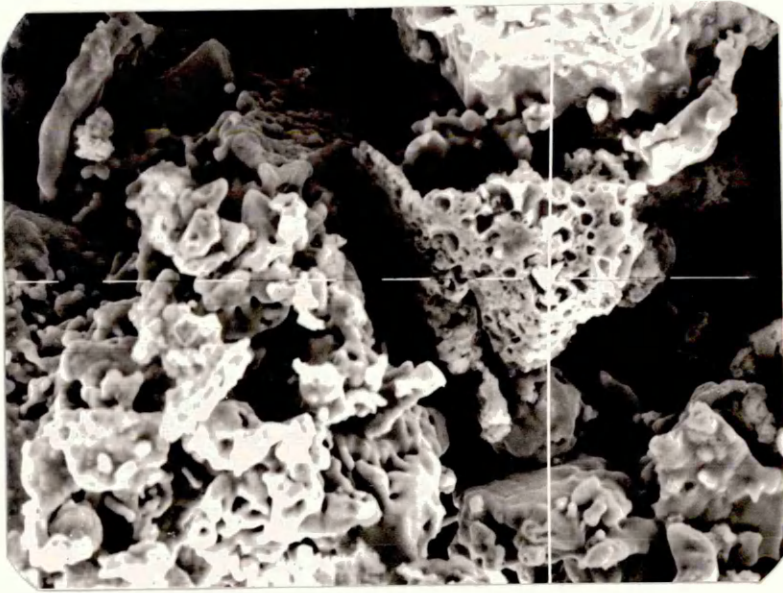


FIG. 39.

- a) Nodular cobalt deposits on iron particles.
Composition of powder Fe-31%Co. Deposit
obtained from 100 g/l CoSO_4 at a PH of
4-4.5.

X 640

- b) Edax analysis, iron and cobalt (on right)
peaks, of the photographed area in fig.
39-a.

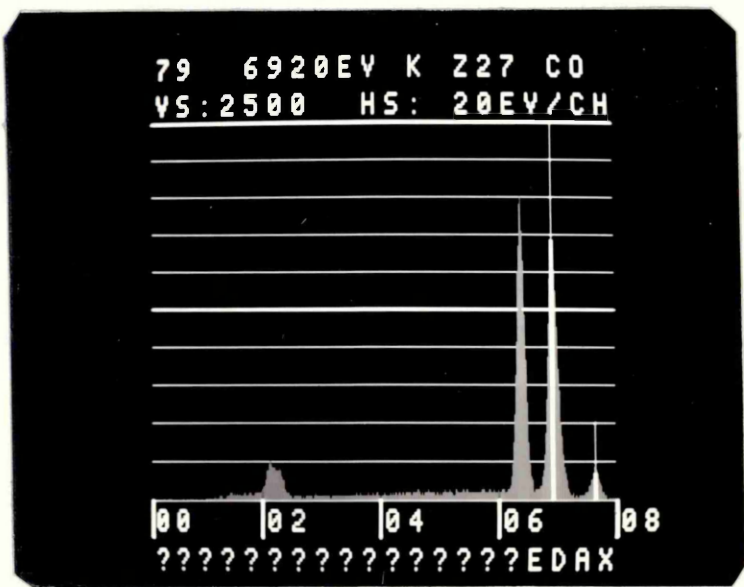
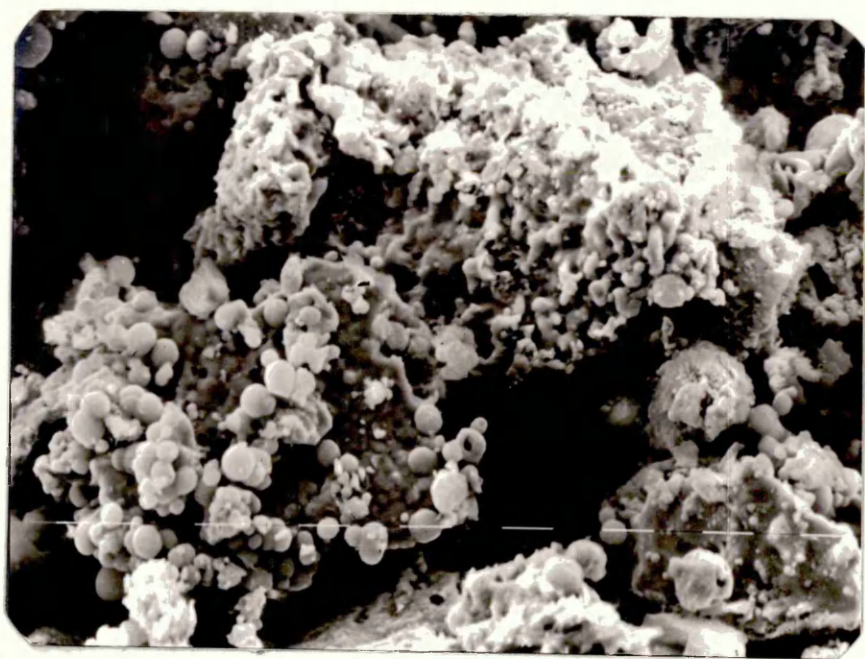
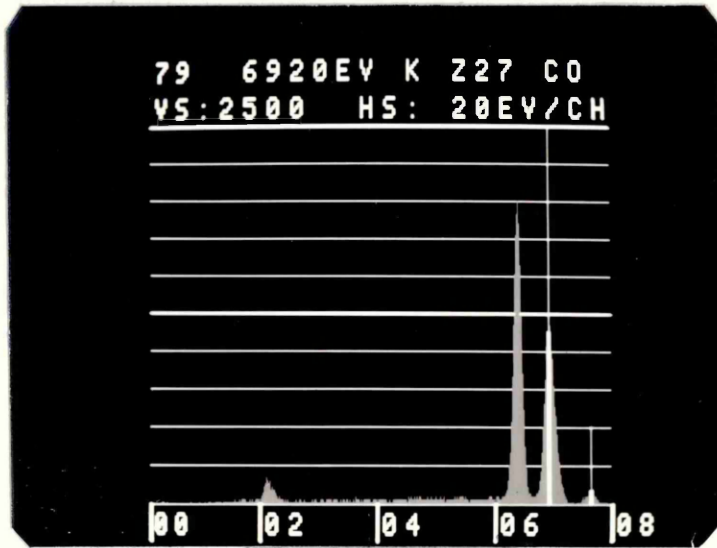
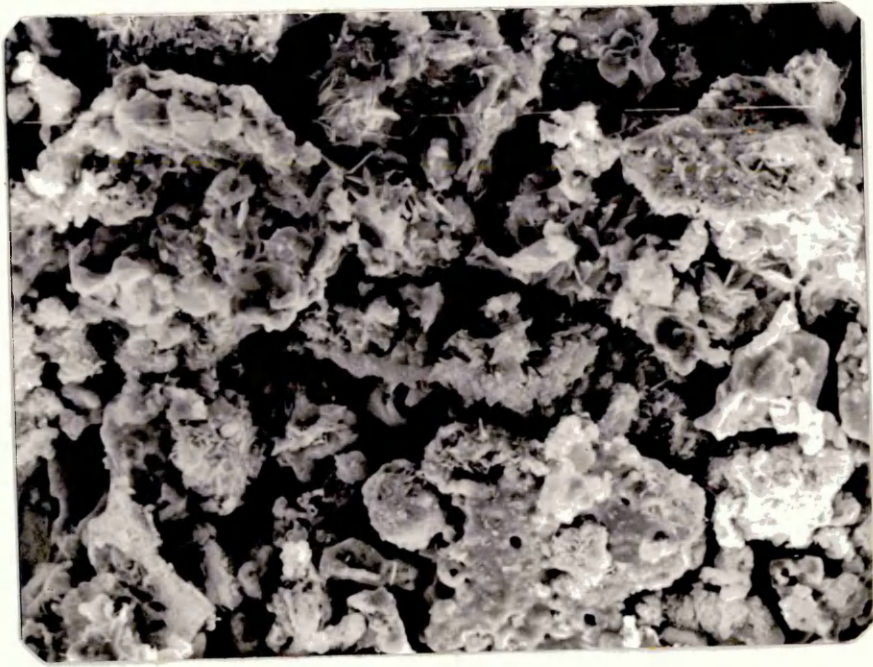


FIG. 40.

- a) Flaky cobalt deposits on iron particles
Composition of powder Fe-8.6%Co.
Deposition obtained from solution
containing 100 g/l of CoSO_4 at a PH of
4-4.5.

X 960

- b) X-ray analysis of iron and cobalt (on left)
peaks of the area in the above photograph.



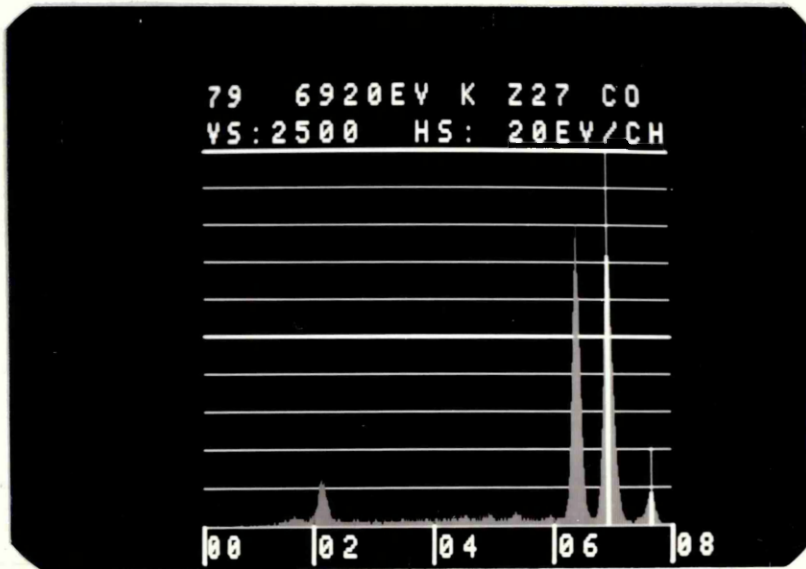
204-B

FIG. 41.

- a) Dendritic cobalt deposits on iron particles. Composition of powder Fe-22.8% Co. Deposit obtained from solution containing 100 g/l of CoSO_4 at a PH of 3.5-4.

X 1120

- b) Edax analysis iron and cobalt (on left) peaks of the area in the above photograph.



205-B

FIG. 42.

Change of the morphology of cemented cobalt.

- a) Nodular cobalt deposits during the first 30 minutes of experiment C.F.28, which was carried out in 100 g/l CoSO_4 , 15 g/l H_3BO_3 solution at PH of 4-4.5, and was including 5%Co.

X 960

- b) Edax analysis iron and cobalt (on left) peaks of the area in fig. 42-a.

(Fig. 42 c and d over)

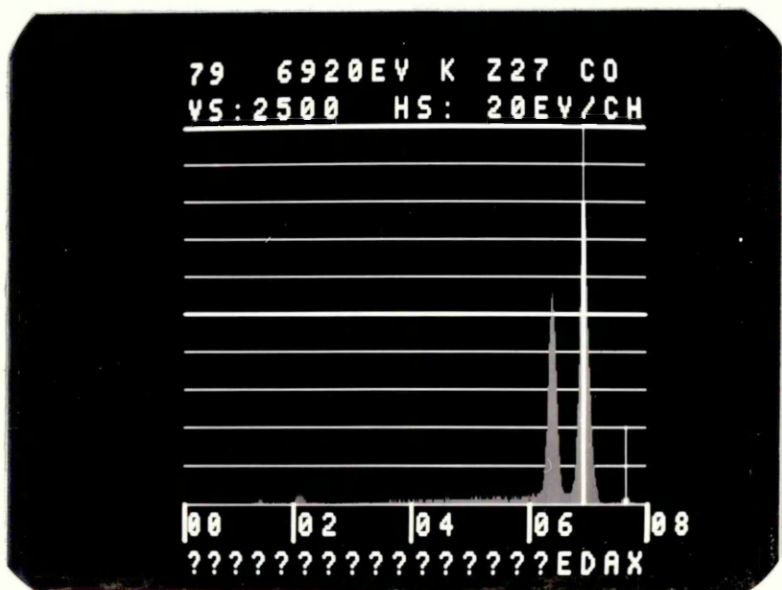
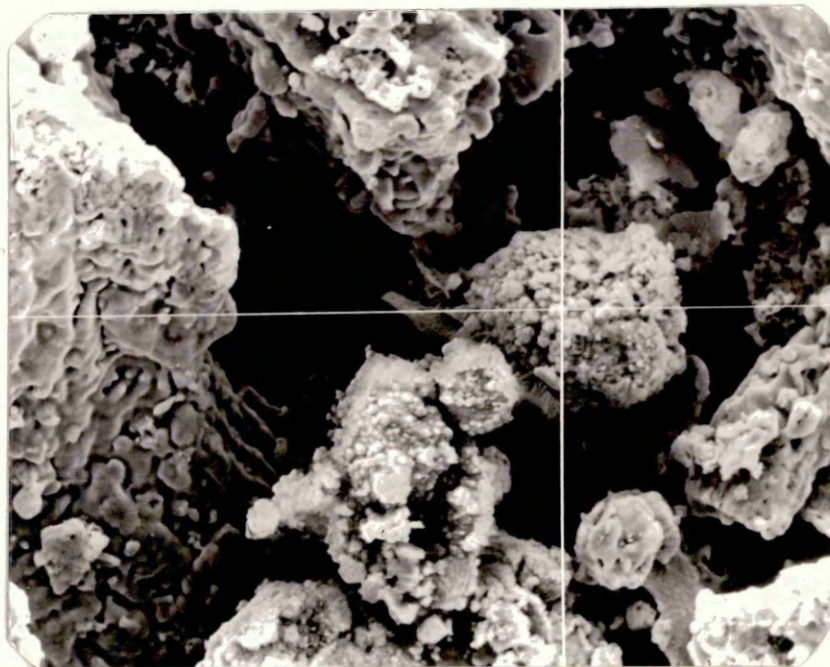


FIG. 42 (continued)

- c) Spongy cobalt deposits in the above solution (42-a), after 90 minutes, total cobalt deposition - 35%.

X 480.

- d) Edax analysis of iron and cobalt (on left) peaks of the area in photograph (c).

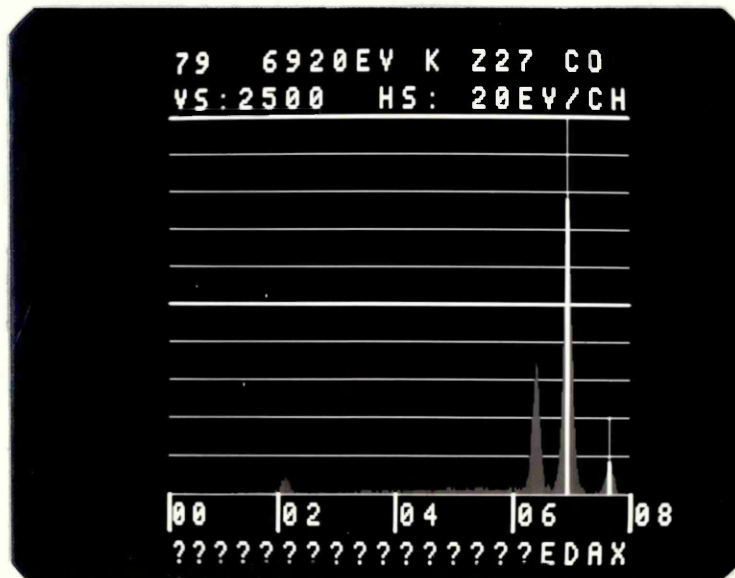
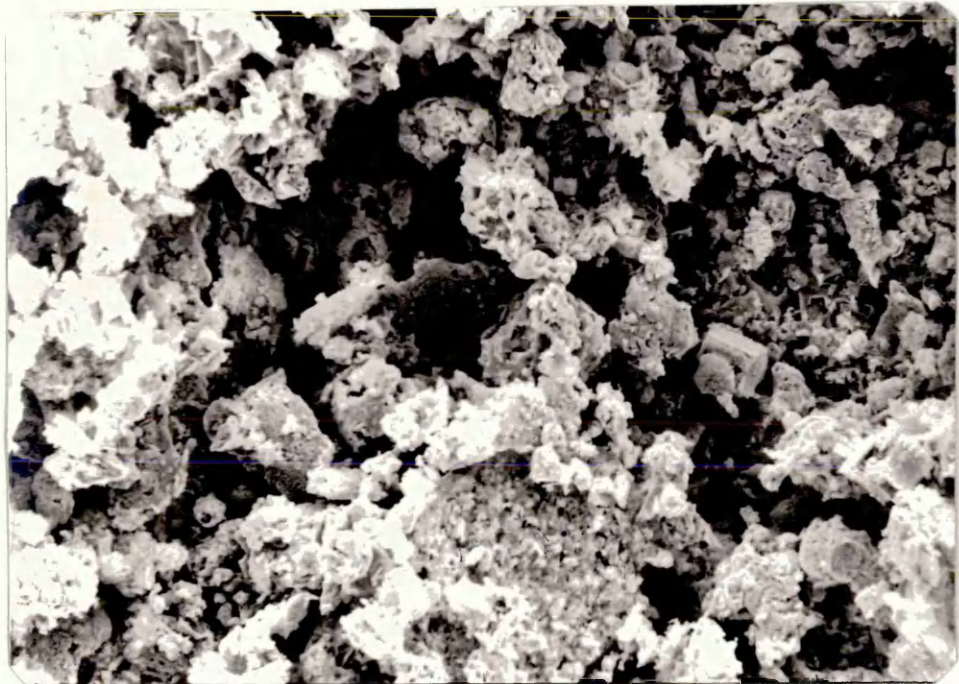
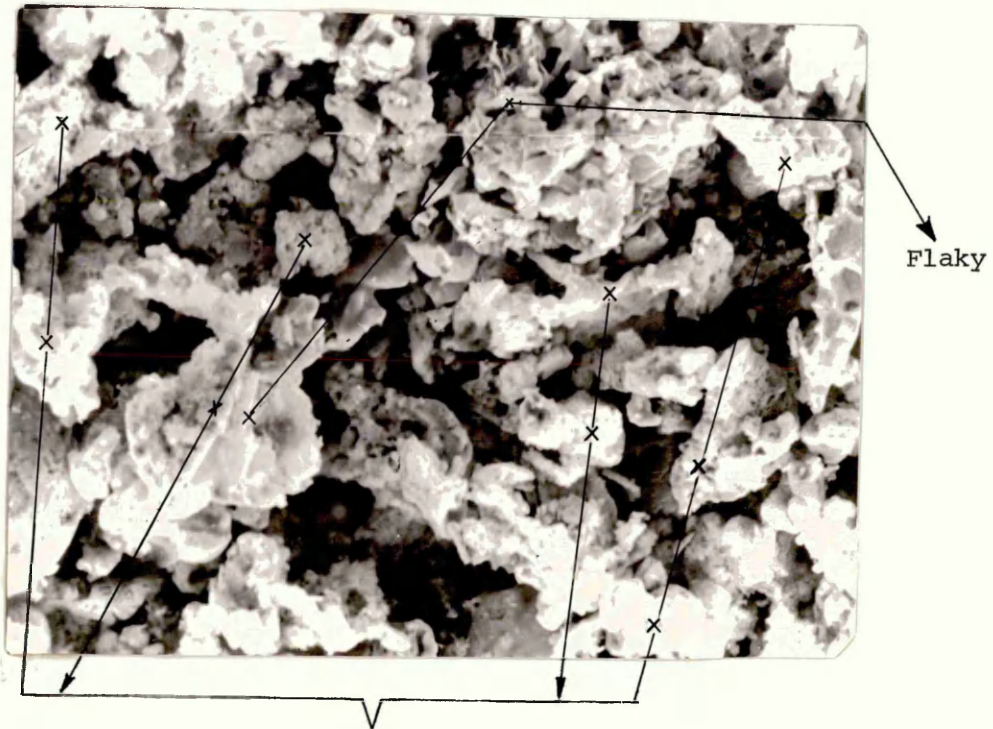


FIG. 43.

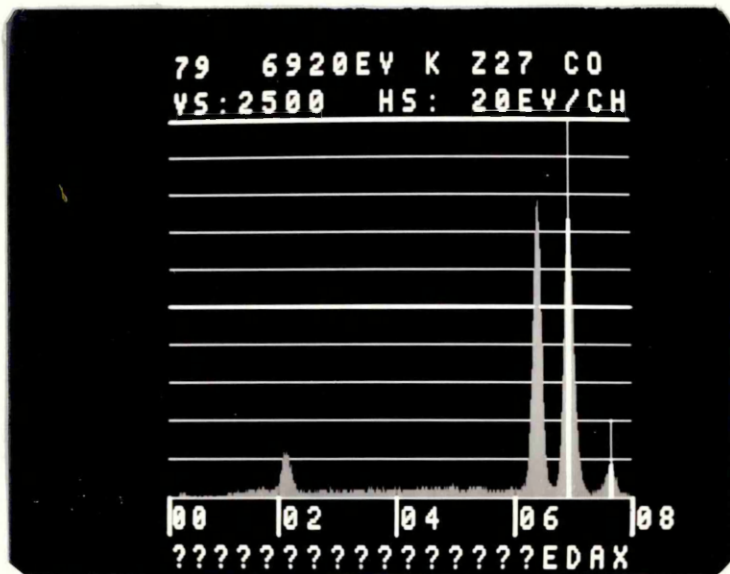
- a) Cobalt deposit with a mixture of spongy and flaky morphology. Composition of powder Fe-14.8% cobalt. Deposit obtained from solution containing 100 g/l of CoSO_4 +15 g/l of H_3BO_3 at a PH of 4-5, and potential of 5.1 volt.

X 480

- b) Edax analysis iron and cobalt (on left) peaks of the area in the above photograph.



Spongy



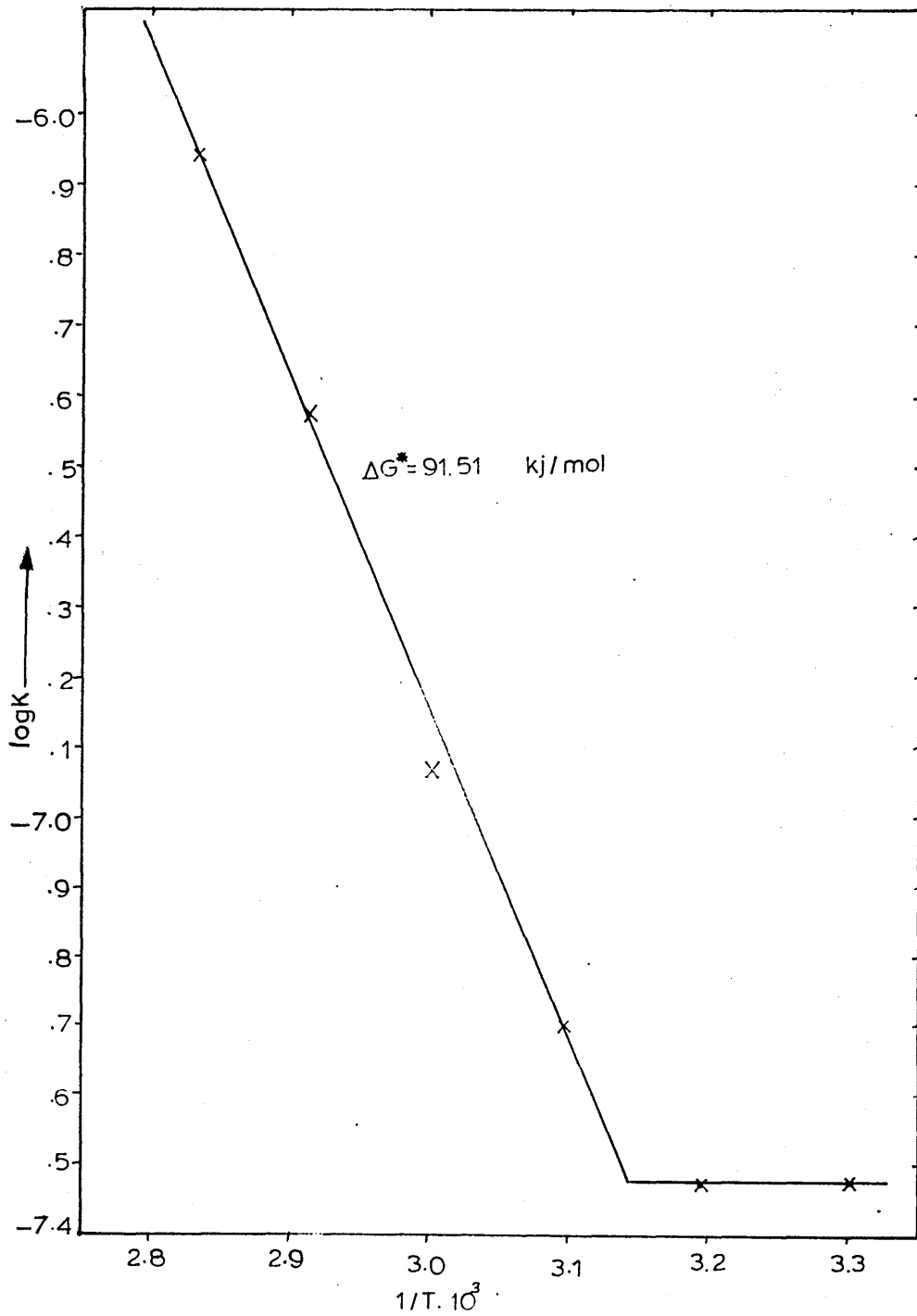


Fig.44: Arrhenius plot for cobalt cementation on iron powder in 100 g/l of cobalt chloride and 50 g/l of iron powder involving solutions at PH of 3 in mechanically stirred beaker.

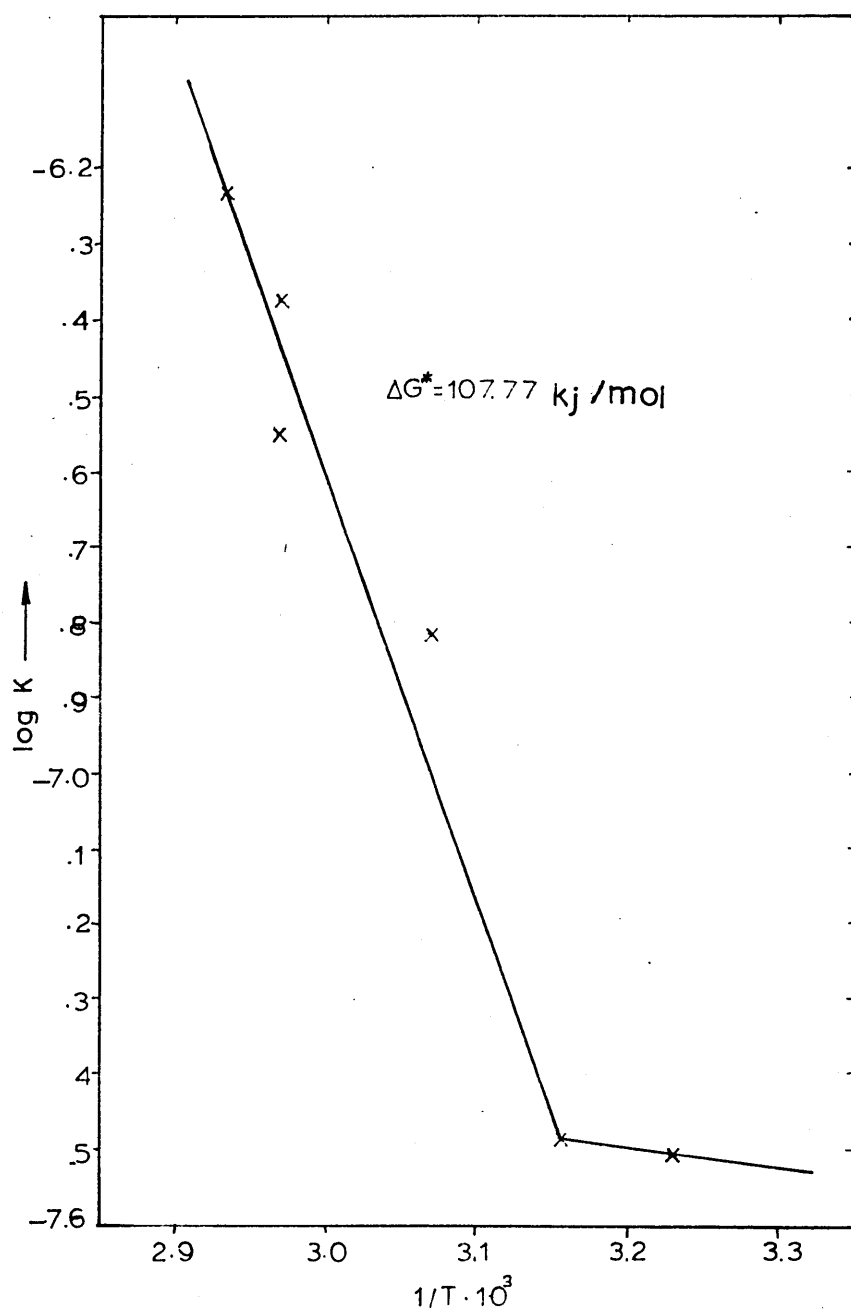


Fig.45: Arrhenius plot of cobalt deposition on iron powder in 100 g/l of cobalt chloride and 100 g/l of iron powder involving solutions, at natural PH (5.6–6.3).

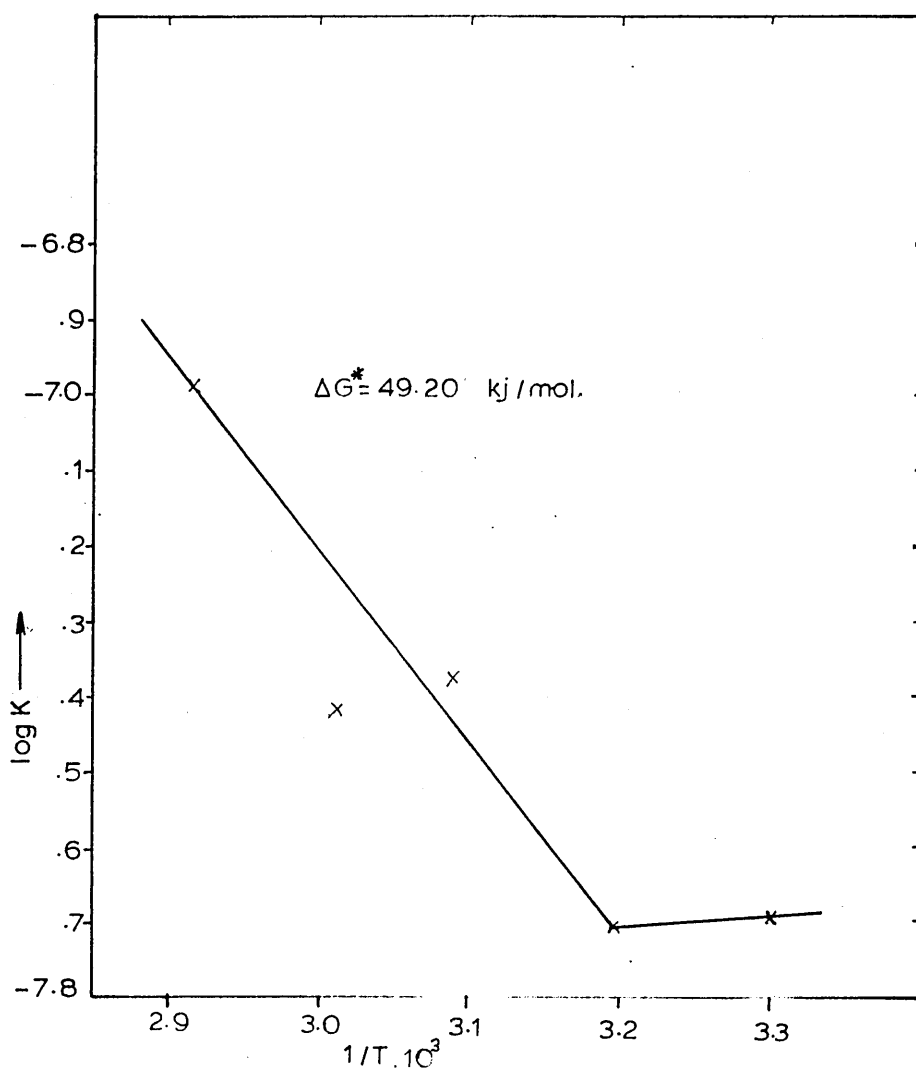


Fig.46: Arrhenius plot for cobalt cementation on iron powder in 100 g/l of cobalt sulphate and 100 g/l of iron powder involving solutions, at natural PH (5.5–7.1)